

Chemical Genetic Studies of Chemical Modulators of Mammalian Adenylyl Cyclases and Phosphodiesterases Expressed in Fission Yeast

Author: Ana Santos de Medeiros

Persistent link: <http://hdl.handle.net/2345/bc-ir:106786>

This work is posted on [eScholarship@BC](#),
Boston College University Libraries.

Boston College Electronic Thesis or Dissertation, 2016

Copyright is held by the author, with all rights reserved, unless otherwise noted.

Boston College
Morrisey College of Arts and Sciences
Graduate School
Department of Biology

**CHEMICAL GENETIC STUDIES OF CHEMICAL MODULATORS OF MAMMALIAN
ADENYLYL CYCLASES AND PHOSPHODIESTERASES EXPRESSED IN FISSION
YEAST**

a dissertation

by

ANA SANTOS DE MEDEIROS

Submitted in partial fulfillment of the requirements for the degree of

Doctor of Philosophy

May 2016

© copyright by ANA SANTOS DE MEDEIROS

2016

ABSTRACT

Cyclic adenosine monophosphate (cAMP) and the second messengers that modulate several biological processes are regulated by adenylyl cyclase (AC) and cyclic nucleotide phosphodiesterases (PDEs). ACs and PDEs are comprised of superfamilies of enzymes that are viewed as druggable targets due to their many distinct biological roles and tissue-specific distribution. As such, small molecule regulators of ACs and PDEs are important as chemical probes to study the roles of individual ACs or PDEs and as potential therapeutics. In the past, our lab has expressed 15 mammalian PDE genes in *S. pombe*, replacing the endogenous Cgs2 PDE. High throughput screens for PDE inhibitors identified novel compounds that show relevant biological activity in mammalian cell culture assays. The aim of this thesis is to develop tools to understand the mechanism of interaction between key regulators of the cAMP pathway and small molecules. The current study is comprised of two parts. In the first part of this thesis, I developed a genetic screen that detected alleles whose proteins remain active in the presence of BC54 and was to confirm the effect of the PDE4BT407A mutation using cell-based assays and *in vitro* enzyme assays. In the second part of this thesis, I developed and carried out HTSs using a PKA-repressed GFP reporter that can identify compounds that reduce PKA activity, which would include PDE activators and AC or GNAS1 inhibitors. To date, I have identified three AC inhibitors that appear to act on several of the ten different mammalian ACs. To our knowledge, this is the first time a large HTS has identified AC inhibitors, where inhibition was assessed inside the cells. The findings in this thesis will be useful in the design of more effective PDE inhibitors and in the development of novel chemical probes for studying cAMP signaling in mammalian cells.

DEDICATION

To my parents and siblings who have given me love, support and encouragement to fulfill my
dreams

ACKNOWLEDGMENT

First and foremost, I would like to thank my advisor, Professor Charles Hoffman. Dr. Hoffman has been an incredible professor and mentor. I thank him for his patience, for his enthusiasm for research, and for all the jokes in the lab. Five years ago, I had a remote idea how far I would go. Charlie 's excitement for Science has been the fuel for my desire to become a better scientist. Every day, I would go back to the lab wondering what lessons I would learn. He thought me to always question my data and to always observe everything. I constantly told myself there was (and still is) so much to learn. Charlie kept supporting and challenging me to seek more knowledge. His guidance and mentorship helped me overcome many obstacles throughout my Ph.D. He taught me that not knowing something is a great opportunity to develop my academic and research skills. I believe I am a better scientist because of him. Looking back, I could not have found and asked for a better mentor. I would like to thank him for giving me the opportunity to join the Hoffman lab. It gave me the opportunity to interact with excellent scientists.

I am also grateful to my committee members for all their support throughout my Graduate study and for taking time from their busy schedules to answer any question I had. I would like to thank Professor Moroianu for her support and for helping and welcoming me to perform experiments in her lab. I also would like to thank Dr. Annunziato for his valuable discussions inside and outside of committee meetings. I also would like to thank Dr. O'Connor for discussions that I believe were very valuable in shaping up my research skills that were essential for the completion of my thesis. I would also like to thank Dr. Cam for being generous and giving me his time to read my thesis and for being on my committee.

The Hoffman las has been an incredible and enjoyable learning environment. I am grateful for Dr. Ceyhan Birsoy and Dr. Wyman who provided me support and training even when they were no longer in the lab. I also would like to thank Rony and Olivia for so much enthusiasm, hard work

and great scientific insights at such young age. I also am thankful to all the Hoffman lab members who worked through these five years and made my PhD an enjoyable experience: Brett, the Charlie's angels (Dayna and Gabby), the boys (Kyle and Alex), Jordan, Sam, Rachel and Grace.

I would like to thank Dr. Demirbas for her support, friendship and for sharing her enthusiasm for Science. Dr. Demirbas is an excellent scientist and I have been privileged to have the opportunity to work with her. Dr. Demirbas has also been very generous in sharing her experience with me and taking the time to teach me.

I am grateful for the opportunity to work in the Moroianu lab for almost a year. I am thankful to have learned from Dr. Slavitskiy and Dr. Onder. It was a wonderful experience to work with great scientists and friends who were so patient and welcoming.

I am blessed to have an incredible group of friends and colleagues that have inspired me and guided me through the tough and happy times: Deb Irene, Veniamin, Zeynep, Brooke, Tomasz, Kaila, Heather, Katie, Andrew, Amit, Sudeshna and Alison. They have been an incredible support and source of knowledge. When I am facing a challenge, I always ask myself if I were one of them what I would do.

I also would like to thank Dr. DiBenedetto, Dr. MuskaVitch, Dr. O'Connor, Dr. Warner, Dr. Annunziato, Dr. Hoffman and Dr. Tanini for allowing me to TA for them. I have learned so much from all of them. Their encouragement and support made me become more confident to teach. Their scientific inquiries helped my research as well.

I also would like to thank all the TA's that I worked in the lab courses and discussion sections. They made TAing a really enjoyable experience. I am very fortunate to have worked with: Brooke, Marisha, Sudeshna, Betty, Alison, Marianne and David. Big thanks to the undergraduate TAs: Jackie and Sam.

I would like to thank Dr. Folker and Dr. Huanchen who made significant contributions to both my research and my scientific development. They took time from their busy schedules to share their knowledge with so much patience. I also would like to thank Dr. Ke for his collaboration and insightful scientific discussions.

I am profoundly indebted to the Department of Biology at Boston college. To Peter Marino for always being so helpful and supportive, from solving issues and answering inquiries so quickly. I would like to thank Diane Butera for encouraging us to join the Seminar lunches with the guest speakers and learn more about Science in a more informal setting. I would like to thank you Donna for placing all the orders for my research and TA assignments so efficiently. I also would like to thank John O'Grady for getting things up and running so I could perform my experiments at any time needed. I would like to thank Colette for her contagious sense of humor and insightful thoughts that put a smile on my face and kept me going when times were tough.

I thank Boston College fund for support my HTS project and making this work possible.

I would also like to thank The ICCB Screening Facility Program at Harvard Medical school, especially Jen Smith, Jen Nale, David Wrobel, Stewart, Sean and Rachel for training me and making the screening process enjoyable. A truly unforgettable experience.

Finally, I would like to thank Susan Shea for her kindness and support throughout my stay at BC. She has been so helpful and a knowledgeable to the International students who seek her guidance like I have. She gave me the tranquility to enjoy the BC experience.

TABLE OF CONTENTS

DEDICATION	I
ACKNOWLEDGEMENT	II
TABLE OF CONTENTS	V
THESIS LIST OF FIGURES	X
FIGURES APPENDIX A	XI
FIGURES APPENDIX B	XI
THESIS LIST OF TABLES	XIII
TABLES APPENDIX A	XIV
LIST OF ABBREVIATIONS	XV
CHAPTER ONE	1
INTRODUCTION	1
1.1 Cyclic nucleotide signaling	1
1.2 Cyclic nucleotide signaling in mammals	1
1.3 Mammalian Cyclic nucleotide Phosphodiesterases (PDEs)	2
1.4 Phosphodiesterase 4 (PDE4) family	3
1.4.1 PDE4 structure and regulation	4
1.4.2 Tissue distribution and Biological roles of PD4B2 and PDE4B3	9
1.4.3 PDE4 inhibitors	10
1.5 Clinical trials of PDE4 inhibitors	18
1.6 Phosphodiesterase 7 (PDE7) family	20
1.6.1 Tissue distribution and biological roles of PDE7	21
1.7 Mammalian adenylyl cyclases	24
1.8 Use of a fission yeast cell –based platform to study mammalian proteins	26
1.8.1 <i>S. pombe</i> glucose/cAMP signaling pathway	27
1.9 PKA in <i>S. pombe</i>	28
1.10 Aims of this dissertation	31
CHAPTER TWO	36
MATERIAL AND METHODS	36

2.1 Materials	36
2.1.1 Growth Media	36
2.1.2 Yeast	36
2.1.3 Bacterial strains	36
2.1.4 Enzymes	37
2.1.5 Buffers for protein purification	37
2.1.5.1 Buffers for protein purification using Affinity column	37
2.1.5.2 Buffers for protein purification using Ion-Exchange column	37
2.1.6 Antibodies	38
2.1.7 Small molecules used in counterscreens and cAMP assays	38
2.2 Methods	38
2.2.1 Strain mating and tetrad dissection	38
2.2.2 Mutagenic PCR	38
2.2.3 Genetic screens	39
2.2.4 Cloning and Plasmid construct	41
2.2.5 DNA sequencing	41
2.2.6 Cell-based assays	41
2.2.6.1 5FOA assays	41
2.2.6.2 GFP assays	42
2.2.7 Site directed mutagenesis	42
2.2.8 Protein purification	42
2.2.9 <i>In vitro</i> assays	49
2.2.10 Protein Measurements	49
2.2.11 High-throughput screens (HTS)	49
2.2.11.1 10,000 HTS for PDE activators	50
2.2.11.2 HTS for PDE activators and AC/GNAS1 inhibitors	55
2.2.12 cAMP assays	56
2.2.13 KCl assays	57
CHAPTER THREE	58
IDENTIFICATION AND CHARACTERIZATION OF COMPOUND RESISTANT ALLELES OF PDE4B TO DUAL PDE4/7 INHIBITOR BC54	58
3.1 Development of a <i>S. pombe</i> genetic screen for compound – resistant alleles of PDE genes	58

3.1.1	Discovery of a dual specificity PDE4/7 inhibitor	58
3.1.2	Cell survival test	59
3.1.3	Optimization of enrichment conditions	60
3.1.4	Screening	60
3.2	Characterization of mutant PDE4B strains in 5FOA assays	61
3.3	Characterization of mutant PDE4B strain in GFP	67
3.4	Biochemical verification of compound resistance	76
3.5	In vitro assays	76
3.5.1	Determining initial velocity, turnover and enzyme efficiency	76
3.5.2	IC ₅₀ assays	83
3.6	Conclusion	86
	CHAPTER FOUR	92
	DEVELOPMENT OF A HIGH THROUGHPUT SCREEN FOR PDE ACTIVATORS	92
4.1	Development of a chemical screen for phosphodiesterase activators	92
4.2	Optimization of fission yeast HTS for PDE activators	93
4.3	Screen with a compound library	94
4.4	Validation of primary screen Hits	100
4.4.1	Selection of compounds for cherry-pick experiments	100
4.4.2	Counter-screen assays	110
4.5	Conclusion	120
	CHAPTER FIVE	121
	HIGH THROUGHPUT SCREEN FOR PDE ACTIVATORS OR AC/GNAS1 INHIBITORS	121
5.1	HTS for small molecules that reduce PKA activity using commercial libraries	121
5.2	Evaluation of the Primary screen	129
5.2.1	Selection of the Primary screen hits	138
5.2.2	Optimization for Cherry-pick experiments	138
5.2.3	Validation of potential candidate hits using Cherry-pick experiments	147
5.3	Secondary assays to confirm potential candidates as final hits	152
5.3.1	Secondary screens for assessment of PKA activity in liquid medium	153
5.3.2	Secondary screens for assessment of PKA activity in solid medium	159

5.4 Conclusion	160
CHAPTER SIX	166
DISCUSSION AND FUTURE DIRECTIONS	166
6.1 Development of a genetic screen to identify BC54-resistant PDE alleles	166
6.1.1 Enrichment is important to screen compound resistant transformants	168
6.1.2 Screening for compound resistance alleles is a successful method to find mutant PDEs	168
6.1.3 The value of knowing the mutants with BC54-resistance	170
6.1.4 BC54 analogs have different chemical groups that decrease their inhibition against strains expressing PDE4B2	174
6.1.5 Conclusion	175
6.2 The 10,000 HTS screen can identify compounds that reduce PKA activity	177
6.2.1 Failure to validate compounds points out to technical issues	177
6.2.2 Conclusion	178
6.3 Development of a HTS for PDE activators and AC/GNAS1 inhibitors	179
6.3.1 Methods to validate candidate hit compounds	180
6.3.2 Difficulty in detecting PDE activators may be related to the limitation in increasing the enzyme activity	181
6.3.3 Progesterone is an AC inhibitor	182
6.3.4 Using non-selective compounds to understand the mechanism of AC regulation	182
6.3.5 Conclusion and Future directions	184
LITERATURE CITED	185
APPENDIX A	201
DEVELOPMENT OF <i>S.POMBE</i> GENETIC SCREEN FOR -COMPOUND- RESISTANT PDE7 ALLELES	201
INTRODUCTION	201
MATERIALS AND METHODS	201
A1. MATERIALS	201
A1.1 Growth media	201
A1.2 Yeast strains	201
A.1. 3 Enzymes	202
A2. Methods	202
A.2.1 Mutagenic PCR	202

A.2.2 Cloning and Plasmid construct	202
A.2.3 DNA sequencing	204
A.2.4 Genetic Screen	204
A.2.5 Cell-based assays	205
A.2.6 Two- step PC to generate single missense mutations	205
RESULTS	206
CONCLUSIONS	218
LITERATURE CITED FOR APPENDIX A	218
APPENDIX B	220
CHARACTERIZATION OF BC54 ANALOGS IN LIQUID AND SOLID MEDIA	220
INTRODUCTION	220
MATERIALS AND METHODS	220
B1. MATERIALS	220
B1.1 Growth media	220
B1.2 Yeast strains	220
B2. METHODS	221
B.2.1 Cell-based assay	221
B2.2 Growth in SC-ura	221
RESULTS	221
B1 Profiling the potency of BC54 analogs	221
B2. Profiling of BC54 analogs in cell-based assays	222
B3. Analyzing the structure of BC54 analogs	222
CONCLUSIONS	223
LITERATURE CITED FOR APPENDIX B	232

THESIS LIST OF FIGURES

Figure 1.1 Overview on cAMP signaling pathway	5
Figure 1.2 Characteristics of mammalian PDEs	7
Figure 1.3 PDE4 Isoforms and regulatory domains	12
Figure 1.4 PDE4B2 crystal structure and residue interactions	15
Figure 1.5 Structure of PDE4 inhibitors	22
Figure 1.6 Phenotypes associated with PKA activity used in the genetic screen	34
Figure 2.1 Development of a genetic screen	46
Figure 2.2 Basis for secondary screen	52
Figure 3.1 Structure of dual specificity PDE4/7 inhibitor (BC54)	62
Figure 3.2. 5FOA growth assays of strain expressing wild type PDE4B2 or wild-type PDE7B	64
Figure 3.3. Stationary cell survival	68
Figure 3.4. Inhibition of growth by PDE inhibitors in SC-ura	70
Figure 3.5. Mutant PDE4B alleles display growth in a halo assay in SC-ura	72
Figure 3.6 Crystal structure of PDE4D bound to cAMP	74
Figure 3.7. 5FOA growth assays of strains expressing wild type PDE4B2, PDE4B2Y233H, or PDE4B2T407A	77
Figure 3.8 The amount of exogenous cAMP needed to activate PKA and repress the GFP reporter is a reflection of PDE activity	79
Figure 3.9. GFP assays strains expressing wild type PDE4B2+ or PDE4B2T407A	81
Figure 3.10. Protein purification of the PDE4BT407A mutant protein	84
Figure 3.11. Vmax values based on a linear reaction with time	87
Figure 3.12. IC50 assays	90
Figure 4.1. Heatmap displaying reproducibility of GPF and OD values from screening and control	95
Figure 4.2. Cells expressing PDE4B require more exogenous cAMP than a strain lacking PDE activity to repress GFP reporter	98

Figure 4.3. Qualitative data overview of 10,000 compound screen	101
Figure 4.4. High throughput screen for PDE4D3 activators	105
Figure 4.5. Results of the HTS	108
Figure 4.6. Pie-chart of candidate hit compounds	111
Figure 4.7. Counter-screen of compounds A1 to A20	114
Figure 4.8. Counter-screen of compounds A11 and A17	117
Figure 5.1. HTS for compounds that reduce PKA activity	122
Figure 5.2. Scatter plot of normalized fluorescence	127
Figure 5.3. Potential candidate hits in the Primary screen	130
Figure 5.4. Qualitative Data Overview	133
Figure 5.5. 3D Histogram of normalized fluorescence	139
Figure 5.6. Selection of small molecules for cherry pick experiments	141
Figure 5.7 GFP assay to validate candidate hits	157
Figure 5.8. Optimization of KCl assays	161
Figure 5.9. KCl assay in solid medium	164

FIGURES APPENDIX A

Figure A1. Development of a genetics screen	207
Figure A2. cAMP curve	210
Figure A3. Growth response of candidate mutant PDE7B alleles to different compounds in 5FOA medium	212
Figure A4. Sequence homology of PDE7A and PDE7B the catalytic domains	216

FIGURES APPENDIX B

Figure B1. Growth phenotype in SC-ura medium	224
Figure B2. 5FOA Growth assays in the presence of BC54 derivatives	226

Figure B3. Chemical structure of BC54 analogs with an effect	228
Figure B4. Chemical structure of BC54 analogs with no effect	230

THESIS LIST OF TABLES

Table 1.1 Properties of PDE enzymes	11
Table 1.2. PDE4 inhibitors currently in clinical trials	17
Table 1.3. Regulation of mammalian AC isoforms and Genome localization	29
Table 1.4. Mammalian AC tissue distribution and biological function	30
Table 1.5. Phenotypes associated with PKA activity	33
Table 2.1. Yeast strain list used in this study	43
Table 2.2. Optimal growth conditions used in 5FOA assays	51
Table 2.3. Optimal growth conditions used in GFP assays	54
Table 3.1. Strains used for cell survival test	66
Table 3.2. Properties of enzyme kinetics for PDE4B2 and PDE4B2^{T407} enzymes	89
Table 4.1. Normalized Fluorescence of optimized HTS	97
Table 4.2. Classification of Hits according to Z-scores of duplicates	107
Table 4.3 List of Chembridge compounds selected for secondary screens	113
Table 4.4. Characterization of candidate PDE4D3 candidates	119
Table 5.1. List of commercial libraries screened at ICCB – Longwood Screening Facility	125
Table 5.2 Analyses of duplicate Z-scores to eliminate false-positives	126
Table 5.3. Elimination of potential candidate hits	132
Table 5.4. Examples for the evaluation of potential hits based on Z-scores	143
Table 5.5. Pilot experiment to evaluate candidate compounds prior to cherry-pick experiments	145
Table 5.6. Results for pilot experiment	146
Table 5.7. Pilot test results of candidate hit compounds at ICCB	148

Table 5.8. Compounds examined in cherry pick experiments with comments on cherry pick results	149
Table 5.9. Small molecules selected for secondary assays	154
Table 5.10. List of strains used for KCl assays in solid medium	163

TABLES APPENDIX A

Table A1. Strain list used in the genetic screen for mating	203
--	------------

List of Abbreviations

5FOA - 5-fluor-ototic acid

AC- Mammalian adenylyl cyclase

AC5- Mammalian adenylyl cyclase type V

AON: Antisense oligonucleotides

ATP- Adenosine triphosphate

sAC – Mammalian soluble adenylyl cyclase

tmAC- Transmembrane adenylyl cyclase

Ba(OH)₂ – Barium hydroxide

BC54 - Ethyl (2Z)-2-(acetylimino)-1-cyclohexyl-5-oxo-1,5-dihydro-3H-dipyrido{1,2-a:2',3'-d]pyrimidine-3-carboxylate

cAMP – Cyclic adenosine monophosphate

cGMP – Cyclic guanosine monophosphate

Cgs1 - PKA regulatory subunit in *S.pombe*

Cgs2 – Phosphodiesterase 1 in *S.pombe*

CLL - Chronic lymphocytic leukemia

CNGs - Cyclic nucleotide-gated ion channels

cNMP- Cyclic nucleotide monophosphate

CNS – Central nervous system

COPD: Chronic obstructive pulmonary disease

ERK – Extracellular-signal-regulated kinase

fbp1 - gene encoding fructose-1,6-bisphosphatase

EPAC - GTPases that are “exchange proteins directly activated by cAMP

GAF domain: Type of protein domain named after some of the proteins: cGMP-specific phosphodiesterases, adenylyl cyclases and FhlA.

GC - Guanylyl cyclase

GFP – Green fluorescent protein

Git1 - Adenylyl cyclase binding protein in *S. pombe*

Git2/Cyr1 - Adenylyl cyclase in *S. pombe*

Git3 - GPCR in *S. pombe*

Git5 - G β subunit in *S. pombe*

Git11 - G γ subunit in *S. pombe*

GNAS1 - Mammalian G α -subunit of heterotrimeric G-protein

Gpa2 - G α subunit in *S. pombe*

GPCR – G-protein coupled receptor

GTP - Guanosine triphosphate

HARBS – High-affinity rolipram binding site

HTS – High throughput screen

IC₅₀ – Inhibitor concentration that reduces enzyme activity in 50%

IPTG – Isopropyl β -D-1-thiogalactopyranoside

KCl- Potassium chloride

LARBS - Low affinity rolipram binding site

LR1 – Linker region 1

LR2- Linker region 2

OD - Optical density

PAS domain – Protein domain involved in the binding of small ligands and protein–protein interaction

PCOS - Polycystic ovary syndrome

PDE – Phosphodiesterase

Pde1 – low affinity PDE in *S. cerevisiae*

Pde2 – high affinity PDE in *S. cerevisiae*

PDE4 – Phosphodiesterase family 4

PDE4B2 - Phosphodiesterase family 4 gene B variant 2

PDE4D2 - Phosphodiesterase family 4 gene D variant 2

PDE4D3 - Phosphodiesterase family 4 gene D variant 3

PDE7 - Phosphodiesterase family 7

PDE7A - Phosphodiesterase family 7 gene A

PDE7B - Phosphodiesterase family 7 gene B

PDE7B1 - Phosphodiesterase family 7 gene B variant 1

PKA – Protein kinase A

Pka1 - PKA catalytic in *S. pombe*

PKC - Protein kinase C

S. cerevisiae - *Saccharomyces cerevisiae* (budding yeast)

S. pombe - *Schizosaccharomyces pombe* (fission yeast)

UCR1 – Upstream conserved region 1

UCR2 - Upstream conserved region 2

ura4 – gene encoding orotidine 5'-phosphate decarboxylase Ura4

ZnSO₄ – Zinc sulfate

CHAPTER ONE

INTRODUCTION

1.1 Cyclic nucleotide signaling

Cyclic nucleotides, cyclic adenosine monophosphate (cAMP) and cyclic guanosine monophosphate (cGMP), are second messengers that modulate several physiological processes, such as cognitive functions, inflammation, and endocrine signaling among others (Beavo and Conti, 2007; Bender and Beavo, 2006). The identification of cAMP led to the development of many studies to uncover the components of the cAMP pathway in many biological processes (Sutherland, 1958). Therefore, understanding their role in different biological responses may be useful for medicinal therapeutics.

In eukaryotes, the cAMP pathway initiates with the recognition of a signaling molecule such as a neurotransmitter by seven-transmembrane domain G protein coupled receptors (GPCRs) that activate heterotrimeric guanine nucleotide-binding proteins (G proteins). The activated G protein then goes on to stimulate adenylyl cyclases (ACs) that convert ATP to cAMP (Offermanns, 2001; Sunahara et al., 1996) (Figure 1.1a). In addition, the rate of conversion of cAMP to 5'AMP is regulated by cyclic nucleotide phosphodiesterases (PDEs) (Beavo and Conti, 2007). Therefore, the intracellular cAMP levels are controlled by the rate of synthesis by ACs and hydrolysis by PDEs, which elicit a cell response to environmental changes (Figure 1.1b) (Beavo and Conti, 2007).

1.2 Cyclic nucleotide signaling in mammals

In mammalian cells, this cAMP signaling cascade is a very complex pathway with superfamilies of proteins that have the same biochemical activity as described in the following sections (Stratakis, 2012; Gancedo, 2013; Maurice et al, 2014, 2006). Once synthesized, cAMP targets numerous

cellular effector proteins, such as: cyclic nucleotide-gated ion channels (CNGs), protein kinase A (PKA) and GTPases that are “exchange proteins directly activated by cAMP”, known as Epacs (Steegborn, 2014) (Figure 1.1a).

1.3 Mammalian Cyclic nucleotide Phosphodiesterases (PDEs)

One of the ways to regulate the intracellular levels of cAMP and cGMP is by their rate of degradation (Figure 1.1b). The temporal and spatial distribution of cyclic nucleotides monophosphate (cNMPs) is controlled, in part, by hydrolysis by PDEs (Bender and Beavo, 2006). In mammals, PDEs are grouped into 11 families encoded by 21 genes that produce more than 100 isoforms. This classification is based on sequence conservation, kinetics and inhibitor sensitivity (Keravis and Lugnier, 2012; Beavo and Conti, 2007) (Table 1.1). Furthermore, PDEs are subdivided according to substrate preference of hydrolyzing either cAMP (PDEs 4, 7 and 8) or cGMP (PDEs 5,6 and 9) or both (PDEs 1,2,3,10 or 11) (Beavo and Conti, 2007) (Figure 1.2a).

Mammalian PDE families also share a conserved catalytic domain of approximately 270 amino acids, located near the C-terminus, and regulatory domains, in most cases located at the protein N terminus (Beavo and Conti, 2007; Bender and Beavo, 2006; Lugnier, 2006), that vary for each PDE from calmodulin binding sites to GAF domains, PAS domains and auto-inhibitory sequences (Lugnier, 2006). Also, PDEs share about 50% sequence homology in the catalytic domains with PDEs from other families (Keravis and Lugnier, 2012). The catalytic domain has been well characterized, especially with respect to three sites. The M site is a metal ion-binding site, which is coordinated by two histidine residues and two aspartic acid residues that form the residue recognition sequence for cNMPs. The Q site is the core pocket that contains the hydrophobic clamp. The S pocket is filled with a water molecule network, and is composed of hydrophilic amino acids including the Q site (Houslay et al., 2005). Moreover, early structural studies suggested that a glutamine residue located in the binding pocket functions in stabilizing the binding of the purine ring to the binding pocket and, consequently, dictating substrate-specificity for each PDE family

(Zhang et al., 2004b; Xu et al., 2000). However, recent studies suggest the differences in preference for either cAMP or cGMP may be due to additional residues in the active site across PDEs, which can also modulate the shape and size of the active sites in the various isoforms (Ke et al., 2011). In addition, individual PDE isoforms display a unique tissue-specific distribution and subcellular localization due to alternative splicing and/or expression from multiple promoters (Lerner and Epstein, 2006; Maurice et al., 2003; Mehats et al., 2002). The distinct intracellular localization of PDEs allows individual PDEs to play greater or lesser roles in the regulation of a myriad of specific physiological processes (Figure 1.2b). Therefore, PDEs are viewed as useful targets for pharmacological inhibition to treat variety of diseases due to their many distinct biological roles, tissue-specific expression and subcellular localization (Lerner and Epstein, 2006; Maurice et al., 2003). However, this subcellular localization is not completely understood and, researchers have suggested three different functional purposes for it, as follows: as a barrier where the PDE is functionally blocking cAMP diffusion; as a sink, by generating low cAMP microdomains; as compartment-sequestered regulator by allowing for equilibrium between compartments by appearing in different concentrations (Richter et al., 2013). The unique temporal and spatial expression of PDEs contributes to their diversity, but it also makes it difficult to understand their biological roles. In order to understand the individual function and utilize them as potential therapeutics, it is essential to identify selective PDE modulators (inhibitors and activators) that target individual PDE families as well as individual subtypes within a family.

1.4 Phosphodiesterase 4 (PDE4) family

In mammals, the PDE4 family is the largest of the PDE families and consists of four genes (*PDE4A*, *PDE4B*, *PDE4C* and *PDE4D*) that undergo alternative splicing and yield many splice variants (Beavo and Conti, 2007; Omori and Kotera, 2007). There are greater than 20 PDE4 isoforms, as follows: 7 PDE4A variants, 4 PDE4B variants, 7 PDE4C variants and 11 PDE4D variants (Figure 1.3a). The PDE4 subtypes have higher affinity for cAMP when compared to cGMP. A compilation

of *in vitro* studies characterized their K_m ranging from 1 to 5 μ M. (Beavo and Conti, 2007) (Table 1.1).

1.4.1 PDE4 structure and regulation

The PDE4 variants have 75% identical catalytic domains with conserved C-termini and variable N-termini such that they can be grouped as length variants (Beavo and Conti, 2007). The PDE4 isozymes differ structurally based on the presence or absence of the regulatory domains termed Upstream Conserved Regions 1 and 2 (UCR1 and UCR2) located in the N-terminus (Maurice et al., 2014). The presence or absence of UCRs determines a variant length and they are classified as long form (possesses both UCR1 and UCR2 regions), short (possesses the UCR2 region only), super-short (contains only half of UCR2 region) (Figure 1.3b) (Richter et al., 2013).

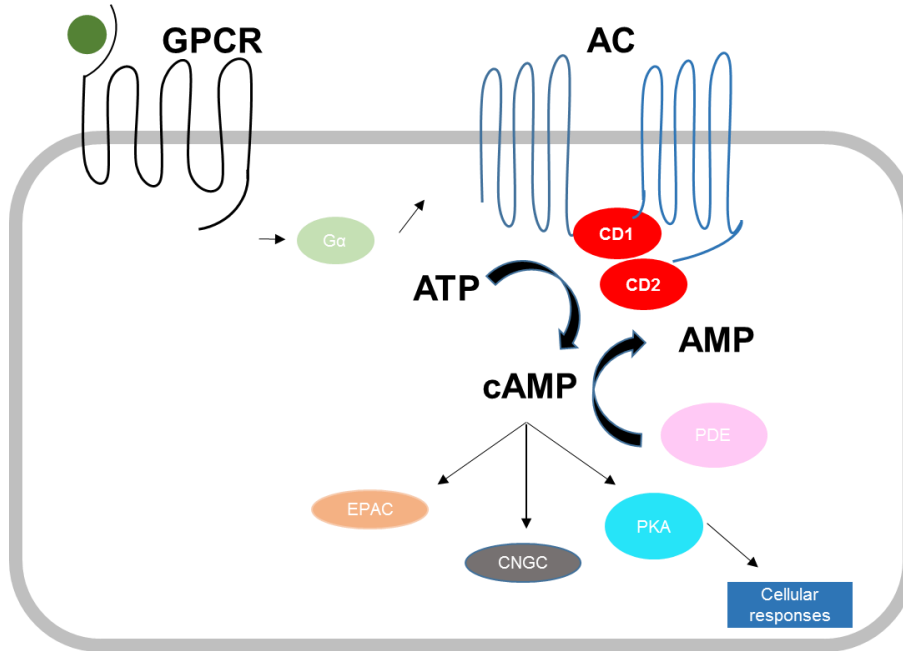
PDE4 enzymes possess various regulatory domains as follows: ERK phosphorylation domain in the C-terminus; the UCRs separated by linker regions 1 and 2 (LR1 and LR2) at the N-terminus; a PKA regulatory domain in the UCR1 directly correlated to the catalytic activity of PDE4 long forms when phosphorylated at a Serine54 (Lerner and Epstein, 2006), and a dimerization site (Figure 1.3b) (Lugnier, 2006). In addition to the PKA domain, the UCR1 site contains a phosphatidic acid binding site that acts as an allosteric activator of the PDE4D3 protein (Grange et al., 2000).

The presence of PKA phosphorylation site in the N-terminus inhibits ERK regulatory activity in the C-terminus in long form variants. Conversely, the absence of PKA domain in the N-terminus allows ERK to activate PDE activity in short forms (Lerner and Epstein, 2006). The UCR-containing region of long form PDE4s is also involved in dimerization. The presence of dimerization promotes sensitivity to rolipram (the drug that defines the PDE4 family) (Richter and Conti, 2004) along with conformational modifications (Conti et al., 2003). These changes in the PDE4 affect the affinity for rolipram and are classified as either low-affinity rolipram binding site (LARBS) and high-affinity rolipram binding site (HARBS) (Houslay et al., 2005). Moreover,

Figure 1.1. Overview on cAMP signaling pathway A) A signaling molecule is recognized by GPCR. This binding causes a conformational change that sends a signal to activate $G\alpha$, which in turn, stimulates AC. AC converts ATP to cAMP, which can then be hydrolyzed by PDE. Once cAMP is produced, it activates the cAMP effectors in mammalian cells: exchange proteins activated by cAMP (EPACS), cyclic nucleotide gated ion channels (CNGs) and PKA that triggers cellular responses. B). cAMP levels are regulated by the rate of synthesis from ATP by adenylyl cyclase and hydrolysis by PDEs producing 5'AMP.

Figure 1.1 Overview on cAMP signaling pathway

A



B

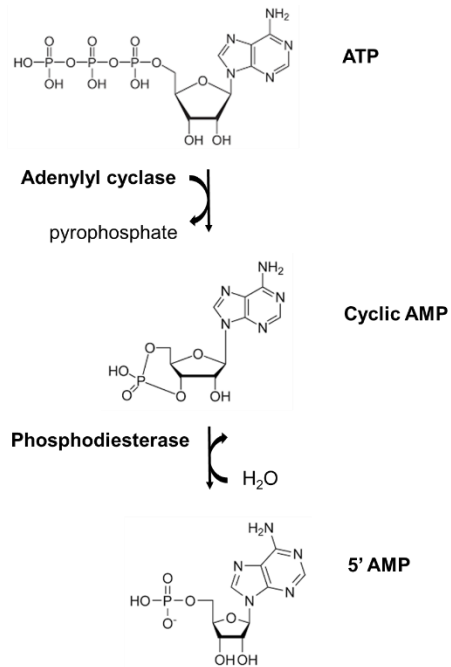


Figure 1.2. Characteristics of mammalian PDEs. A) Mammalian PDE families subdivided according to substrate specificity. cAMP specific PDEs are in the pink circle, cGMP specific PDEs are in the blue circle and dual PDEs are in both circles. B) cAMP specific PDEs are involved in several biological processes (from left to right: cognition and memory, endocrine function, heart and respiratory tract function, inflammation, cell proliferation and differentiation), implicating in many potential therapeutics (Images found using Google search engine).

dimerization is important for stabilization of PDE4 long forms and the regulation of its activity via post-translational modifications, but not required for high-affinity rolipram binding (Richter and Conti, 2004).

According to the PDE4B2 crystal structure, the catalytic domain structure is composed of residues 152 to 487. The catalytic site is comprised of three functional groups of residues that are responsible for the following: hydrolysis, nucleotide recognition and hydrophobic clamp (Figure 1.4a) (Houslay et al., 2005). Crystal structure studies of PDE4 enzymes have facilitated our understanding of residues involved in substrate binding, conformational changes that are essential for PDE4 catalytic activity, and the residues involved in binding of PDE4 inhibitors (Figure 1.4b) (Xu et al., 2000, Conti et al., 2003, Houslay et al., 2005). These studies also have allowed drug design targeting PDEs as a therapeutic approach for many biological disorders. Many PDE small molecule inhibitors have been the subjects of clinical trials (Table 1.2).

1.4.2 Tissue distribution and Biological roles of PD4B2 and PDE4B3

The PDE4 mRNAs have a ubiquitous tissue distribution (Lerner and Epstein, 2006; Beavo and Conti, 2007). They can be found in cardiovascular tissue, smooth muscles and inflammatory cells, muscle and brain (Keravis and Lugnier, 2012). More specifically, PDE4B subtypes are localized in human immune and inflammatory cells, consistent with their immune response and inflammatory roles (Keravis and Lugnier, 2012) and they are predominantly found in human monocytes and neutrophils (Wang et al., 1999). Moreover, both PDE4B and PDE4D are expressed in cardiomyocytes of rodents and humans (Maurice et al., 2003) with PDE4D3 being highly expressed in the heart muscle (Houslay et al., 2007). In addition, PDE4D mRNA is highly expressed in the mural granulosa cells, cells from female reproductive system (Tsafiriri et al., 1996).

PDE4 proteins are found at relatively high concentrations in the brain (Richter et al., 2013) where they play a role in cognition (Richter et al., 2013) as the main PDE involved in learning and memory

(Keravis and Lugnier, 2012). As such, PDE4B and D mutations are associated with anxiety behavior and in neurogenesis along with depression and memory, respectively (Titus, et al., 2014). Therefore, PDE4 proteins are seen as a good pharmacological target for the treatment of conditions affecting a myriad of biological processes, such as: immune and inflammation, myocardium and smooth muscle contractility, angiogenesis, and cognition, among others (Figure 1.2b) (Ricciarelli and Fedele, 2015; Richter et al., 2013, Maurice et al., 2014; Houslay et al., 2005). However, the broad tissue distribution of the PDE4 family suggests the likelihood of side effects, as the emetic response associated with PDE4D inhibition (Robichaud, 2002).

1.4.3 PDE4 inhibitors

PDE4 has been targeted for drug development for the treatment of many biological disorders mentioned in the previous section (Houslay et al., 2005). The difficulty in developing PDE inhibitors lies in generating effectiveness against isoforms that share a conserved catalytic domain sequence and in understanding of the LARBS and HARBS conformational states (Wang et al., 2007). These characteristics create a challenge to generate selective PDE4 inhibitors for specific isoforms that can decrease or abolish side effects (Wang et al., 2007, Xu et al., 2000). However, most PDE4 compounds do not show subtype selectivity (Wang et al., 2007).

As already mentioned, in recent years, crystal structure studies have allowed scientists to better understand amino acid interactions involved in the PDE activity, which, in turn, have stimulated the development of drug design studies for therapeutic approaches. These studies aim to identify compounds that either interact with the catalytic domain directly or, indirectly, via allosteric sites (Wang et al., 2007; Card et al., 2004). Most inhibitors, but not all, bind to enzymes at the active site, competing directly with the substrate (Copeland, 2000). However, other inhibitors are allosteric effectors, binding to a distinct site other than the active site, inhibiting the enzyme in a non-competitive manner by promoting a conformational change in the enzyme (Copeland, 2000).

Table 1.1 Properties of PDE enzymes*

PDE family	Genes	No of isoforms	Substrate specificity	Km in μM (cAMP)	Km in μM (cGMP)	Tissue distribution	Regulatory properties	Commonly used compounds
PDE1	PDE1A-C	~21	Dual-specificity	0.3–124	0.6–6	Heart, brain, lung, smooth muscle	Ca ²⁺ /calmodulin-stimulated	Nimodipine, IC86340, IC224, IC295, dioclein
PDE2	PDE2A	3	Dual-specificity	15	15	Adrenal gland, heart, lung, liverplatelets, endothelial cells	cGMP-stimulated	EHNA, BAY-60-7750, PDP, IC933, oxindole, ND7001
PDE3	PDE3A-B	4	Dual-specificity	0.2–0.4	0.02-0.3	Heart, smooth muscle, liver, platelets, adipocytes, immunocytes	cAMP-selective, cGMP-inhibited	Cilostamide, milrinone, siguazodan, cilostazol
PDE4	PDE4A-D	>20	cAMP	1-10	300	Brain, Sertolli cells, kidney, liver, heart, smooth muscle, lung, endothelial cells, immunocytes	cAMP-specific, cGMP-insensitive	Rolipram, roflumilast, cilomast, NCS 613
PDE5	PDE5A	3	cGMP	150	1	Brain, Sertolli cells, kidney, liver, heart, smooth muscle, lung, endothelial cells, immunocytes	cGMP-specific	Zaprinast, DMPPO, sildenafil, tadalafil, vardenafil
PDE6	PDE6A-C	-	cGMP	2000	60	Photoreceptors, pineal gland, Lung	cGMP-specific, transducin activated	Zaprinast, DMPPO, sildenafil, vardenafil
PDE7	PDE7A-B	~5	cAMP	0.03-0.2	1000	Skeletal muscle, heart, kidney, brain, pancreas, T lymphocytes	cAMP-specific, high-affinity rolipram-insensitive	BRL 50481, IC242, ASB16165
PDE8	PDE8A-B	9	cAMP	0.06	N/A	Testes, eye, liver, skeletal muscle, heart, kidney, ovary, brain, T lymphocytes, thyroid	cAMP-selective, IBMX insensitive rolipram-insensitive	PF-04957325
PDE9	PDE9A	20	cGMP	N/A	0.07-0.17	Kidney, liver, lung, brain	cGMP-specific, IBMX insensitive	BAY-73–6691, PF-04447943
PDE10	PDE10A	18	Dual-specificity	0.2-1	13-14	Testes, brain, thyroid	cGMP-sensitive, cAMP-selective	Papaverine, TP-10, MP-10
PDE11	PDE11A	4	Dual-specificity	0.5-2	0.3-1	Skeletal muscle, prostate, pituitary gland, liver, heart	cGMP-sensitive, dual specificity	None selective

*Modified from Keravis and Lugnier (2012) and Bender and Beavo (2006)

Figure 1.3. PDE4 Isoforms and regulatory domains. The PDE4 family is composed of four genes (*PDE4A-D*). A) Each gene has multiple variants: at least, 7 PDE4A variants, 4 PDE4B variants, 7 PDE4C variants and 11 PDE4D variants. Asterisks indicate the PDE4 isoforms addressed in this study (PDE4B2, super short form; PDE4D2, short form; and PDE4D3, long form). B) The domains represented as barrels connected by wires indicating linker regions. Long red barrels correspond to the catalytic domains and short red barrels correspond to the conserved C-termini; Blue circles represent phosphorylation sites for protein kinase A (PKA) and extracellular signal-regulated kinase 2 (ERK2). The lengths of PDE4 variants are distinguished by the complete or partial presence of the UCR1/UCR2 regions (in pink and purple barrels) respectively, and UCR domain regions mediating dimerization are represented by a black rectangle (Modified from Houslay et al., 2005).

Figure 1.3 PDE4 Isoforms and regulatory domains

A

PDE4 genes

PDE4 variants

PDE4 A

PDE4A1
PDE4A4
PDE4A5
PDE4A6
PDE4A7
PDE4A8
PDE4A10

PDE4 B

PDE4B1
PDE4B2 *
PDE4B3
PDE4B4

PDE4 C

PDE4C1
PDE4C2
PDE4C3
PDE4C4
PDE4C5
PDE4C6
PDE4C7

PDE4 D

PDE4D1
PDE4D2 *
PDE4D3 *
PDE4D4
PDE4D5
PDE4D6
PDE4D7
PDE4D8
PDE4D9
PDE4D10
PDE4D11

B

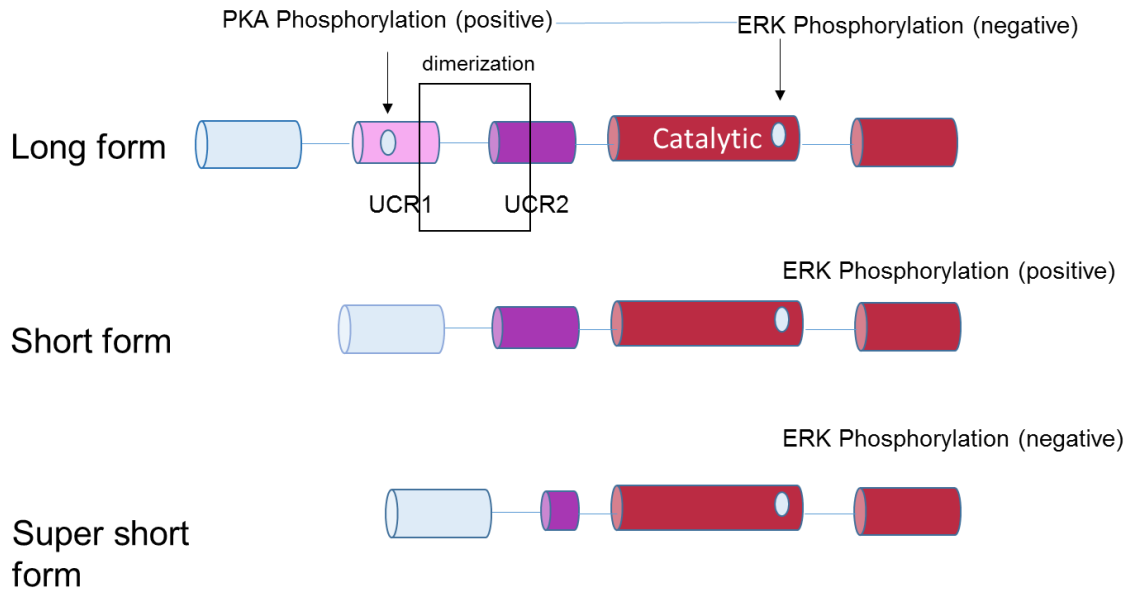
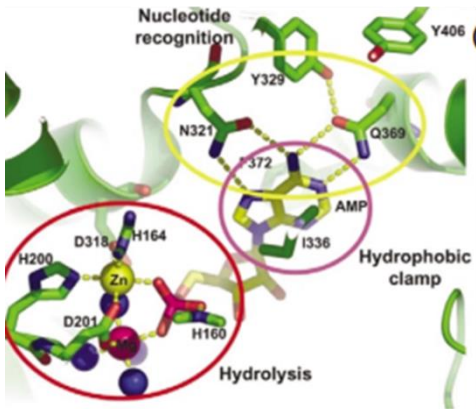


Figure 1.4. PDE4B2 crystal structure and residue interactions. A) Three groups involved in aspects of PDE function: hydrolysis, nucleotide recognition and hydrophobic clamp (image belongs to Houslay et al., 2005) B) PDE4B2 catalytic domain (residues from 152 to 487) is formed by 17 α -helices that are divided in three groups, as follows: the yellow group (residues 152 to 274) located in the C-terminus, the middle group in green (residues 275 to 347 and blue group (residues 348 to 487) located in the N-terminus domain (Modified from Xu et al., 2000).

Figure 1.4 PDE4B2 crystal structure and residue interactions

A



B

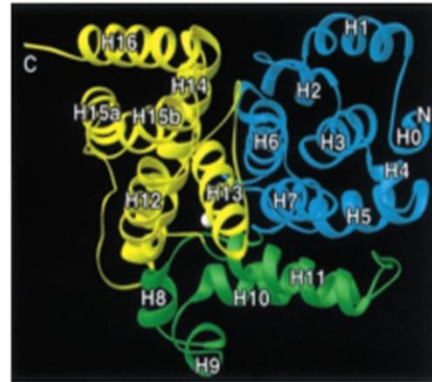


Table 1.2. PDE4 inhibitors currently in clinical trials

Agents (Sponsors)	Indication	Status	ClinicalTrials.gov Identifiers
Rolipram (NIH)	Depression	Phase I	NCT00369798
Rolipram (GlaxoSmithKline)	Huntington's disease	Phase I	NCT01602900
GSK356278 (GlaxoSmithKline)	Huntington's disease	Phase I	NCT01602900
ASP9831 (Astellas Pharma)	Non-alcoholic steatohepatitis	Phase II	NCT00668070
GSK256066 (GlaxoSmithKline)	Rhinitis	Phase II	NCT00464568
CHF6001 (Chiesi Pharmaceutici)	Asthma; COPD	Phase II	NCT01730404
Apremilast (Celgene)	Ankylosing spondyloarthritis	Phase III	NCT01583374
Apremilast (Celgene)	Acne	Phase II	NCT01074502
MK0952 (Merck Sharp & Dohme)	Alzheimer's disease	Phase II	NCT00362024
CHF6001 (Chiesi Pharmaceutici)	COPD	Phase II	NCT01730404
Roflumilast (Takeda)	Atopic dermatitis	Phase II	NCT01856764
Roflumilast (Takeda)	Dementia	Phase II	NCT01433666
Roflumilast (The National heart, Lung and Blood Institute)	Obesity	Phase II	NCT01862029

Modified from Maurice et al., 2014 (not all PDE4 inhibitors are listed)

There are different ways to develop new PDE inhibitors. The first approach is to generate allosteric modulators. To date, researchers have successfully used this approach to target many GPCRs for treatment of CNS disorders (Conn et al., 2009) or to inhibit PDE4D, the PDE4 subtype involved in several CNS conditions, with the ability to reduced emetic response by determining the emetic threshold in three species via oral administration (Burgin et al., 2010). In addition, inhibitors have been computationally designed based on co-crystal structure of PDE4 enzymes bound to inhibitors (Houslay et al, 2005). The second approach is through chemical screens using either *in silico* (Card et al., 2004) or cell-based assays (Ceyhan et al., 2012; Demirbas, et al., 2010). Recently, several studies have tested compounds targeting more than one PDE family, such as PDE4 and PDE7 that are both cAMP-specific PDE involved in inflammatory response (Maurice et al., 2014). A third approach has been used to identify compounds that produce synergistic effects by either inhaling the inhibitors or developing antisense oligonucleotides targeting specific PDEs (Maurice et al., 2014). For instance, treatment of combined PDE7A and PDE4 family using specific antisense oligonucleotides (AON) effectively reduced the inflammatory response to sub-acute smoke-induced model exposure in mice correlating reduction of neutrophils recruitment with reduction of mRNA levels of PDEs tested, and reduction of chemokine levels in human broncho-epithelial cells *in vitro* (Fortin et al., 2009). Our lab has identified a dual-specificity PDE4/7 inhibitor (BC54) that seems less active against PDE4D (the PDE4D responsible for emesis) than it is against PDE4A and PDE4B in our yeast assay, although it displays similar potency to all three subtypes *in vitro* (Hoffman laboratory, unpublished data). Thus, BC54 may be able to elicit a greater anti-inflammatory response with reduced side effects. Chapter 2 of my thesis describes a genetic approach to examine the interaction of BC54 with PDE4B, while Appendix B examines the effectiveness of BC54 derivatives as a way of investigating functional groups of the compound.

1.5 Clinical trials of PDE4 inhibitors

Over the years, a large number of trials for PDE4 enzymes have been conducted (US National Institutes of Health, 2015). These involve compounds that fall into four main chemical classes: catechol, xanthane, pyrozole and purine analogs (Figure 1.5a) (Houslay et al., 2005). The first generation of PDE inhibitor studies were carried out with non-selective PDE inhibitors such as theophylline, a weak PDE4 inhibitor that is a xanthine derivative (Houslay et al., 2005). It has been tested for asthma and chronic obstructive pulmonary disease (COPD) treatment along with bronchodilators. However, it produces too many side effects to be used in these conditions (Spina, 2008).

Rolipram, a first generation PDE4 inhibitor, is selective PDE inhibitor (Castro et al., 2005). Rolipram has been used as a model to generate selective PDE4 inhibitors (Houslay et al., 2005). Over the years, many clinical trials were conducted testing second generation PDE4 inhibitors (Figure 1.5b). The second generation of PDE4 inhibitors were developed following the discovery of rolipram and its distinct binding affinity to the long (IC_{50} varying from 1 to 50 nM) or short forms (IC_{50} varying from 0.1 to 1 μ M) of PDE4 (Houslay and Adams, 2003).

Early studies in rats and humans identified rolipram as a PDE4 inhibitor that promoted antidepressant and behavioral effects (Wachtel, 1982; Wachtel, 1983; Zeller et al., 1984). In 2005, clinical trials for asthma tested many compounds, such as: rolipram, zardaverine, filamilast, piclamilast, tetomilast among others. But many of these compounds have been discontinued due to side effects or lack of effectiveness (Houslay et al., 2005). After that, compounds that appear to be less emetic were developed for asthma and entered either Phase I (tofamilast, an indazole or ibudilast; and pyrazolopyridine, used for asthma, but also tested for multiple sclerosis trials) or Phase II trials (YM-976, pyridopyrimidinone, and liramilast, but both were discontinued possibly due to emetic effects) (Houslay et al., 2005).

Although rolipram causes emesis, it has shown some promise, but it is not a good drug to treat conditions like depression and Huntington's disease (Maurice et al., 2014). It inhibits the production of TNF-alpha, a pro-inflammatory cytokine produced by monocytes, macrophages and

T cells (Jimenez et al., 2001). In recent years, Roflumilast, a catechol inhibitor that resembles rolipram, has been approved for the treatment of COPD (FDA, 2011). In a recent clinical trial, roflumilast was tested in 36 obese women w/ polycystic ovary syndrome (PCOS) and the combined treatment of roflumilast and metformin, an antidiabetic medication, promoted body weight reduction via fat mass loss (Jensterle et al., 2014).

The latest generation of PDE4 inhibitors, apremilast, seemed promising for trials for autoimmune conditions, presenting fast absorption (Kumar et al., 2013). Inhibition of PDE4 by apremilast has promoted TNF α inhibition in human cells (Harrison, 2013) and was approved by the FDA for psoriatic arthritis last year (FDA, 2014).

Currently, there are many ongoing trials testing compounds that target PDE4 enzymes for different pathologies (Table 1.2) (Maurice et al., 2014). For PDE4 isoenzymes targeted for therapeutics, the conditions range from autoimmune disorders like psoriasis, apondylitis and arthritis (Kumar et al., 2013; Loukides et al., 2013; Castro et al., 2005; Ariga et al, 2004), fertility (Jin et al, 1999); asthma and COPD (Fabbri et al., 2009; Schalkwyk, et al, 2005), airway smooth muscle contraction (Mehats et al, 2003), CNS conditions (Houslay et al., 2005), and cancer (Lin et al., 2013).

Although many PDE4 inhibitors have been designed and placed in clinical trials, there have been a wide range of side effects associated to their use. The common side effects are nausea, headache and emesis (Kumar et al., 2013; Spina, 2008; Calverley et al., 2007; Houslay et al., 2005; Lipworth, 2005). Therefore, there is still a need to discover new PDE4 inhibitors that can be both selective and potent, yet produce relatively few side effects.

1.6 Phosphodiesterase 7 (PDE7) family

The PDE7 family consists of two genes (*PDE7A* and *PDE7B*). Each *PDE7* gene has three splice variants (Conti and Beavo, 2007). In addition, *PDE7B* gene codes for an additional variant (Keravis and Lugnier, 2012). To date, there are no known regulatory sites in the N-termini of PDE7 proteins (Keravis and Lugnier, 2012). The PDE7 proteins have wide tissue distribution and subcellular

location, being expressed in lymphocytes and proinflammatory cells (PDE7A1), skeletal and cardiac muscle (PDE7A2), striatal neurons (PDE7B1) (Keravis and Lugnier, 2012). This tissue specific expression and localization has suggested that PDE7A1 has immune and inflammatory roles (Giembycz and Smith, 2006; Lee et al., 2002) and PDE7B1 may be involved in cognition and memory (Sasaki et al., 2004).

Expression of PDE7A is required during regulation of CD3- and CD8- for T cell activation and IL-2 production (Soderling and Beavo, 2000; Linsong et al., 1999). PDE7B splice variants (PDE7B1, PDE7B2 and PDE7B3) are also expressed in several tissues including brain, heart, skeletal muscle and pancreas (Sasaki et al., 2002; Hetman et al., 2000; Sasaki et al., 2000) and PDE7B1 transcript was the only one activated by agonist response in striatal neurons via the cAMP pathway, suggesting a role in memory function (Sasaki et al., 2004). Overall, there is a 70% homology between PDE7A and PDE7B within the 270 amino acids in the catalytic domain (Gardner et al., 2000).

1.6.1 Tissue distribution and biological roles of PDE7

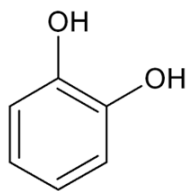
The PDE7 family is expressed in several tissues including brain, heart and muscle. Inhibiting both PDE7A and PDE4 family using specific antisense oligonucleotides (AON) effectively reduced the inflammatory response in a sub-acute smoke-induced exposure model in mice (Fortin et al., 2009). Inhibition of PDE7A enzyme reduced spinal cord tissue injury and inflammation (Paterniti et al., 2011). Furthermore, PDE7B expression is increased in B cells during chronic lymphocytic leukemia (CLL) and use of PDE7 inhibitor along with dual PDE4/7 inhibitor appears to decrease leukemic cells at concentrations that have low toxicity effects in normal B cells (Zhang et al., 2008). In disease studies, understanding the functions of PDE7 enzymes has the potential to develop good therapeutic targets.

However, there is a lack of selective inhibitors for PDE7 enzymes (Maurice et al., 2003). There are a couple of PDE7 inhibitors currently undergoing clinical trials (Maurice et al., 2014) (Table 1.2)

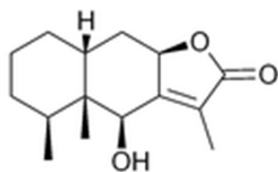
Figure 1.5. Structure of PDE4 inhibitors. A) There are four main compound classes used in the design of PDE4 inhibitors, as follows: catechol, xanthane, pyrazole, purine analogs (Images modified from Wikipedia) B) Many PDE4 inhibitors have been used for clinical trials: Rolipram, Zarvaderine, cilomilast roflumilast, Piclamilast, are second generation of PDE4 inhibitors and Theophylline, a non-selective first generation PDE4 inhibitor (Modified from Houslay et al., 2005).

Figure 1.5 Structure of PDE4 inhibitors

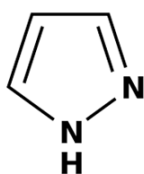
A



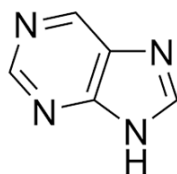
Catechol



Xanthane

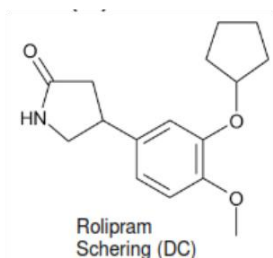


Pyrozole

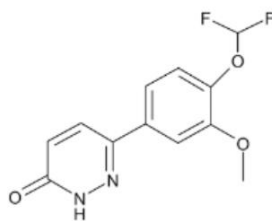


Purine

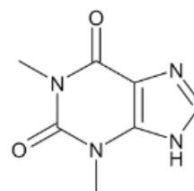
B



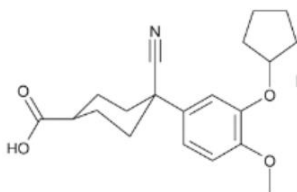
Rolipram
Schering (DC)



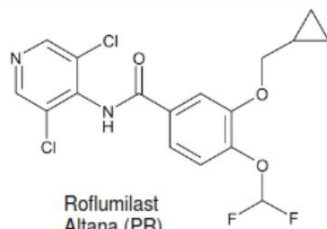
Zardaverine
Byk Gulden (DC)



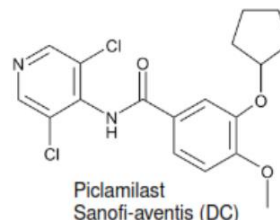
Theophylline
Elan (LC)



Cilomilast
GSK (PR)



Roflumilast
Altana (PR)



Piclamilast
Sanofi-aventis (DC)

and, thus far, there is only one commercially-available compound BRL50481 (Smith et al, 2004), which it is not very active against PDE7B (Alaamery et al., 2010). A previous study from our lab identified compounds that inhibit PDE7B, but the mechanism of inhibition is not completely understood due to a lack of PDE7B crystal structure characterization (Alaamery et al., 2010). Moreover, additional data suggest that some of these compounds may bind allosterically to PDE enzymes, instead of blocking the cAMP binding site (Alaamery et al., 2010). Therefore, it is reasonable to think that PDE7s can be regulated at another site other than the cAMP binding site. As mentioned above, one idea in drug development is to target both PDE4 and PDE7 proteins (Maurice et al., 2014). These proteins are expressed in inflammatory cells (Maurice et al., 2014; Keravis and Lugnier, 2012) and treatment of both PDE4 and PDE7 have reduced inflammation in many studies (Giembycz and Newton, 2011; Tenor et al., 2011; Fortin et al., 2009; Smith et al., 2004), suggesting a possible synergistic effect in the reduction of inflammation (Maurice et al., 2014). Therefore, a dual PDE4/7 inhibition approach could be a good therapeutic treatment for inflammatory conditions like COPD and asthma. The dual PDE4/7 inhibitor BC54 that is the focus of Chapter 2 of this thesis could possibly generate a greater anti-inflammatory response before reaching levels that cause emesis, however more needs to be known about its mechanism of action to help guide its development from a promising lead compound to an actual drug (Section 1.8.1).

1.7 Mammalian adenylyl cyclases

Adenylyl cyclases (ACs) and guanylyl cyclases (GCs) are enzymes responsible for the conversion of adenosine triphosphate (ATP) or guanosine triphosphate (GTP) to cAMP and cGMP, respectively, with release of pyrophosphate (Hartwig et al., 2014; Kamenetsky et al., 2006). ACs along with GCs comprise six distinct classes of proteins that are evolutionarily defined by sequence homology within their catalytic domain (Kamenetsky et al., 2006). In mammalian cells, there are 10 isoforms of AC enzymes and they belong to nucleotidyl cyclase family class III (Nicol and Gaspar, 2014; Kamenetsky et al., 2006). AC isoforms are encoded by ten different genes (Table

1.3) (Hanoune et al., 1997). These isoforms are divided in two types: AC1 to AC9 are transmembrane adenylyl cyclases (tmACs), while the tenth AC is a soluble adenylyl cyclase, known as sAC (Kamanetsky et al., 2006).

The activity of mammalian ACs can be regulated at different levels, such as: at post-translational modifications; at the translational level by either covalent modifications or interactions with small molecules that stimulate or inhibit AC activity (Table 1.3) or other proteins and at the transcriptional level or via mRNA stability (Kamanetsky et al., 2006). sAC, encoded by the *ADCY10* gene, is sensitive to variation of ATP levels and activated synergistically by calcium and bicarbonate (Ho et al, 2010) through decreasing the K_m for ATP and increasing sAC's V_{max} , respectively (Gancedo, 2013).

In contrast to sAC modulation, the activity of tmACs is regulated by heterotrimeric G proteins and all tmACs are stimulated by the GNAS1 $G_s\alpha$ protein (Table 1.3) (Nicol and Gaspar, 2014; Gancedo, 2013). Moreover, tmACs can be subclassified according to other regulatory responses, as follows: Group 1 (AC1, AC3, AC8) and group 2 (AC5 and AC6) are either stimulated or inhibited by Ca^{++} and calmodulin, respectively; Group 3 (AC2, AC4 and AC7) is stimulated by protein kinase C (PKC) and $\beta\gamma$ activation; Group (AC9), which is stimulated by $\beta\gamma$ subunit and it is calcium insensitive; $G_i\alpha$ subunits inhibit AC1, AC5 and AC6 (Table 1.3) (Nicol and Gaspar, 2014; Hanoune and Defer, 2001).

The AC isoforms are expressed in many different tissues (Table 1.4) (Sunahara et al, 1996), their distinct physiological role and pharmacological properties (Hanoune and Defer, 2001). sAC is expressed in various tissues in the cytoplasm, as well as in the mitochondria and in the nuclei cells, which reflects the variety of physiological functions, such as: apoptosis, sperm motility, and mitochondrial respiration (Gancedo, 2013; Kamenetsky et al., 2006; Hanoune et al., 1997). All tmACs are expressed in the CNS, except for AC7 and AC4, where the latter AC has its expression restricted to blood vessels in CNS (Table 1.4) (Nicol and Gaspar, 2014; Hanoune and Defer, 2001). AC1, AC2 and AC9 seem to be the most abundant in the brain (Hanoune and Defer, 2001).

In mammals, AC1 through AC9 are transmembrane proteins that are composed of 1064 to 1353 amino acids with mass varying from 120-150 kDa (Hanoune et al., 1997). The tmAC structure consists of a short N-terminus, two sets of hydrophobic repeats of six transmembrane domains and two cytoplasmic catalytic domains (CD1 ad CD2) that heterodimerize to form an active AC (Figure 1.1) (Kamenetsky et al., 2006). The cytoplasmic regions responsible for the catalytic activity share 50-70% amino acid sequence identity and the possible site for regulation (Steebhorn, 2014; Hanoune and Defer, 2001).

The distinct tissue distribution and structure of tmACs makes it difficult to develop inhibitors to target individual ACs. For instance, many studies have focused on a pharmacological approach to discover drugs that target AC5, the most abundant isoform in the cardiac tissue, as an alternative therapy for heart disease (Vatner et al., 2013; Okumura, et al., 2009). However, it has been difficult to identify AC5 inhibitors mainly due to compound membrane impermeability (Ho et al., 2010). Therefore, new screens are needed for AC inhibitors that are able to get into cells.

1.8 Use of a fission yeast cell –based platform to study mammalian proteins

S. pombe and *S. cerevisiae* are unicellular eukaryotes that possess highly conserved protein-encoding genes, some of which are homologs to human disease loci (Wood et al., 2012; Wood et al., 2002). They are both useful for the expression of biologically-active mammalian proteins. Therefore, they have served as important model organisms for the study of many biological processes conserved in humans (Demirbas et al., 2011a; Bahler and Wood, 2004; Hayles and Nurse, 1992). Both yeasts have been used to study PDE genes by cloning and expressing mammalian genes to identify and understand mammalian protein function and changes in its activity through mutagenesis (Atienza and Colicelli, 1998; Pillai et al., 1993; Nikawa et al., 1987b). This approach was used to study the human p53 protein expressed in *S. pombe* (Bischoff et al., 1992), facilitating the isolation of loss of function mutations as a way of understanding the functional domains of this protein. In past studies, *S. cerevisiae* was found to express two PDE proteins, Pde1 (low affinity)

and Pde2 (high affinity) enzymes (Nikawa et al., 1987a). In addition, strains carrying deletions of both PDE genes, showed increased intracellular cAMP levels, which interfered with the normal response to nutrient starvation and conferred heat-shock sensitivity in stationary phase cells (Michaeli et al., 1993; Colicelli et al., 1991). Expression of a mammalian PDE gene restored resistance to heat shock (Michaeli et al., 1993; Colicelli et al., 1991; Colicelli et al., 1989). Moreover, rolipram, prevented the heterologously-expressed PDE4B enzyme from conferring survival to heat shock (Pillai et al., 1993). This study demonstrated that regulation of PDE activity by specific PDE inhibitors can be assessed in yeast cells.

1.8.1 *S. pombe* glucose/cAMP signaling pathway

In unicellular organisms, nutrient sensing mechanisms are important for growth and sexual development (Hoffman, 2005b). In both *Schizosaccharomyces pombe* and *Saccharomyces cerevisiae*, a glucose sensing mechanism promotes a transient cAMP response that activates the cAMP-dependent protein kinase (PKA) (Hoffman, 2005). In fission yeast, the glucose/cAMP pathway and requires at least seven genes to trigger adenylyl cyclase activation (Hoffman, 2005a; Hoffman, 2005b).

Most of the genes of the *S. pombe* glucose/ cAMP signaling pathway were identified in a screen for mutants that are defective in transcriptional regulation of the *fbp1* gene, encoding fructose-1,6-bisphosphatase (Hoffman and Winston 1990). Growth phenotypes used to identify mutants in the cAMP/PKA pathway were conferred by an *fbp1-ura4* construct (Hoffman and Winston, 1991), a PKA-repressed reporter driving *ura4* expression, which produces reciprocal growth patterns on media containing 5FOA (5-fluor-ototic acid) or lacking uracil (de Medeiros et al., 2013). Mutations that conferred constitutive expression of this reporter affected proteins involved in glucose/cAMP signaling (Hoffman and Winston, 1991), such as: Git3 (GPCR) (Welton and Hoffman, 2000), Gpa2 (G α subunit) (Landry et al., 2000; Isshiki et al., 1992), Git5 (G β subunit) and Git11 (G γ subunit) (Landry and Hoffman, 2001; Landry et al., 2000), Git2/Cyr1 (adenylyl cyclase; Hoffman and

Winston, 1991), Git1 (adenylyl cyclase binding protein) (Kao et al., 2006) and Pka1 (PKA catalytic subunit) (Jin et al., 1995). In addition, negative PKA regulators were identified in genetic screens for suppressors using this system. For example, a strain carrying a mutation of the *cgs2* gene, the only fission yeast PDE gene, suppressed an activation-defective form of adenylyl cyclase (*git2*) (Wang et al., 2005). As demonstrated by these studies, the *fbp1-ura4* reporter can be used to identify mutants that confer growth in medium containing 5FOA or lacking uracil by either stimulating or decreasing PKA activity, respectively. The successful use of a PKA repressed reporter in genetic screens allowed our lab to develop a platform to screen for small molecule inhibitors of PDEs using genetically-engineered strains that express heterologous PDEs in place of the *S. pombe* Cgs2 PDE (Demirbas et al., 2013; Ceyhan et al., 2012; Demirbas et al., 2011; Ivey et al., 2008; Alaamery et al., 2010). The *fbp1-ura4* reporter was also used to screen for PDE mutants with either altered behavior in the presence of PDE inhibitors or altered substrate specificity (de Medeiros et al., 2013). While work by our lab and others have generated a collection of selective PDE inhibitors, there is a near absence of small molecule PDE activators that can be beneficial as therapeutics and as chemical probes to expand our understanding of PDEs' biological roles. In recent years, our lab has developed a new cell-based assay using a GFP reporter that is better-suited for identifying compounds that reduce PKA activity, which would include PDE activators or AC and GNAS1 ($G\alpha_s$ in humans) inhibitors (de Medeiros et al., 2015).

1.9 PKA in *S. pombe*

Protein kinase A (PKA) is a serine/threonine kinase that is activated by cAMP (Søberg et al., 2013). Once PKA is in its active state it can phosphorylate various proteins, such as: regulatory enzymes, ion channels and transcription factors (Gancedo, 2013). PKA activation occurs by binding of cAMP to the regulatory subunits (Gancedo, 2013). In mammals, PKA is a heterotetramer comprised of two regulatory and two catalytic domains and PKA is inactive in its heterotetrameric form (Stratakis, 2012).

Table 1.3. Regulation of mammalian AC isoforms and Genome localization

Isoforms	Stimulation by	Inhibition by	Chromosome	
AC1	G _s α	PKC*	G _i α Gβγ CaMK	7p12
AC2	G _s α Gβγ	PKC		5p15
AC3	G _s α - Ca ⁺⁺ / calmodulin*	PKC	Gβγ CaMK	2p22-24
AC4	G _s α Gβγ*	PKC*		14q11.2
AC5	G _s α Gβγ*	PKC	G _i α Ca ⁺⁺ PKA	3q13.2-q21
AC6	G _s α Gβγ*		G _i α Ca ⁺⁺ PKA PKC	12q12-13
AC7	G _s α Gβγ	PKC		16q12-13
AC8	G _s α Ca ⁺⁺ / calmodulin		Gβγ	8q24
AC9	G _s α		Calcineurin PKC	16p13.3
		CaMK*		
sAC	G _s α - Ca ⁺⁺ / calmodulin			1q24

*Indicates inconclusive data. Table modified from Nicol and Gaspar (2014), Gancedo (2013) and Hanoune et al. (1997)

Table 1.4. Mammalian AC tissue distribution and biological function*

AC isoform	Tissue distribution	Role
AC1	Neurons , adrenal gland (medulla)	Learning and memory, circadian rhythm, etc
AC2	Brain, skeletal muscle, lung , heart	Synaptic plasticity, cell proliferation arrest
AC3	Brain, olfactory epithelium , male germ cells, pancreas	Odorant stimulation
AC4	Blood vessels (brain) , heart, kidney, liver, lung, uterus	?
AC5	Brain, heart , kidney, liver, lung, uterus	Heart, metabolism, aging
AC6	Various	Cell proliferation
AC7	Brain, platelets , others	Ethanol dependency
AC8	Brain, lung , testis, adrenal, heart, uterus	Synaptic plasticity, drug dependency
AC9	Brain, skeletal muscle , others	
sAC	Testis , all tissues	

*Data collected from Hanoune and Defer, 2001. Tissues in bold represent the tissue in which the AC isoform has higher expression levels.

In *S. pombe*, the regulatory and catalytic subunits of PKA are encoded by *cgs1* and *pkal* (Stiefel et al., 2004; Hoffman, 2005b). PKA activation occurs when the cAMP pathway produces a cAMP response that leads to the binding of cAMP to Cgs1 followed by release of Cgs1 from Pka1 (Hoffman, 2005b). The use of null mutant alleles involved in cAMP pathway facilitated our understanding of the roles of PKA in fission yeast. Studies assessing growth in KCl (Stiefel et al., 2004), entry into stationary phase and mating have associated these processes with PKA activity (Mochizuki and Yamamoto, 1992; DeVoti et al., 1991). Furthermore, Maeda and colleagues (1994) reported a delay in spore germination by disruption of *pkal*⁺. It was also confirmed that the cAMP/PKA signaling pathway regulates spore germination (Hatanaka and Shimoda, 2001).

Nutritional signaling of glucose via the cAMP pathway represses sexual development in fission yeast, as was already mentioned (section 1.8). Deletions of *cyr1/git2* (Stiefel et al., 2004; Kawakumai et al., 1991), *pkal* (Maeda et al., 1994), *git3*, *gpa2*, *git5*, *git11*, and *git1* (Welton and Hoffman, 2000; Landry and Hoffman, 2001; Kao and Hoffman, 2006) derepress sexual development. In addition, *pkal* disruption causes a delay in vegetative growth, but is not lethal (Maeda et al., 1994). Conversely, deletions in the *cgs2/pde1* inhibit mating and stationary phase entry (Mochizuki and Yamamoto, 1992; DeVoti et al., 1991). Furthermore, overexpression of the *cyr1* gene results in elongated cells with a sterile mating phenotype similarly seen in cells expressing high cAMP levels (Kawakumai et al., 1991).

In *S. pombe*, the transcription of *pkal* and *cgs1* are induced under a variety of stress responses tested (Chen et al., 2003). In addition, disruption of the *git2* adenylyl cyclase gene in yeast cells confers KCl-growth sensitivity that is suppressed by mutations in *cgs1* that restore PKA activity (Stiefel et al., 2004). Finally, in strains expressing the *fbp1-ura4* reporter, elevated PKA activity is associated with a failure to grow in SC-Ura medium and the ability to grow in 5FOA medium (de Medeiros et al., 2013). The phenotypes associated with PKA activity are summarized in Table 1.5.

1.10 Aims of this dissertation

This dissertation is comprised of two distinct studies with the objective to expand the tools for the understanding of the modulation of the cAMP regulators. In the first study, the aim is to characterize a novel dual specificity PDE4/7 inhibitor, previously identified in a screen carried out by our lab. To accomplish this goal, I have developed a genetic screen that allowed me to identify mutations that confer compound-resistance to PDE genes. In this study, growth in SC-Ura medium (in Chapter 3) was used to identify mutations that confer compound resistance to PDE gene (Figure 1.6): The discovery of PDE4B2 mutant alleles with altered behavior in the presence of dual specificity PDE4/7 inhibitor will allow us to understand which amino acids are essential for PDE activity and its modulation. The second aim of this study was to develop a chemical screen that can identify small molecules that reduce PKA activity by activating PDEs or inhibiting either AC or GNAS1. For the second study, I have carried out a 10,000 HTS to detect PDE4D3 activators as a proof of concept. Based on the lessons learned from that screen, I carried out a larger HTS using two yeast strains that allowed me to target five mammalian proteins. The screening strain expresses PDE4D3 and AC5, while the counter-screen strain expresses PDE7B, AC1 and GNAS1. The identification of PDE activators and or AC/GNAS1 inhibitors will provide us with new research tools to advance our understanding of cAMP-regulated processes and can lead to the development of new therapeutics. AC5 or PDE4D3 are enzymes are expressed in various tissues and are seen is good drug targets for many diseases like heart and CNS diseases, respectively.

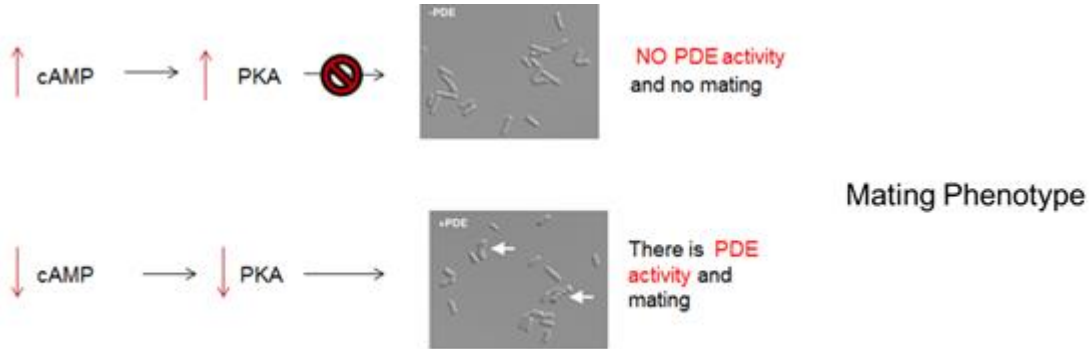
Table 1.5. Phenotypes associated with PKA activity

Low PKA activity	High PKA activity
Mating	Absence of mating
Short cells -10 μm long	Long cells - 14 μm long
Growth in SC-ura medium	Failure to grow in SC-ura medium
Entry in stationary phase	Failure to enter stationary phase
KCl sensitivity	KCl resistance

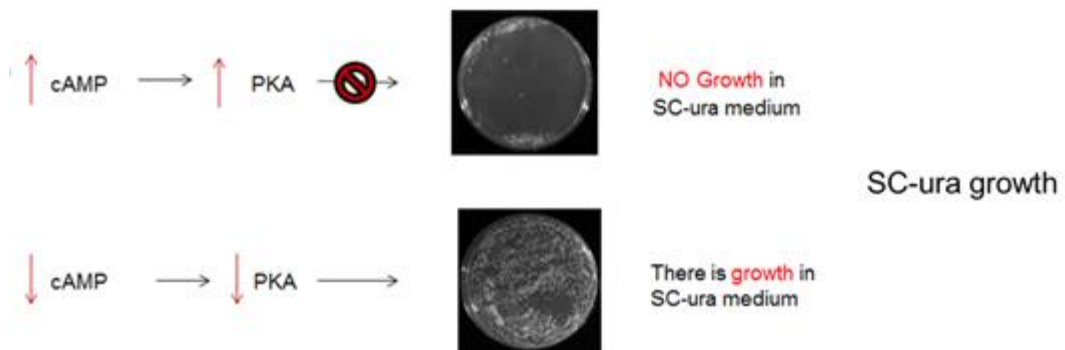
Figure 1.6. Phenotypes associated with PKA activity used in the genetic screen. A) Mating occurs in the presence of low cAMP levels along with low PKA activity and active PDE enzymes. B) SC-Ura growth occurs in yeast cells with low cAMP levels and reduced PKA activity.

Figure 1.6 Phenotypes associated with PKA activity used in the genetic screen

A



B



CHAPTER TWO

MATERIALS AND METHODS

2.1 Materials

2.1.1 Growth Media

YES-rich medium is as follows: one liter of medium contains 30g of Glucose, 5g of Yeast extract and supplemented with required nutrients (Adenine, Histidine, Lysine, Leucine and Uracil) at 225 mg/L (and 20g agarose for plates). 1M KCl is used for KCl assays. EMM-defined medium is made as previously described (Demirbas et al., 2011b). Resistance or sensitivity to PDE inhibitors was determined in 5FOA and SC-Ura solid medium as described by Hoffman and Winston (1990). *E. coli* were grown in Luria Bertani (LB) broth (1% tryptone, 0.5% yeast extract and 1% NaCl) with ampicillin (100mg/L).

2.1.2 Yeast

The genotypes of all yeast strains used in this study are listed in Table 2.1. The strains in this thesis carried either the *fbp1-ura4⁺* or the *fbp1-GFP* reporter. Both constructs are translational fusions integrated at the *fbp1⁺* locus, as previously described by Hoffman and Winston (1990) and de Medeiros et al. (2013), respectively. Strains were grown at 30°C.

2.1.3 Bacterial strains

ElectroTen-Blue electroporation competent cells (Agilent Technologies - Stratagene) were used as the host strain to amplify plasmids (Invitrogen, San Diego). BL21 (DE3) competent cells (New England BioLabs®, Inc.) were used as host strain to express mutant and wild-type PDE4B proteins

from the pET15b plasmid for protein purification. Bacterial transformants were selected on LB with ampicillin (100mg/L) plates. Cells were grown at 37°C overnight unless otherwise described.

2.1.4 Enzymes

Restriction endonuclease enzymes and their buffers were purchased from New England Biolabs (NEB, Ipswich, MA) and used according to NEB instructions. The restriction digestion patterns were predicted by NEBcutter software. Failsafe enzyme along with Failsafe kit were purchased from Epicentre Technologies (Madison, WI). *PfuTurbo* DNA polymerase was purchased from Stratagene (La Jolla, CA) for site-directed mutagenesis PCR. DNase I (RNase-free) was purchased from New England BioLabs Inc. (Ipswich, MA) and used for protein purification.

2.1.5 Buffers for protein purification

2.1.5.1 Buffers for protein purification using Affinity column

Affinity-purification of his-tagged proteins was carried out using Talon beads by Clontech (Mountain View, CA). The sonicate buffer was at a 50mL final concentration 0.004 mg/mL stocks of leupeptin and aprotinin each, 10mg of 1 mg/mL lysozyme, 10% glycerol, PMSF 0.01M and 0.1% DNase I (RNase free) and 0.2% Triton-x100 filled with modified Buffer A (described in 2.1.5.2 section). The binding buffer was a modified Buffer A (described in section 2.1.5.2) without imidazole. The elution buffer was prepared with 10 mL of 20 mM Tris-HCl, pH 7.5, 50 mM NaCl, 0.4 M imidazole and 1mM β ME was used for protein elution.

2.1.5.2 Buffers for protein purification using Ion-Exchange column

The Ion-exchange column used was a Q-Sepharose column by GE Healthcare Sciences (Marlborough, MA). The buffers were prepared as followed: Buffer A was prepared to a 500 mL final volume with 20 mM Tris-HCl, pH 7.5, 20 mM Imidazole, 300 mM NaCl, 1 mM β ME; Buffer

B, only differ from Buffer A with the following reagents: 50 mM NaCl, 1mM β ME. Buffers C1, C2, C3 and C5 contained 20 mM Tris-HCl, pH 7.5, 1 mM EDTA, 1mM β ME with varying final concentrations of NaCl (100 mM, 200 mM, 300 mM, 500 mM, respectively).

2.1.6 Antibodies

For the immunodetection, the primary antibody (rabbit polyclonal IgG, a His probe, sc-803-G) and the secondary antibody (goat anti-rabbit IgG-HRP, sc-2004) were purchased from Santa Cruz (Dallas, TX) and used in 1:500 and 1:1500 dilutions, respectively.

2.1.7 Small molecules used in counterscreens and cAMP assays

Small molecules were purchased from ChemDiv, IFLab2, Enamine and Maybridge. 20mM stocks were prepared by dissolving the small molecules in DMSO and storing at -80°C.

2.2 Methods

2.2.1 Strain mating and tetrad dissection

Yeast strains were patched onto YES solid medium prior to mating. The freshly streaked strains were mated on EMM solid medium for 24 h at 30°C. After that, asci were separated and dissected using a dissection needle to YES plate. After germination and colony formation, progeny was scored by replica plating to selective medium. In some cases, whole cell PCR was carried out to confirm what AC or PDE was present in the progeny for crosses.

2.2.2 Mutagenic PCR

Mutagenesis PCR was performed to clone either the mammalian PDE4B2 (Genbank accession number L20971) or PDE7B1 (Genbank accession number NM_018945) by flanking *Schizosaccharomyces pombe* *cgs2* gene sequence. PCR products were generated by FailSafe PCR

kit using "Premix" buffers B, C, J and L (Epicentre Biotechnologies, Madison, WI) to increase mutations (Clontech, 2001). The custom DNA primers ordered from Integrated DNA Technologies (Coralville, IA) were the following: *cgsmut5'* (5'TCATAGCATA-CTTCTTCACCAAGC3') and *cgsmut3'* (3'AAAGTGTCCGATGAGAAAAGCGTG). FailSafe PCR kit used for Mutagenic PCR system was optimized to 20 cycles to decrease the number of mutations per clone and to increase the chances in targeting single amino acid substitutions to produce phenotypic changes. The PCR products containing PDE4B2 or PDE7B1 were co-transformed into *StuI*-linearized plasmid pKG3-dropout vector (Hoffman lab, unpublished) by gap-repair DMSO transformation protocol (Bahler et al., 1998) followed by a genetic screen, described in 2.2.5 section. Plasmids pKG3-PDE4B2 or pKG3-PDE7B1 were transformed in yeast strains as a control. PCR products were verified by gel electrophoresis.

2.2.3 Genetic screens

A genetic screen was developed in the present study to identify and isolate BC54 compound-resistant PDE4B2 alleles by their ability to confer growth on SC-Ura plates in the presence of BC54. (BC54 inhibits PDE4B2 to elevate cAMP-levels and repress *fbp1-ura4* expression, thus preventing growth on SC-Ura medium.) After mutagenic PCR and gap-repair transformation of strain CHP1346, the PDE4B2-expressing transformants cultured from EMM-Leu plates were collected in 10mL in water, resuspended in 1 mL of 15% glycerol and stored at -80°C to allow for screening of individual pools of transformants. The screening steps were as follows:

1. Generate a pool of transformants by PCR;
2. Collect pools of transformants and make frozen stocks for subsequent screening;
3. Transfer aliquot of frozen transformants to 10mL of EMM-Leu liquid medium on a rotating wheel overnight at 30 °C;
4. Thaw an aliquot of transformants, dilute 10-fold in 4mL EMM-Leu liquid medium and incubate for 6-8 hours on a rotating wheel at 30 °C;

5. Transfer 5×10^5 cells into an eppendorf tube and pellet by microcentrifugation (5 seconds);
6. Enrich for cells that are able to enter stationary phase by resuspending cells in 100 μ L YES medium with 10 μ M BC54 and incubating for 3 days without shaking at 30 °C to allow cells to grow to stationary phase;
7. Dilute samples 10-fold and count live cells;
8. Repeat enrichment steps 4 to 6 two more times;
9. Transfer 50 μ L of 10-fold diluted samples to 100 μ L of sterile distilled water and spread onto EMM-Leu plates to select for cells with candidate plasmids;
10. Collect cells from EMM-Leu and plate 5×10^5 transformants onto SC-ura plates in the presence of 10mM BC54. Incubate at 30°C for three days;
11. Rescue plasmids from colonies that form in the zone of inhibition and transform *E. coli* for plasmid preps.
12. Sequence *PDE4B* allele in plasmid candidates;
13. Re-test purified candidate transformants on SC-ura plate containing a spot of BC54 for final assessment.

Candidate plasmids were rescued out of yeast into *E. coli* as previously described (Hoffman and Winston, 1987) and were sent out for sequencing. Upon confirmation of mutations, mutant plasmids were digested for linearization before integration. Both mutant plasmids were incubated overnight in YES liquid medium for integration to the chromosome and plated in 5FOA medium to confirm mutant PDE4B was replaced a copy of *ura4* in the *cgs2* locus. Following confirmation, mating phenotype was assessed by iodine stain for 2 minutes and strains were constructed that express PDE4B2^{Y233H} or PDE4B2^{T407A} in combination with either the *fbp1-ura4* or *fbp1-GFP* reporter for further validation of compound resistant phenotype with cell-based assays (Table 2.1). A schematic for the genetic screen is depicted in Figure 2.1.

2.2.4 Cloning and Plasmid construction

Mutant plasmid candidates were rescued out of yeast into *E. coli* by using the Smash and Grab method (Hoffman and Winston, 1987) and sent out for sequencing. After sequencing, plasmids containing candidate alleles *PDE4B2*^{T407} and *PDE4B2*^{Y233H} were integrated into the chromosome of *S. pombe* CHP1662, replacing the *ura4*⁺ gene that was inserted into the *cgs2* locus.

Once integrated, these mutant alleles were combined with either the *fbp1-ura4* or *fbp1-GFP* reporter by traditional yeast crosses. These strains also carried the *git2Δ* that prevents endogenous cAMP production so as to allow for the characterization mutant PDE4B2 activity in strains exposed to varying levels of exogenous cAMP or cGMP.

2.2.5 DNA sequencing

The purified plasmids were sent out to Eurofins MWG Operon (Huntsville, Alabama) for DNA sequencing and confirmation of base-pair change. The following primers were used to amplify the mutant candidate gene: PDE4BAMPF (ATATTCCAGGAAAGAGACCTCC) and, 1157R (5' TTGCGAAGGACCTGAATGCG3'). The PDE4BAMPF primer was also used for the sequencing analysis of the site-directed mutagenesis products.

2.2.6 Cell-based assays

Plasmids were integrated into strains as described in the previous section to assess if these mutations were responsible for the altered behavior in the presence of BC54 (PDE4B inhibitor) in two cell-based assays.

2.2.6.1 5FOA assays

This cell-based platform is a counterselectable assay used to study genetically engineered strains expressing mammalian PDEs and carrying the *fbp1-ura4* reporter. In these strains, the *fbp1* promoter drives the expression of the *ura4* gene. When the *fbp1* promoter is derepressed as is the

case when PKA activity is low, yeast cells fail to grow in 5-fluorotic acid (5FOA) medium (Demirbas et al., 2011a; Demirbas et al., 2011b). Compounds that reduce PDE activity to increase cNMP levels to activate PKA can be detected by their ability to confer 5FOA-resistant growth (Figure 2.2a). For this assay, cells must be grown under conditions that lead to the repression of the *fbp1-ura4* reporter prior to their transfer to 5FOA medium (Table 2.2).

2.2.6.2 GFP assays

This cell-based platform was used as another method to assess either PDE or AC activity in genetically engineered strains carrying the *fbp1-GFP* reporter (Figure 2.2b). The activity of these enzymes could be tested for mutant PDEs in the presence of an inhibitor, PDE activators or AC inhibitors, as previously described (de Medeiros et al., 2015). The enzymatic activity of PDE was correlated with the levels of GFP signal, which was normalized by OD₆₀₀ to decrease well-to well variation. Growth conditions were determined for the pre-growth steps to shut off of the GFP reporter and proper assessment of small molecules (Table 2.3).

2.2.7 Site directed mutagenesis

The mutants were generated as described by QuickChange II site-directed mutagenesis kit from Agilent Technologies (Santa Clara, CA). The PCR method was performed on pET15b vector expressing wild-type PDE4B catalytic domain (acquired from Dr. Hengming Ke) to generate the mutant PDE4B alleles by using the following primers: T407-F (5'AATTGTACGGCAATGGGCAGACCGCATCATGGAGGA3'), T407-R (5'TCCTCCATGATGCGGTCTGCCCATTGCCGATAACAATT3'), Y233H-F (5'CCATTCTGACGTGGCACATCACAACAGCCTGAC3'), and Y233H-R (5'GTGCAGGCTGTTGTGATGTGCCACGTCAGAATGG3'). The products were confirmed by DNA sequencing.

2.2.8 Protein purification

Table 2.1. Yeast strain list used in this study

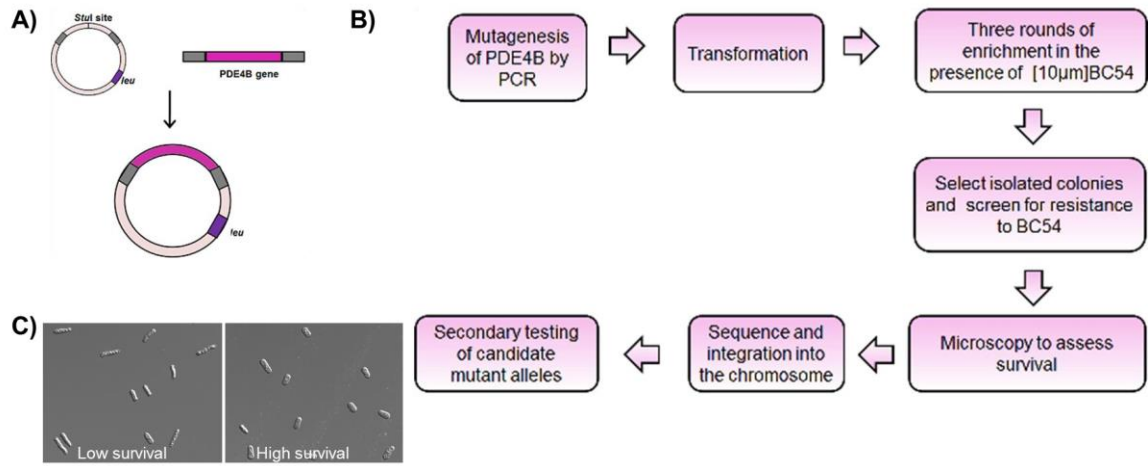
Human PDE and/or AC	Strain ID	Genotype
–	CHP1040	<i>h⁻ fbp1⁺ ura⁺ leu1-32 ade6-M216 lys⁺ his⁺ pap1⁺ cgs2⁺ lys2::his7⁺ git⁺</i>
PDE4D3	CHP1167	<i>h⁻ fbp1::ura4 ura4::fbp1-lacZ leu1-32 ade⁺ lys⁺ his⁺ pap1D::ura4- cgs2::PDE4D3 git2⁺</i>
–	CHP1207	<i>h⁻ fbp1::ura4 ura4::fbp1-lacZ leu1-32 ade⁺ lys⁺ his7-366 pap1D::ura4- cgs2-2 git2-2::his7+(7)</i>
PDE7B1	CHP1209	<i>h⁻ fbp1::ura4 ura4::fbp1-lacZ leu1-32 ade⁺ lys⁺ his⁺ pap1D::ura4- cgs2::PDE7B git3::kan</i>
–	CHP1265	<i>h⁻ fbp1::ura4 ura4::fbp1-lacZ leu1-32 ade⁺ lys⁺ his⁺ pap1D::ura4- cgs2-2 his3-D1 gpa2::his3+</i>
PDE4B2	CHP 1268	<i>h⁻ fbp1::ura4 ura4::fbp1-lacZ leu1-32 ade⁺ lys⁺ his⁺ pap1D::ura4- cgs2::PDE4B2 git3::kan</i>
–	CHP1346	<i>h⁺ fbp1::ura4 ura4::fbp1-lacZ leu1-32 ade⁺ lys⁺ his⁺ cgs2-2 pap1D::ura4- git2⁺</i>
PDE4B2	CHP1401	<i>h⁻ fbp1::ura4 ura4::fbp1-lacZ leu1-32 ade⁺ lys⁺ his⁺ pap1D::ura4- cgs2::PDE4B2 git2-2::his7+(7)</i>
–	CHP1610	<i>h⁺ fbp1::ura4 ura4::fbp1-lacZ leu1-32 ade⁺ lys⁺ his⁺ cgs2⁺ git11::kan</i>
–	CHP1611	<i>h⁺ fbp1::ura4 ura4::fbp1-lacZ leu1-32 ade⁺ lys⁺ his⁺ cgs2⁺ git3::kan</i>
PDE4B2	CHP1641	<i>h⁻ fbp1::GFP ura4::fbp1-lacZ leu1-32 ade⁺ lys⁺ his7-366 ??? pap1D::ura4- cgs2::PDE4B2 git2-2::his7+(7)</i>
–	CHP1662	<i>h⁹⁰ fbp1::GFP ura4::fbp1-lacZ leu1-32 pap1::ura4- cgs2D::ura4 git2⁺</i>
PDE4B2 ^{Y233H}	CHP1679	<i>h⁻ fbp1::GFP ura4::fbp1-lacZ leu1-32 ade⁺ lys⁺ his7-366 pap1::ura4- cgs2::PDE4B(Y233H) Ana7 git2-2::his7+(7)</i>
PDE4B2 ^{Y233H}	CHP1680	<i>h⁻ fbp1::ura4 ura4::fbp1-lacZ leu1-32 ade⁺ lys⁺ his7-366 pap1::ura4- cgs2::PDE4B(Y233H) Ana7 git2-2::his7+(7)</i>

PDE4D3	CHP1702	<i>h⁻ fbp1::GFP ura4::fbp1-lacZ leu1-32 ade⁺ lys⁺ his⁺ pap1D::ura4- cgs2-2 ars1[pNMT1-GNAS1+ LEU2+] git2-2::his7+(7)</i>
PDE4B2 ^{T407}	CHP1712	<i>h⁻ fbp1::GFP ura4::fbp1-lacZ leu1-32 ade⁺ lys⁺ his7-366 pap1::ura4- cgs2D::PDE4B2(T407A) Ana1 git2-2::his7+(7)</i>
PDE4B2 ^{T407}	CHP1713	<i>h⁻ fbp1::ura4 ura4::fbp1-lacZ leu1-32 ade⁺ lys⁺ his7-366 pap1::ura4- cgs2D::PDE4B2(T407A) Ana1 git2-2::his7+(7)</i>
AC5 and GNAS1	CHP1731	<i>h⁻ fbp1::GFP ura4::fbp1-lacZ leu1-32 ade⁺ lys⁺ his⁺ pap1D::ura4- cgs2-2 ars1[pNMT1-GNAS1R201C LEU2+]adh::[pLEV3-AC5-10-2:3 LEU2+] git2-2::his7+(7)</i>
PDE4D2	CHP1742	<i>h⁻ fbp1::GFP ura4::fbp1-lacZ leu1-32 ade⁺ lys⁺ his⁺ pap1::ura4- cgs2::PDE4D2(confirmed by PCR) git11::kan</i>
PDE4D3 and AC1	CHP1805	<i>h⁻ fbp1::GFP ura4::fbp1-lacZ leu1-32 ade⁺ lys⁺ his⁺ pap1D::ura4- cgs2::PDE4D3 adh::[pLEV3-AC1] LEU2+] git2-2::his7+(7)</i>
PDE4D3 and AC4	CHP1807	<i>h⁻ fbp1::GFP ura4::fbp1-lacZ leu1-32 ade⁺ lys⁺ his⁺ pap1D::ura4- cgs2::PDE4D3 adh::[pLEV3-AC4] LEU2+] git2-2::his7+(7)</i>
AC1	CHP1811	<i>h⁻ fbp1::GFP ura4::fbp1-lacZ leu1-32 ade⁺ lys⁺ his⁺ pap1D::ura4- cgs2-2 [pLEV3-AC1] git2-2::his7+(7)</i>
AC4	CHP1812	<i>h⁻ fbp1::GFP ura4::fbp1-lacZ leu1-32 ade⁺ lys⁺ his⁺ pap1D::ura4- cgs2-2 [pLEV3-AC4] git2-2::his7+(7)</i>
AC7	CHP1813	<i>h⁻ fbp1::GFP ura4::fbp1-lacZ leu1-32 ade⁺ lys⁺ his⁺ pap1D::ura4- cgs2-2 [pLEV3-AC7] git2-2::his7+(7)</i>
PDE7B1 and AC5	CHP1822	<i>h[?] fbp1::GFP ura4::fbp1-lacZ leu1-32 ade⁺ lys⁺ his⁺ pap1D::ura4- cgs2:: PDE7B1 adh::[pLEV3-AC5-10-2:3 LEU2+] git2-2::his7+(7)</i>
PDE4D3 and AC5	CHP1823	<i>h⁻ fbp1::GFP ura4::fbp1-lacZ leu1-32 ade⁺ lys⁺ his⁺ pap1D::ura4- cgs2::PDE4D3 adh::[pLEV3-AC5-10-2:3 LEU2+] git2-2::his7+(7)</i>
-	CHP1841	<i>h⁺ fbp1::GFP ura4::fbp1-lacZ leu1-32 ade⁺ lys⁺ his⁺ pap1::ura4- cgs2+::intLEU2 git11::kan</i>
PDE4D2 and AC5	CHP1852	<i>h⁺ fb1::GFP ura4::fbp1-lacZ leu1-32 ade⁺ lys⁺ his⁺ pap1D::ura4- cgs2::PDE4D2 lys2-97 [pJV1-AC5 (lys2+)] ars1[pNMT1-GNAS1R201C LEU2+] git2-2::his7+(7)</i>

AC5 and GNAS1	CHP1854	<i>fbp1::GFP ura4::fbp1-lacZ leu1-32 ade+ lys+ his+ pap1D::ura4- cgs2-2 lys2-97 [pJV1-AC5 (lys2+)] ars1[pNMT1-GNAS1R201C LEU2+] git2-2::his7+(7)</i>
—	CHP1871	<i>h+ fbp1::GFP ura4::fbp1-lacZ leu1-32 ade+ lys+ his+ pap1D::ura4- cgs2+::intLEU2 gpa2::ura4+</i>
PDE7B1 and AC1 and GNAS1	CHP1883	<i>h+ fbp1::GFP ura4::fbp1-lacZ leu1-32 ade+ lys+ his+ pap1D::ura4- cgs2::PDE7B lys2-97 [pJV1-AC1 (lys2+)] ars1[pNMT1-GNAS1R201C LEU2+] git2-2::his7+(7)</i>
PDE1C4 and AC6	CHP1962	<i>h+ fbp1::GFP ura4::fbp1-lacZ leu1-32 ade+ lys+ his+ pap1D::ura4- cgs2::kan-adh1-PDE1C4 lys2-97 [pJV1L-AC6:4] git2-2::his7+(7)</i>
PDE10A and AC1	CHP1964	<i>h+ fbp1::GFP ura4::fbp1-lacZ leu1-32 ade+ lys+ his+ pap1D::ura4- cgs2-2 lys2-97 [pJV1-AC1 (lys2+)] [pLEV3-PDE10ALEU2+] git2-2::his7+(7)</i>
PDE10A and AC5	CHP1967	<i>h+ fbp1::GFP ura4::fbp1-lacZ leu1-32 ade+ lys+ his+ pap1D::ura4- cgs2-2 lys2-97 [pJV1-AC5 (lys2+)] [pLEV3-PDE10ALEU2+] git2-2::his7+(7)</i>
AC6	CHP1981	<i>h+ fbp1::GFP ura4::fbp1-lacZ leu1-32 ade+ lys+ his+ pap1D::ura4- cgs2-2 lys2-97 [pJV1L-AC6:4] git2-2::his7+(7)</i>
AC3 + GNAS1	CHP1990	<i>h+ fbp1::GFP ura4::fbp1-lacZ leu1-32 ade+ lys+ his+ pap1D::ura4- cgs2-2 lys2-97 [pJV1L-AC3] ars1[pNMT1-GNAS1R201C LEU2+] git2-2::his7+(7)</i>
AC8	CHP2015	<i>fbp1::GFP ura4::fbp1-lacZ leu1-32 ade+ lys+ his+ pap1D::ura4- cgs2-2 lys2-97 [pJV1t-AC8:3] git2-2::his7+(7)</i>
AC2	CHP2016	<i>fbp1::GFP ura4::fbp1-lacZ leu1-32 ade+ lys+ his+ pap1D::ura4- cgs2-2 [pLEV3-AC2 LEU2+] git2-2::his7+(7)</i>
Sac	CHP2017	<i>fbp1::GFP ura4::fbp1-lacZ leu1-32 ade6-M216? lys+ his7+? pap1D::ura4- cgs2-2 lys2-97 [pJV1L-sAC] git2-2::his7+(7)</i>
AC9	CHP2024	<i>fbp1::GFP ura4::fbp1-lacZ leu1-32 ade+ lys+ his+ pap1D::ura4- cgs2-2 lys2-97 pJV1tif-AC9:4(9) git2-2::his7+(7)</i>
PDE7B1 and AC6	CHP2028	<i>h? fbp1::GFP ura4::fbp1-lacZ leu1-32 ade+ lys+ his+ pap1D::ura4- cgs2::PDE7B1 lys2-97 [pJV1L-AC6:4] git2-2::his7+(7)</i>
ExoY, PDE9A and PDE5A	CHP2053	<i>h+ fbp1::GFP ura4::fbp1-lacZ leu1-32 ade+ lys+ his+ pap1D::ura4- cgs2::PDE9A lys2-97::PDE5A[lys2+] ars1::pnmt81-exoY[LEU2] git2-2::his7+(7)</i>

Figure 2.1. Development of a genetic screen. A) Gap repair was performed to clone candidate mutant alleles of PDE4B generated by PCR into the plasmid. B) Genetic screen protocol. C) Microscopic examination of cells in stationary phase in the presence (left) or absence (right) of compound BC54. Inhibition of PDE4B in these cells confers a rapid loss of viability in stationary phase.

Figure 2.1 Development of a genetic screen



E. coli competent cells carrying pEt15b vector, expressing the catalytic domain of either wild-type or mutant proteins, were grown in 100 mL LB medium batch with 0.1 g/mL ampicillin resistance overnight. The cultures were (1:90 fold) diluted to 900mL LB medium and 0.1 g/mL ampicillin and grown for at 37°C for 2-3 hours. OD's were targeted to 0.6-0.7 absorbance for induction using IPTG (0.2 mM, as the final concentration) at 16°C for 18-20 hours. Induced samples were centrifuged down in 85mL Nalgene tubes at 8500 rpm for 10 minutes at 4°C. Pellets were resuspended in sonication buffer and incubated on ice for 30 minutes and sonicated 3 times for 30 seconds with intervals of 10 seconds followed by centrifugation for 30 minutes at 8500rpm twice. A cobalt column was chosen for the affinity purification since the proteins studied carry a 6-His tag (attached to N- terminus of the protein). The Talon[®] Metal affinity resins manual from Clontech Laboratories, Inc (Mountain View, CA) was used for affinity chromatography with the following modifications: 4mL of beads (per culture) were suspended and washed once with 10mL Sonicate buffer. Next, supernatant samples were transferred and incubated with talon beads in a shaker at 4°C for 3.5 hours or overnight, PDE4B^{wt} and PDE4^{T407A} or PDE4B^{Y233H} sample, respectively for binding. After that, samples were flown under gravity and eluted by 12 mL of elution buffer. In each step of the procedure, aliquots were collected to confirm purification by SDS-PAGE and Western blot analysis. For further purification (removal of elution buffer), an Ion – exchange chromatography was performed with Q-Sepharose column using 2mL Q-beads washed with 10 mL buffer B twice. After that, samples were loaded, flowed under gravity and washed with 10mL Buffer C1. Flow through was collected in every step. Samples were eluted with 4.5 mL buffers C2, C3, C5 in 1.5 mL fractions. Purified proteins sizes were confirmed by SDS- PAGE and Western blot analysis. Commassie blue was used to detect proteins. Precision Plus Porinte[™] Kaleidoscope from Bio-rad was used as the protein standard ladder. After that, centrifugation was performed using Amicon ultra-15 for protein concentration according to manufacture specifications (EMD Millipore) and aliquoted into -80°C freezer.

2.2.9 *In vitro* assays

In vitro enzyme assays were performed using the barium precipitation method as previously described (Wang et al, 2005a). In this method, samples are incubated in a heating block set at 25°C. Reactions are stopped with a final concentration of 0.2M of ZnSO₄ (Zinc sulfate) and, after that final concentration of 0.25N Ba(OH)₂ (Barium hydroxide) is added to precipitate the product. Samples are centrifuged in a microcentrifuge at maximum speed for 15 minutes and supernatant is collected for analyses. The amount of product produced during the reaction was estimated as: $(C_T - C_0)/C_T$, where C_T represents cpm at time (without enzyme) and C_0 represents the starting cpm. The activity of recombinant human PDE4B2 enzyme and its mutant forms (Y233H and T407A) were tested as followed: To calculate the V_{max} of PDE4WT and mutant proteins, the assay was saturated with 10 μM of cold substrate (cAMP). To investigate the enzymatic activity of these proteins, *in vitro* assays were performed to measure enzyme efficiency (Wang et al., 2007) and IC₅₀ assays (by Ceyhan et al., 2012). The IC₅₀ was estimated as the concentration of BC54 or Rolipram that reduced enzyme activity by 50%. The substrate concentration of 0.5 μM was used for both enzymes based on a K_m of 5 μM for PDE4B2, as previously described (Beavo and Conti, 2007). Reactions proceeded for 25 and 40 minutes for PDE4B2 wild-type and T407 mutant, respectively, during which time in the production of product was linear with time. The amount of hydrolysis was generally limited between 42-50% and the IC₅₀ values were calculated from the means of at least three independent experiments. Substrate concentration was ≤ 0.1 K_m for each enzyme with IC₅₀ values representing approximate the inhibitor K_i values.

2.2.10 Protein Measurements

Purified enzyme concentrations were determined using BCA assays according to manufacturer's protocol (Pierce in Rockford, IL).

2.2.11 High-throughput screens (HTS)

2.2.11.1 10,000 HTS for PDE activators

High-throughput chemical screens were performed at the ICCB facility at Harvard Medical School. Prior to the screening, a collection of strains was created expressing the short and long forms of mammalian PDE4D proteins. After that, the optimal cell density was determined by detecting the basal GFP signals of a PDE-expressing strain in comparison to a strain not expressing PDE (de Medeiros et al., 2015). This allows for the proper assessment of a compound that reduces PKA activity. The strains used were CHP1702 (expressing PDE4D3), our experimental sample, and strain CHP1742 (expressing PDE4D2) (Table 2.1). Strain CHP1702 expresses the PDE4D3 long form that has a PKA autoregulatory domain and strain CHP1742, the PDE4D2 short form, was used as the genetic mimic of a positive control due to lack of known PDE4D activators. A PDE4D2 lacks the inhibitory domain present in PDE4D3, it displays a higher PDE activity and higher GFP values, similar to what a PDE activator might confer upon the screening strain. Once the screening conditions were optimized using a 384-well microtiter dish with black walls and clear bottom to measure GFP signals. Finally, the optimal cell concentration for each strain was determined for inoculation in the microtiter dishes in order to produce a Z-factor > 0.5 (see below) as a reflection of the HTS quality. The starting cell concentrations used are seen in Table 2.3. For this HTS, strains were pre-grown to exponential phase in EMM complete medium without or with 20mM cAMP overnight (CHP1742) and cells were prepared for pinning of compounds, as previously described (de Medeiros et al., 2015). The stock solutions of compounds tested were generally 5mg/mL with the exception of ChemDiv6 where compounds are 10mM. Plates were incubated in a container with “moist” paper towel to prevent evaporation for 48h at 30°C. GFP fluorescence and optical densities (OD_{600}) of cultures were measured using an Envision plate reader, with a 485 eGFP excitation filter and 535 eGFP emission filter and 485 filters and 505 mirror for OD bottom readings. GFP values were normalized by OD values to decrease well-to-well variation.

Compounds hits for the 10,000 HTS were determined by Z-scores of the experimental wells that were calculated using the mean and standard deviation of the negative controls for each plate (cells

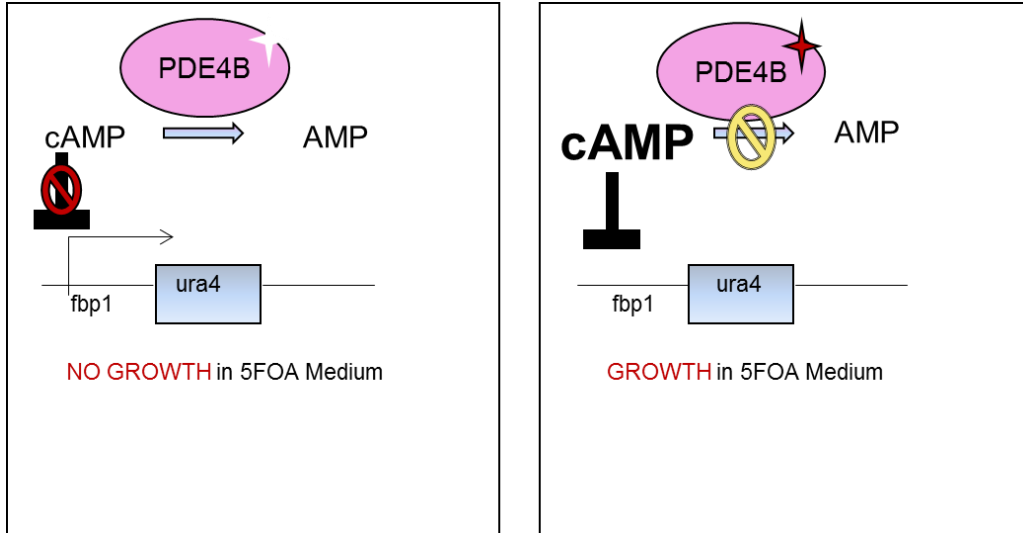
Table 2.2. Optimal growth conditions used in 5FOA assays

Strain / Protein (s) expressed	Pregrowth Supplement	Cyclic nucleotide in 5FOA medium	Cell density (cells/mL)
CHP1209 (PDE7B)	2.5 mM cAMP	N/A	1×10^5
CHP1268 (PDE4B2 wild-type)	5mM cAMP	N/A	2×10^5
CHP1401 (PDE4B2 wild-type)	20 μ M rolipram + 2.5mM cAMP	0.4mM cAMP	0.5×10^5
CHP1680 (PDE4B2 ^{Y233H})	5mM cGMP	0.4mM cAMP	0.5×10^5
CHP1713 (PDE4B2 ^{T407})	5mM cGMP	0.4mM cAMP	0.5×10^5
CHP1742 (PDE4D2)	20mM cAMP	N/A	2×10^6

Figure 2.2. Basis for secondary screen. A) Basis for 5FOA assay. When cAMP levels are low, the *fbp1* promoter is derepressed and the *ura4* gene is expressed (left). In the presence of a PDE4B inhibitor, cAMP levels increase, the *fbp1* promoter is repressed, and *ura4* is not expressed (right) resulting in 5FOA-resistant growth. B) Basis for GFP assay. Reduction of PKA activity by either PDE activator or AC/GNAS1, decrease cAMP levels followed by detection of GFP signal (left). Increase in PKA activity by PDE inhibition or AC activation, increases cAMP levels increase and reduce GFP signal (right).

Figure 2.2 Basis for secondary screen

A



B

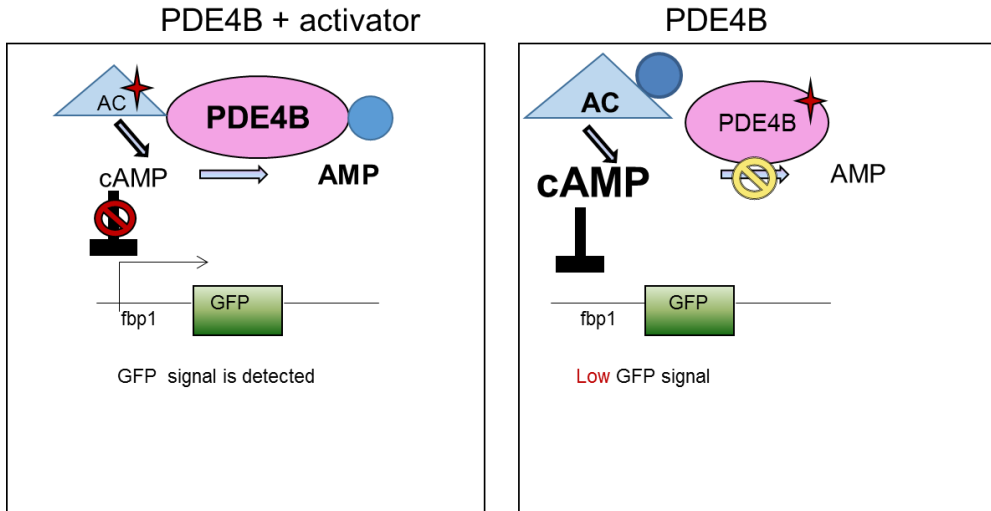


Table 2.3. Optimal growth conditions used in GFP assays

Strain / Protein (s) expressed	Pregrowth Supplement	Cyclic nucleotide in EMM medium	Cell density (cells/mL)
CHP1641 (PDE4B2 wild type)	1.5 mM cAMP	0.25mM cAMP	3 x 10 ⁶
CHP1679 (PDE4B2 ^{Y233H})	1.5mM cAMP	0.25mM cAMP	3 x 10 ⁶
CHP1702 (PDE4D3)	20mM cAMP	N/A	4 x 10 ⁶
CHP1712 (PDE4B2 ^{T407})	1.5mM cAMP	0.25mM cAMP	3 x 10 ⁶
CHP1742 (PDE4D2)	20mM cAMP	N/A	2 x 10 ⁶
CHP1805 PDE4D3 and AC1	N/A	N/A	4 x 10 ⁶
CHP1807 PDE4D3 and AC4	20mM cAMP	N/A	4 x 10 ⁶
CHP1812 (AC4)	20mM cAMP	N/A	4 x 10 ⁶
CHP1822 (PDE7B1 and AC5)	N/A	N/A	2 x 10 ⁶
CHP1841 (Δ)	N/A	N/A	2 x 10 ⁶
CHP1823 (PDE4D3 + AC5)	N/A	N/A	2 x 10 ⁶
CHP1882/CHP1883 (PDE7B1 + AC1)	N/A	N/A	2 x 10 ⁶
CHP1962 (PDE1C4 and AC6)	N/A	N/A	2 x 10 ⁶
CHP1964 (PDE10A and AC1)	N/A	N/A	2 x 10 ⁶
CHP1967 (PDE10A and AC5)	N/A	N/A	2 x 10 ⁶
CHP2053 (<i>ExoY</i> + <i>PDE5A</i> + <i>PDE9A</i>)	N/A	N/A	2 x 10 ⁶

growing in DMSO) as described previously (Ceyhan et al., 2012). Cherry pick was performed as using pocket tips. Bioinformatic analyses were performed using the Vortex Software provided by ICCB. Cherrypicked compounds were retested in 75uM concentration to validate the hits using strains CHP1702 (PDE4D3), CHP1807 (PDE4D3 and AC4) and CHP1812 (AC4). Counter-screen assays were performed for further validation and characterization of final candidate PDE4D3 activators.

2.2.11.2 HTS for PDE activators

After the 10,000 HTS was concluded, a collection of strains was created expressing a combination of mammalian AC and PDE proteins for a larger HTS for compounds that reduce PKA activity as previously mentioned in section 2.2.12.1. In this HTS, we chose strains CHP1823 (expressing PDE4D3 and AC5), CHP1882 and CHP1883 (expressing PDE7B1 and PDE4D2) that expressed similar basal GFP signals for our experimental sample and counter-screen strains, respectively, along with strain CHP1742 (expressing PDE4D2) as the genetic positive control (Table 2.1). Strain CHP1823 expresses the long form PDE4D3 protein that has a PKA regulated autoinhibitory domain. As there are no known small molecule activators of PDE4 enzymes, strain CHP1742, which expresses the PDE4D2 short form, was used as the genetic positive control that produces a high GFP value due to high PDE4 activity. The initial counter-screen strain CHP1883 was substituted by strain CHP1882 that has the same genotype, but display a better growth behavior, which facilitated the elimination of false positive compounds. Finally, the optimal cell concentration for each strain was determined for inoculation in the microtiter dishes in other to produce a Z-factor > 0.5 (see below) as a reflection of the HTS quality. The starting cell concentrations used are seen in Table 2.3. For this HTS, strains were pre-grown to exponential phase in EMM complete medium without or with 20mM cAMP overnight (CHP1742) and procedure was performed as previously described (de Medeiros et al., 2015). The stock solutions of compounds tested were generally 5mg/mL with the exception of ChemDiv6 library where

compounds were stored at 10 mM. Plates were incubated in a container with “moist” paper towel to prevent evaporation for 48h at 30°C. Prior to readings, plates were vortexed with a plate mixer to prevent clumping 90 minutes before data collection. GFP fluorescence and optical densities (OD₆₀₀) of cultures were measured using an Envision plate reader, using 485 eGFP excitation filter and 535 eGFP emission filter and 485 filters and 505 mirror for OD bottom readings. Compounds hits for the 100,000 HTS were chosen by analyzing median and mean absolute deviation (MAD) of the experimental samples for each plate in order to assign Z-scores to each well. This approach takes into consideration the variation within treated samples and is more practical than using mean and standard deviation of negative controls. Z-scores were calculated by subtracting the median value of the normalized GFP values for the experimental samples in a plate from the value of each individual well and dividing this by the MAD value for each plate (MADs were generally ~4-7% of the median). In addition, a differential Z-score was calculated by addition of Z-scores from the duplicate experimental or counter-screen strains followed by subtraction of the former to the latter. Compounds that produced OD₆₀₀ values of < 0.6 were excluded as being toxic. Bioinformatics analyses were performed using the Vortex Software provided by ICCB. Cherry picked compounds were retested in a dose-dependent manner (from 0.675uM to 5uM) to validate the hits against PDE4D3 – and AC1- expressing strain (CHP1805), PDE7B1- and AC5- expressing strain (CHP1822), PDE4D3- and AC5- expressing strain (CHP1823) and PDE7B1- and AC6- expressing strain (CHP2028). Counter-screen assays were performed for further validation and characterization of final candidates in terms of specificity to either PDE4D3 or AC5.

2.2.12 cAMP assays

Cells were treated with small molecules at a final concentration of 20 µM for 1 and a half hours in the rotating wheel at 30°C and collected by filtration onto glass filters (Fisher). Filters were incubated in 1mL of 1M formic acid for 20 minutes and filters were removed and samples were evaporated in a Speedvac as previously described (Byrne and Hoffman, 1993). After that, pellets

were resuspended in the same volume of 0.1 HCl and assayed using cAMP Direct Kit according to Enzo Life Sciences specifications.

2.2.13 KCl assays

Yeast strains were pre-cultured in YES medium and transferred to YES with 1M KCl to assess KCl-resistance. The initial cell concentration of all strains tested in KCl assays was 2×10^5 cells/mL. After that, a 2.5-fold serial dilution (from 20 μ M to 1.28 μ M) of candidate PDE4D activators or AC5 inhibitors was performed to determine whether the compounds affected the activity of either enzyme.

CHAPTER THREE

IDENTIFICATION AND CHARACTERIZATION OF COMPOUND RESISTANT ALLELES OF *PDE4B* TO DUAL PDE4/7 INHIBITOR BC54

3.1 Development of a *S. pombe* genetic screen for compound – resistant alleles of PDE genes

This chapter describes the development of and results from a fission yeast genetic screen to identify mutant PDE4 and PDE7 alleles that have altered sensitivity to compounds previously identified in our lab, including BC54, a potent inhibitor of both PDE4 and PDE7 enzymes.

3.1.1 Discovery of a dual specificity PDE4/7 inhibitor

Previously, the Hoffman lab constructed a collection of strains in which mammalian PDEs replaced the *cgs2/pde1* (Demirbas et al., 2011a) and have used the strains to identify small molecule inhibitors of the mammalian PDEs. Our lab has taken advantage of the *fbp1-ura4* reporter, a PKA repressed reporter, to develop HTS for small molecules that can be detected by their ability to increase PKA activity (Demirbas et al., 2013; Ceyhan et al., 2012; Alaamery et al., 2010; Ivey et al., 2008). Thus, the Hoffman lab has identified a collection of PDE inhibitors. One of these compounds, BC54, is a small molecule that has a dual specificity role of inhibiting both PDE4 and PDE7 enzymes (Figure 3.1) (Demirbas et al., 2011a).

BC54 has been tested in different assays discussed further in this chapter. In the cell-based assay for 5FOA-resistant growth, BC54 is a potent inhibitor of both PDE4 and PDE7 enzymes as seen by its ability to confer 5FOA^R growth to strains expressing PDE4B2 (CHP1268) and PDE7B (CHP1209) (Figure 3.2a). In addition, treatment of strain expressing PDE4B2 (CHP1268) with

BC54 seemed as potent as rolipram treatment (Figure 3.2b). After that, we decided to develop a genetic screen to identify mutations in PDE genes that would confer resistance to a specific inhibitor as a way of learning more about the interactions of these compounds with their target proteins, as this information could help guide future efforts to design more effect derivatives of these compounds.

The assay development involved 3 steps: (1) To select the strain that can differentiate cell survival in the presence of PDE4/7 inhibitors; (2) To develop enrichment conditions to increase cell viability in the presence PDE4/7 inhibitors; (3) To optimize the conditions to assess growth in SC-ura medium.

3.1.2 Cell survival test

Failure to enter stationary phase is associated with high PKA activity (DeVoti et al., 1991).

Therefore, cells lacking PDE activity rapidly die in a saturated culture. This could then allow one to selectively enrich a population of cells for those that retain PDE activity in the presence of a PDE inhibitor. The following experiment was carried out to test our ability to selectively kill off cells with different levels of PKA activity. Six different strains carrying various combinations of mutations involved in cAMP metabolism were chosen. The summary of the strains genotypes and cAMP production and/ or PDE activity are listed in Table 3.1.

The cell survival phenotype was assessed by both microscopy and spot plating. The 100-fold diluted cultures were prepared as described (section 2.2.3). The percentage of live and dead cells were counted under the microscope after each round of enrichment (data not shown). This step will be discussed in more detail (section 3.1.3).

Spot plating was performed as followed: a four serial dilution of an initial 100-fold diluted culture was performed and spotted on YES plate using an initial culture concentration of 5×10^5 cells/ mL. Each dilution was a 10-fold dilution of the previous dilution. After incubation, cell survival was scored by counting the number of colony-forming units from the most diluted sample. The

transformant strain that produced cAMP and expressed PDE4B2 (CHP1346) had a 10-fold reduction in survival in the presence of PDE4 or PDE7 inhibitors in comparison to strain not treated with such compound (Figure 3.3), consistent with the idea that PDE inhibition would elevate PKA activity and reduce cell viability in stationary phase.

3.1.3 Optimization of enrichment conditions

The purpose of the enrichment is to increase the percentage of transformants that can survive in the presence of the inhibitors due to the expression of a compound resistance PDE alleles. The details for the enrichment are provided in Chapter 2. The optimal concentration of inhibitor is 10 μ M, which allows cell survival of the mutants under conditions that would inhibit stationary phase entry and otherwise kill most of the cells. In addition, mutant cell survival must be higher than wild-type cell survival. The number of cells used allowed for growth in the absence of inhibitors and for proper assessment of strain expressing wild-type PDE4 and PDE7 enzymes in the presence of their respective inhibitors (Figure 3.4). Thus, compound resistant transformants are expected to grow in the zone of inhibition (Figure 3.5). The zone of inhibition is formed after the compound is added directly to the center of the plate and the compound diffuses during incubation.

3.1.4 Screening

The screening strain (CHP1346) carries a frameshift mutation in the *cgs2* gene and, consequently has no PDE activity (Table 2.1). In addition, CHP1346 has the wild-type *git2* gene that encodes adenylyl cyclase. Therefore, CHP1346 strain produces its own cAMP. In addition, cells lacking PDE activity have a faster loss of survival, which allows for enrichment of cells surviving in the presence of compounds (de Medeiros et al., 2013). In order to generate PDE4B and PDE7B mutant alleles, a random mutagenic PCR was performed and PDE4B and PDE7B PCR products were cloned by gap repair into the pKG3 plasmid (Figure 2.1) so as to place these PDE ORFs under the control of the *cgs2* promoter. Pools of PCR products were cloned by gap repair into strain CHP1346

(Table 2.1), as previously described (section 2.2.2), and mutant PDE4B and PDE7B transformants were enriched as described in section 2.2.3. After enrichment, transformant cells were cultured in solid media (EMM-Leu and SC-Ura) in the presence of BC54 (section 2.2.3). Seven mutants for each PDE4B and PDE7B allele candidates were isolated after screening for survival in stationary phase in the presence of the inhibitor and sent for sequencing. Upon sequencing analysis, two candidate alleles were identified. The PDE4B mutants had either Y233H or T407A altered residues located near the cAMP-binding pocket that could interact directly with the adenosine of cAMP (Figure 3.6). Each mutant allele expressed in plasmid was integrated into the chromosome of CHP1662 strain (Table 2.1) by replacing the *cks2::ura4⁺* marker. After that, mutant alleles were selected for in 5FOA – resistant transformants. Strains were constructed that express PDE4B2^{Y233H} or PDE4B2^{T407A} in combination with either the *fbp1-ura4* or *fbp1-GFP* reporter (Table 2.2) for further characterization using cell-based assays.

3.2 Characterization of mutant PDE4B strains in 5FOA assays

In order to reconfirm the compound resistant PDE4B phenotype, I used the following approach: mutant PDE4B strains were characterized by 5FOA growth assays in response to varying doses of BC54 (Figure 2.2a). The strains used in this cell-based assay have a deletion of the *git2* adenylyl cyclase gene, which allows for the regulation of the *fbp1-ura4* reporter expression by exogenous cAMP added to the 5FOA medium. Prior to the 5FOA assay, a cAMP growth curve was carried out (data not shown) to assess the hydrolytic activity of the candidate mutant PDEs and identify conditions for detecting compound sensitivity. Pre-growth conditions are described in Table 2.2. After that, 5FOA assays were performed in the presence of either BC54 or rolipram, a well-known PDE4 inhibitor. The growth of the strain expressing wild-type PDE4B (WTPDE4B) in 5FOA medium represents sensitivity to BC54 (Figure 3.7a) and rolipram (Figure 3.7b). Both PDE4B2^{T407A} and PDE4B2^{Y233H} are resistant to BC54 (Figure 3.7a) and rolipram (Figure 3.7b) in comparison to strain expressing WTPDE4B, as seen by the inability of these compounds to confer

Figure 3.1. Structure of dual specificity PDE4/7 inhibitor (BC54). BC54, (ethyl (2Z)-2-(acetylimino)-1-cyclohexyl-5-oxo-1,5-dihydro-3H-dipyrido{1,2-a:2',3'-d}pyrimidine-3-carboxylate, was identified from the ChemDiv 3 library in screens carried out at the Broad Institute Screening Facility.

Figure 3.1 Structure of dual specificity PDE4/7 inhibitor (BC54)

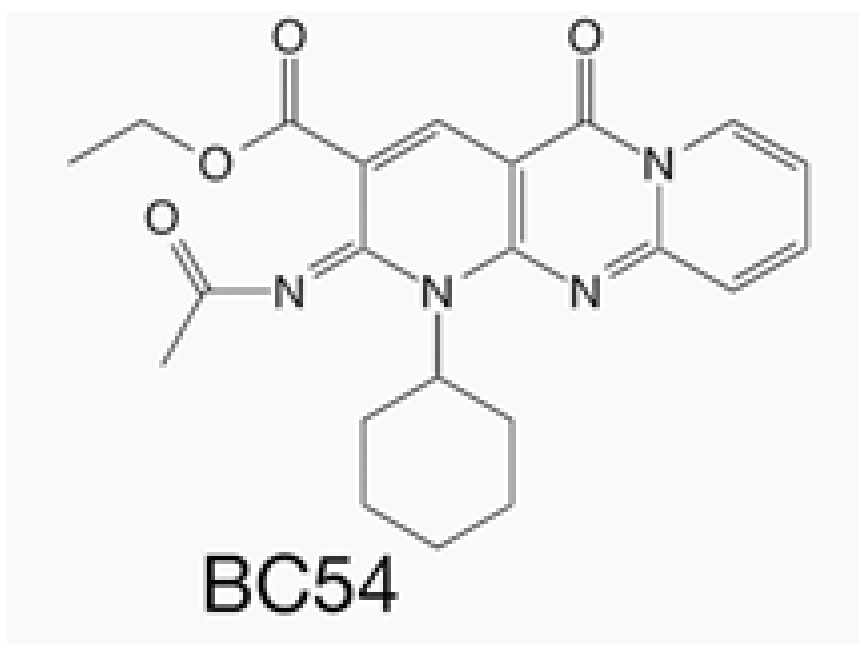
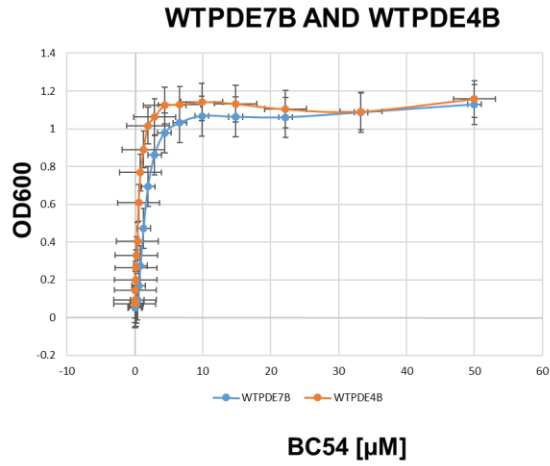


Figure 3.2. 5FOA growth assays of strain expressing wild type PDE4B2 or wild-type PDE7B. A) Growth treatment of strains (PDE7B and PDE4B) in the presence of BC54. B) Growth treatment of strain expressing PDE4B2 (CHP1268) in the presence of either BC54 or rolipram. Values represent the average of $OD_{600} \pm$ standard error from three independent experiments. The values within each experiment represent an average of four replicate wells. Each experiment was incubated for a 48h growth at 30°C.

Figure 3.2 5FOA growth assays of strain expressing wild type PDE4B2 or wild-type PDE7B

A



B

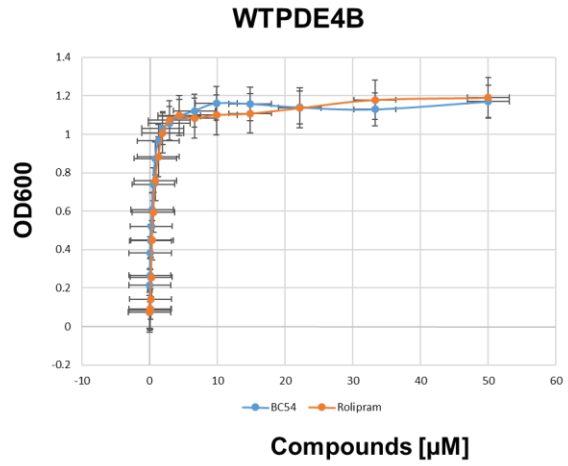


Table 3.1. Strains used for cell survival test

Strains	Genotypes	cAMP production and/ or PDE activity
CHP1207	<i>git2</i> (AC) mutant and <i>cgs2-2</i> (PDE) mutant	No cAMP production and no PDE activity
CHP1265	<i>gpa2</i> (α subunit of heterotrimeric G- protein) mutant and <i>cgs2-2</i> (PDE) mutant	Very low cAMP production and no PDE activity
CHP1346	Wild-type <i>gpa2</i> , <i>gii3</i> , and <i>git2</i> ; <i>cgs2-2</i> (PDE) mutant	High cAMP production and no PDE activity
CHP1610	<i>git11</i> (γ subunit of heterotrimeric G-protein) mutant and wild-type <i>cgs2</i>	Moderate cAMP production and active PDE
CHP1611	<i>gii3</i> (G-protein coupled receptor) mutant and wild-type <i>cgs2</i>	Low cAMP production and active PDE

5FOA^R growth.

3.3 Characterization of mutant PDE4B strain in GFP assays

The compound-resistant nature of these mutant PDE4B alleles was also confirmed independently via GFP assays (Figure 3.9a, b). Prior to the GFP assay, a cAMP curve for a GFP assay was performed to assess the hydrolytic activity of the candidate mutant strains, PDE4B2^{Y233H}, PDE4B2^{T407A} and wild-type PDE4B2 (Figure 3.8). In addition, the cAMP curve is used to identify conditions for measuring compound sensitivity, such as the concentration of cAMP that would repress GFP expression in a strain lacking PDE activity, but not in strains expressing these PDE4 enzymes.

The concentration of exogenous cAMP needed to activate PKA to repress *fbp1-GFP* reporter expression reflects PDE activity (Figure 2.2b), as previously described (section 2.2.6.2; more cAMP is required in the presence of an active PDE. In this cAMP curve, the addition of 1.5 mM cAMP was found to be optimal for pre-culture conditions, promoting cell growth while repressing *fbp1-GFP* reporter and keeping the PDE activity low (Figure 3.8). The exogenous cAMP concentration of 0.25 mM was used for assessment of strains in the presence of inhibitors (Table 2.3). PDE4B2^{T407A} strain (CHP1712) hydrolyzed more cAMP than the PDE4B^{wt} strain (CHP1641) (Figure 3.8). However, the mutant PDE4B^{Y233H} strain (CHP1679) hydrolyzed less cAMP than the PDE4B^{wt} strain (Figure 3.8), which supports growth observations that this mutant expresses a weak PDE enzyme. After that, GFP assays were performed in the presence of either BC54 or rolipram. In this assay, the inhibition of PDE activity leads to a reduction in fluorescence, which corresponds to sensitivity to BC54 and rolipram (Figure 3.9a, b). The reduction of GFP values in the treatment of PDE4B^{wt} strain (CHP1641) with either BC54 (Figure 3.9a) or rolipram (Figure 3.9b) confirms the wild-type PDE4B strain sensitivity to both compounds. In addition, BC54 is much more effective on wild type PDE4B than is rolipram. The mutant PDE4B^{T407A} strain (CHP1712) has a partial altered behavior consistent to its lower sensitivity to BC54 (Figure 3.9a). The mutant

Figure 3.3. Stationary cell survival. Host strain producing cAMP and expressing PDE activity has a 10-fold survival reduction in the presence of PDE inhibitor. Cell survival is not affected if the host strain does not produce cAMP or does not express a PDE. The culture with initial cell concentration of 5×10^5 cells/ mL was diluted 100-fold, followed by four series of a 10-fold dilutions and spotted on YES plate. YES plates were incubated for 3 days at 30°C.

Figure 3.3 Stationary cell survival

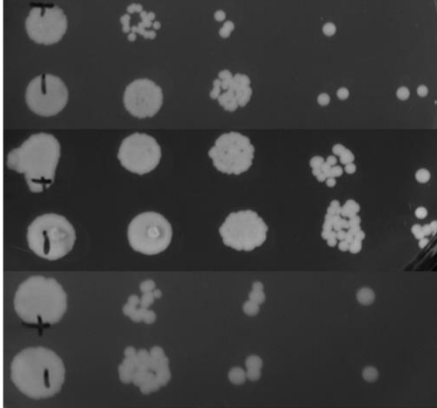
Host cAMP production			Compound	
+	PDE4B		+	
			-	
-	PDE4B		+	
			-	
+	None		+	
			-	

Figure 3.4. Inhibition of growth by PDE inhibitors in SC-ura. Growth phenotype of strains expressing either PDE7B (top) or PDE4B (bottom) in SC-ura medium. Growth is due to PDE activity that reduces PKA activity to allow *fbp1-ura4* expression and is unaffected by DMSO (the vehicle for the compounds). The PDE inhibition prevents growth by activating PKA in the presence of family-specific inhibitor or dual PDE7B/4B inhibitor. Such growth inhibition should allow us to screen for compound-resistant alleles that promote growth in inhibition zone. Compounds are directly delivered to the plate. Four spots for compounds were formed in each plate.

Figure 3.4 Inhibition of growth by PDE inhibitors in SC-ura

Plasmid –
expressed
PDE gene

DMSO

Family - Specific
inhibitor

PDE4/7 inhibitor

PDE7B

PDE4B

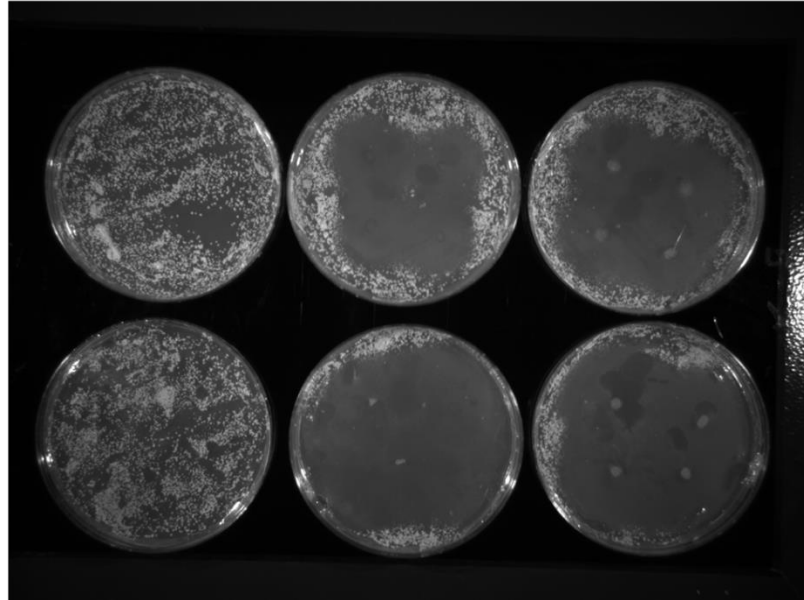


Figure 3.5. Mutant *PDE4B* alleles display growth in a halo assay in SC-ura. Growth phenotype of transformants expressing either wild type PDE4B (left), PDE4B^{T407} (middle) or PDE4B^{Y233H} (right) in SC-ura medium. Approximately 5×10^5 transformants are spread onto an SC-ura plate onto which BC54 was directly delivered to the center of the plate on one single spot. Growth is due to compound- resistance phenotype that reduces PKA activity to allow *fbp1-ura4* expression. SC- ura plates with transformants expressing either wild type PDE4B or PDE4B^{T407} were incubated for 4 days. SC- ura plate with transformant expressing PDE4B^{Y233H} was incubated for 7 days.

Figure 3.5 Mutant *PDE4B* alleles display growth in a halo assay in SC-ura

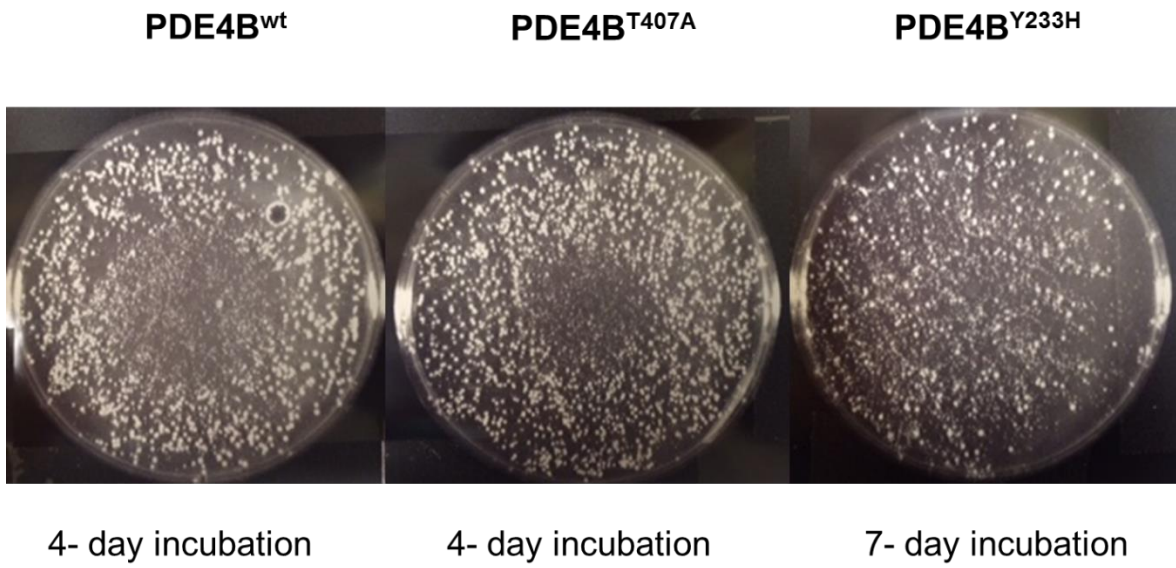
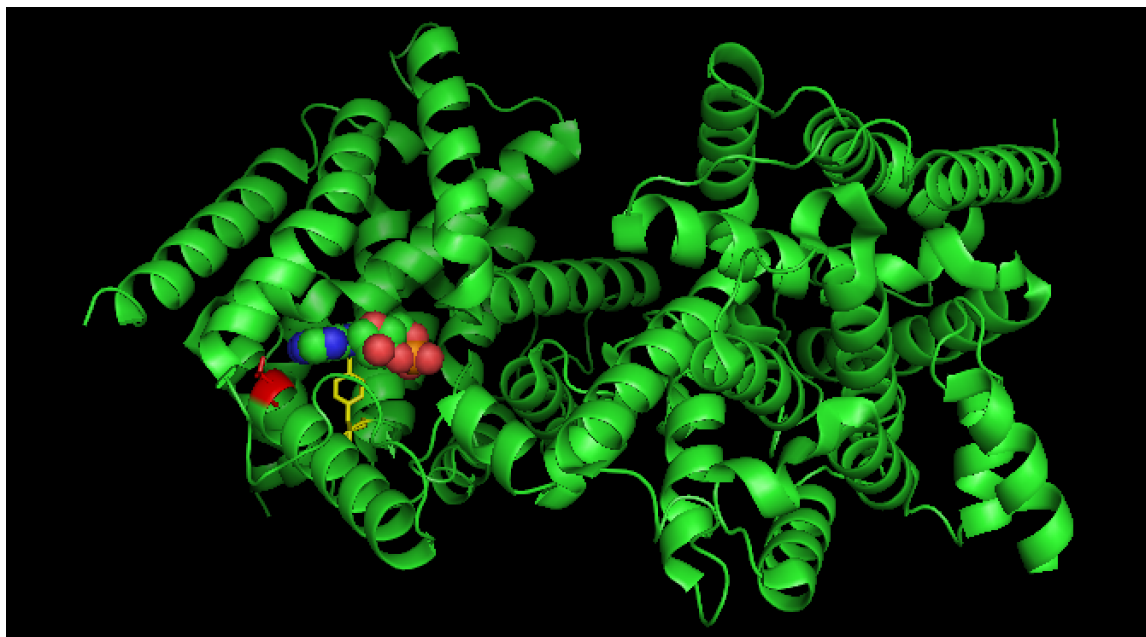


Figure 3.6. Crystal structure of PDE4D bound to cAMP (PDB: 2PW3: Ke et al., 2008). The crystal structure highlights altered residues of PDE4B, threonine (T) in red and Tyrosine (Y) in yellow, in close proximity to cAMP. There is no crystal structure of PDE4B bound to cAMP. For this reason, PDE4D crystal structure was used. The PDE4D bound to cAMP crystal structure was displayed and modified using PyMOL software.

Figure 3.6 Crystal structure of PDE4D bound to cAMP



PDE4B^{T407A} strain has an altered behavior consistent to its partial resistance to rolipram in comparison to wild-type PDE4B (Figure 3.9b).

3.4 Biochemical verification of compound resistance

I used site-directed mutagenesis PCR to introduce mutant allele coding for mutant PDE4B^{T407A} protein in pET15b vector. This approach was followed by transformation of both mutant PDE4BT407A and WTPDE4B⁺ expressing vectors in *E. coli* competent cells for protein purification (Figure 3.10). *E. coli* transformants expressing the catalytic domain of either wild-type PDE4B⁺ or mutant PDE4BT407A T407A proteins were purified by two steps: affinity and ion-exchange purifications. Both enzymes were successfully purified as seen in the SDS gel images (Figure 3.10). Purified proteins were confirmed by Western blot (data not shown).

3.5 *In vitro* assays

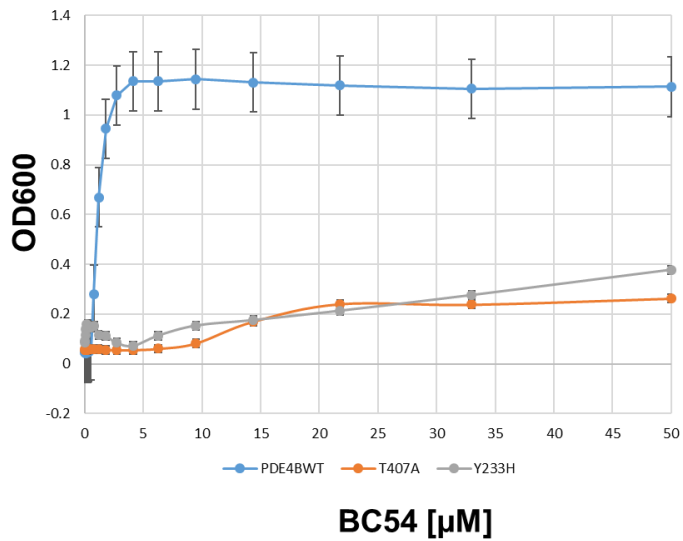
3.5.1 Determining initial velocity, turnover and enzyme efficiency

After protein purification, I performed *in vitro* assays to characterize PDE4B⁺ and PDE4B^{T407A} enzymes. The purpose of these experiments is to determine if the amino acid substitution is increasing the enzyme's activity rather than reducing its sensitivity to BC54. One possibility is that the altered behavior in the presence of BC54 is due to an increase in its effectiveness in hydrolyzing cAMP and not necessarily, a loss of inhibition by BC54. To test this hypothesis, I carried out *in vitro* assays to determine the maximum velocity (V_{max}). Due to the nature of this assay, it is difficult to determine V_{max} directly. Therefore, I used the conditions to test the initial velocity as an indirect measurement of V_{max} . The initial velocity (V_0) of these enzymes is dependent on the concentration of substrate. However, in this case, the enzymes are saturated with 10 μ M cAMP, above the known K_m for PDE4B, in a time-course that represents a linear reaction over time. Thus, V_{max} is determined from the V_0 with saturated substrate. From each experiment,

Figure 3.7. 5FOA growth assays of strains expressing wild type PDE4B2, PDE4B2^{Y233H}, or PDE4B2^{T407A}. A) Growth treatment of strains in the presence of BC54. B) Growth treatment of strains in the presence of rolipram. Values represent the average of OD₆₀₀ ± standard error from three independent experiments. The values within each experiment represent an average of four replicate wells. Each experiment was incubated for 48h at 30°C.

Figure 3.7. 5FOA growth assays of strains expressing wild type PDE4B2, PDE4B2^{Y233H}, or PDE4B2^{T407A}

A



B

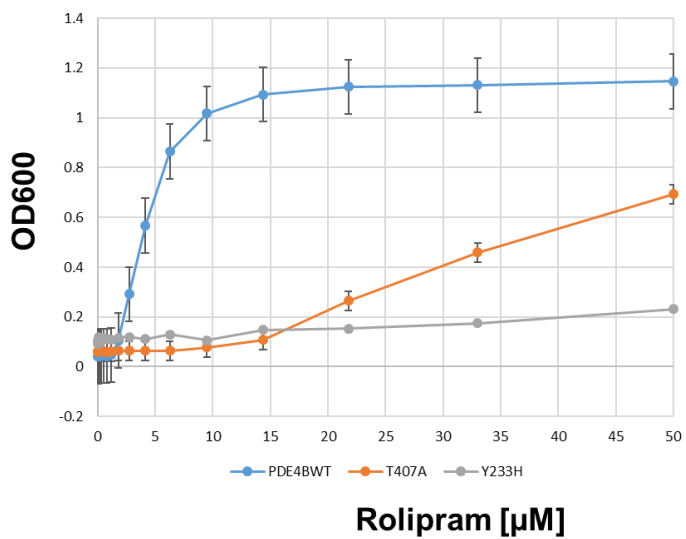


Figure 3.8. The amount of exogenous cAMP needed to activate PKA and repress the GFP reporter is a reflection of PDE activity. A rightward shift reflects increased PDE activity, while a leftward shift indicates reduced PDE activity. Values represent the average of normalized GFP to $OD_{600} \pm$ standard error from three independent experiments. The values within each experiment represent an average of four replicate wells. Each experiment was incubated for a 48h growth at 30°C.

Figure 3.8 The amount of exogenous cAMP needed to activate PKA and repress the GFP reporter is a reflection of PDE activity

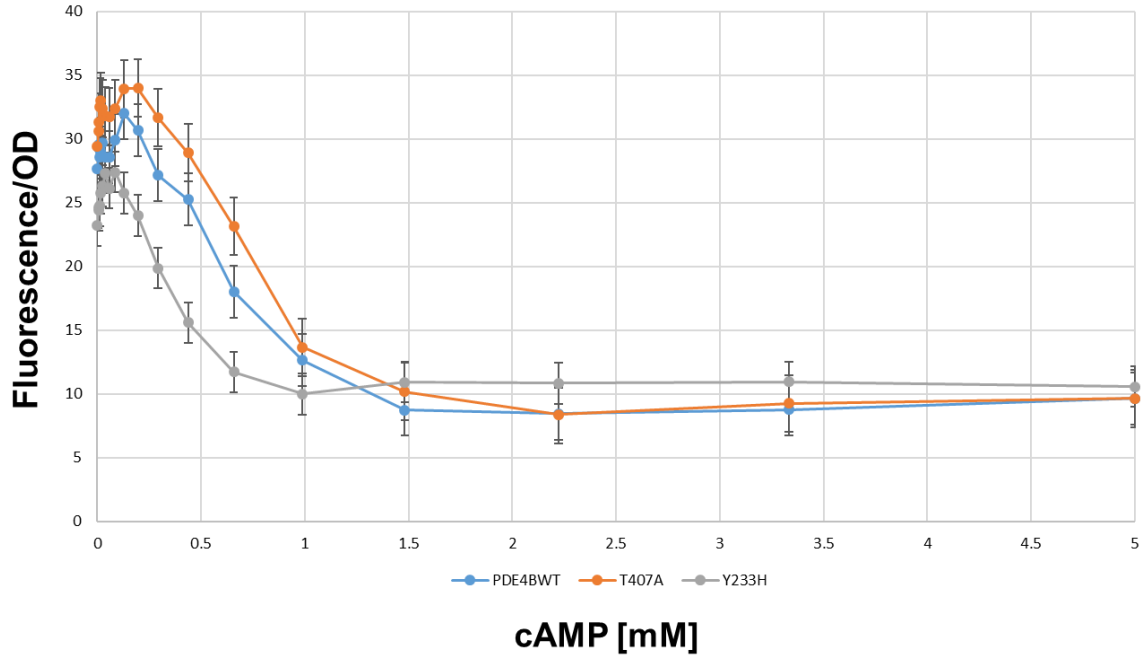
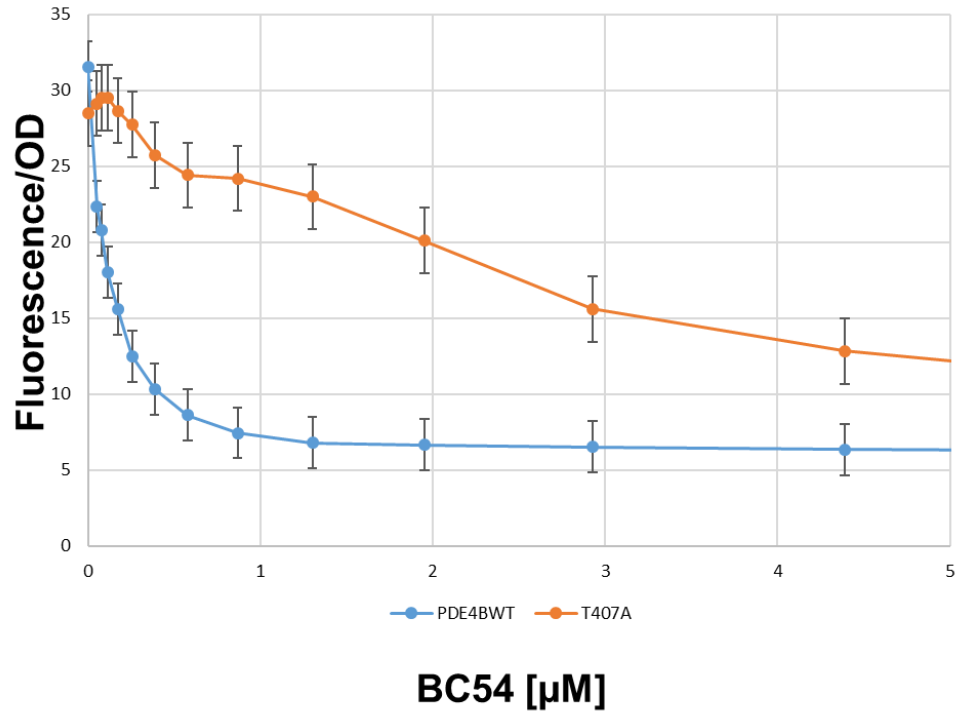


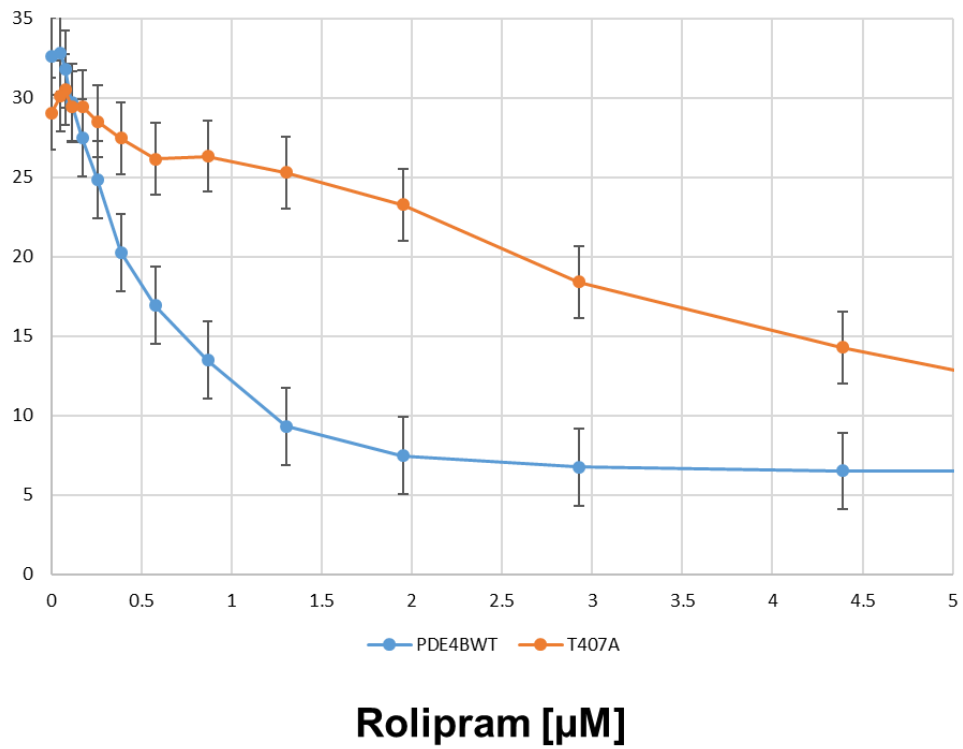
Figure 3.9. GFP assays strains expressing wild type PDE4B2⁺ or PDE4B2^{T407A}. A) Treatment of strains in the presence of BC54. B) Treatment of strains in the presence of rolipram. Values represent the average of normalized GFP to OD₆₀₀ ± standard error bars from three independent experiments. The values within each experiment represent an average of four replicate wells. Each experiment was incubated for a 48h growth at 30°C.

Figure 3.9 GFP assays strains expressing wild type PDE4B2⁺ or PDE4B2^{T407A}

A



B



a linear equation was obtained and used to calculate V_{max} (Figure 3.11a, b). The V_{max} values of wild type PDE4B⁺ (Figure 3.11a) were higher than in the PDE4B^{T407A} enzyme in every experiment (Figure 3.11b). The protein concentration was determined by a BCA assay and was used to identify the concentration of the enzymes used in the V_{max} experiment. The concentrations of PDE4B⁺ and PDE4B^{T407A} are 0.65 $\mu\text{g}/\mu\text{L}$ and 0.84 $\mu\text{g}/\mu\text{L}$, respectively. The turnover number was calculated by correcting the V_{max} for the protein concentration. The enzyme efficiency was calculated based on the V_{max} values previously obtained and adjusted according to the concentration of the proteins used for the assay (Figure 3.11). Based on these experiments, the wild type PDE4B⁺ is more efficient than the PDE4B^{T407A} enzyme (Table 3.2). In addition, the turnover (number of molecules converted per time) is higher for PDE4B⁺ than for PDE4B^{T407A} (Table 3.2).

The results for V_{max} , turnover, enzyme concentration and efficiency are summarized in Table 3.2. Overall, PDE4B⁺ is more efficient than PDE4B^{T407A}, achieving a higher V_{max} under the same conditions but using less protein, and converting more molecules into product over time. The next step is to perform IC_{50} for further characterization of enzyme activity in the presence of PDE4B inhibitors.

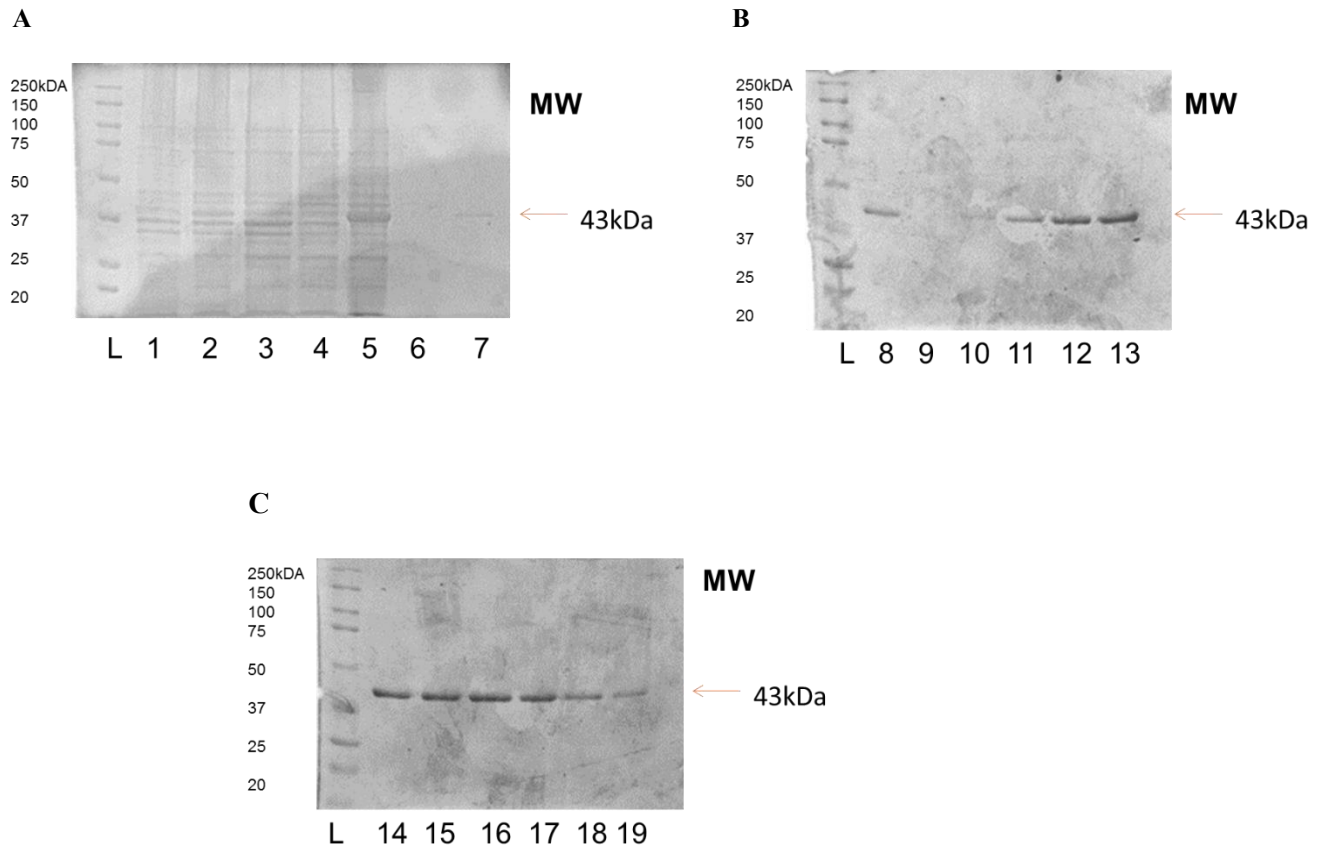
3.5.2 IC_{50} assays

To quantitate the sensitivity of PDE4B^{T407A} to PDE4B inhibitors in comparison to PDE4B⁺, *in vitro* enzyme assays (IC_{50} assays) were performed with both enzymes in the presence of either BC54 or Rolipram. In these assays, their IC_{50} values were determined based on the concentration of the inhibitor with the ability to reduce the enzyme activity for each assayed enzyme in 50%.

Nonlinear regression curves were used to determine IC_{50} values for both enzymes under each treatment (Figure 3.12). In the treatment with BC54, mutant PDE4B^{T407A} was less sensitive to the inhibitor in comparison to PDE4B⁺ treatment where the IC_{50} value for the mutant PDE4B^{T407A} was 19-fold higher in comparison to inhibition of PDE4B⁺ by BC54 (Figure 3.12a). However, the IC_{50} value for the mutant PDE4B^{T407A} in the rolipram treatment was only about 4-fold higher in

Figure 3.10. Protein purification of the PDE4B^{T407A} mutant protein. A) Affinity purification using talon beads. Purification steps were as followed: uninduced, induced, initial lysate, unbound, beads before elution, wash and elution (Lanes 1 to 7). B) and C) Ion-exchange purification using Q-Sepharose column. Washes A and B (Lanes 8 and 9, respectively) were performed before elution. Elution initiated with buffer C1 (lane 10) and continued with the collection of three fractions per buffer used: buffers C2 (lanes 11-13), C3 (lanes 14-16) and C5 (Lanes 17-19). Samples 13 to 16 were used for further concentration in Amicon tubes. This experiment was performed with T407A and it is representative for WTPDE4B purification steps. The IPTG induction of the lac promoter was performed as described in section 2.2.8. The SDS –PAGE gel was the method of detection used using Commassie blue stain. L corresponds to the Protein ladder described in chapter 2. All protein stocks were stored at -80°C.

Figure 3.10 Protein purification of the PDE4B^{T407A} mutant protein



comparison to WTPDE4B (Figure 3.12b). Overall, IC_{50} assays demonstrated that PDE4B^{T407A} is has a decreased affinity to both PDE4 inhibitors tested.

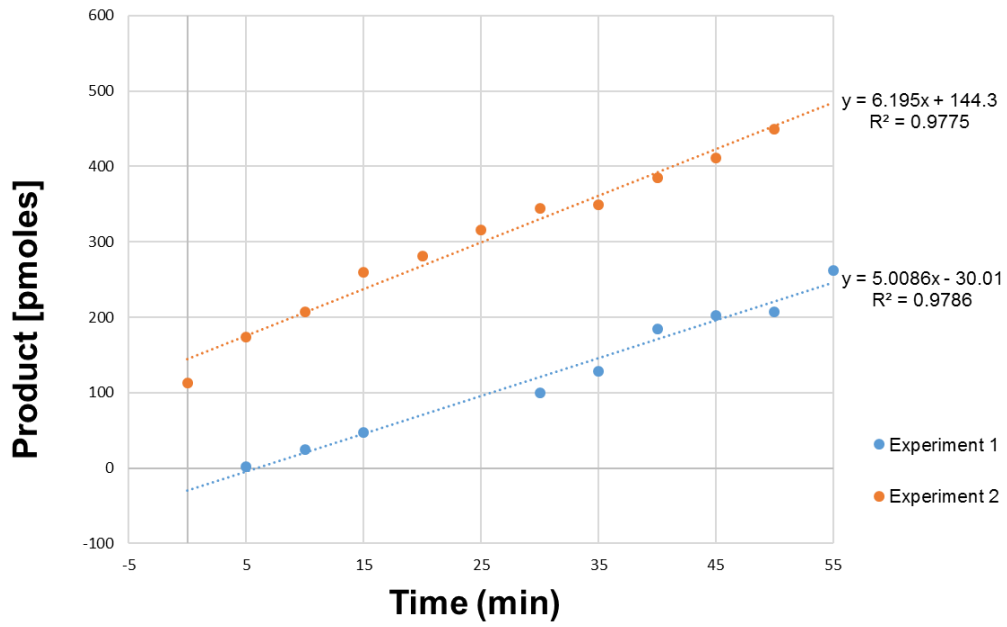
3.6 Conclusion

In this chapter, I demonstrated the development of a genetic screen to identified PDE4 alleles with altered behavior in the presence of BC54. This screen was used the survival phenotype associated with PKA activity. Furthermore, I have identified and characterized two PDE4B-resistant alleles to BC54 using two cell-based assays along with in vitro assays. The two mutant enzymes have single amino acids as followed: PDE4B^{Y233H} and PDE4B^{T407A}. Both mutant proteins are resistant to BC54 as well as rolipram. In addition, our data suggest that both PDE4B mutant proteins are less active than the wild type PDE4B. This decrease in activity does not seem correlate with increase in hydrolysis of cAMP. I can conclude this genetic screen is a great tool to generate PDE mutants. In the future, we can generate a larger collection of PDE mutants for further characterization of their enzymatic activity. Another approach is to introduce these two mutations in other PDE4 isoforms and assess differences in enzyme activity and inhibition. I believe the generation of mutants and treatment in the presence of compounds will help us have a better understanding in the mechanism of interaction of PDEs and their regulators.

Figure 3.11. Vmax values based on a linear reaction with time. A) Vmax of WTPDE4B enzyme. B) Vmax of T407A enzyme. Values represent the V_0 of two separate experiments. Linear equation (on the right) in every experiment was used to calculate V_0 that under saturating conditions represent Vmax. The dilutions used for the WTPDE4B and T407A were 1:10,000 and 1:20,000 and 40 μ L was assayed for each enzyme.

Figure 3.11 Vmax values based on a linear reaction with time

A



B

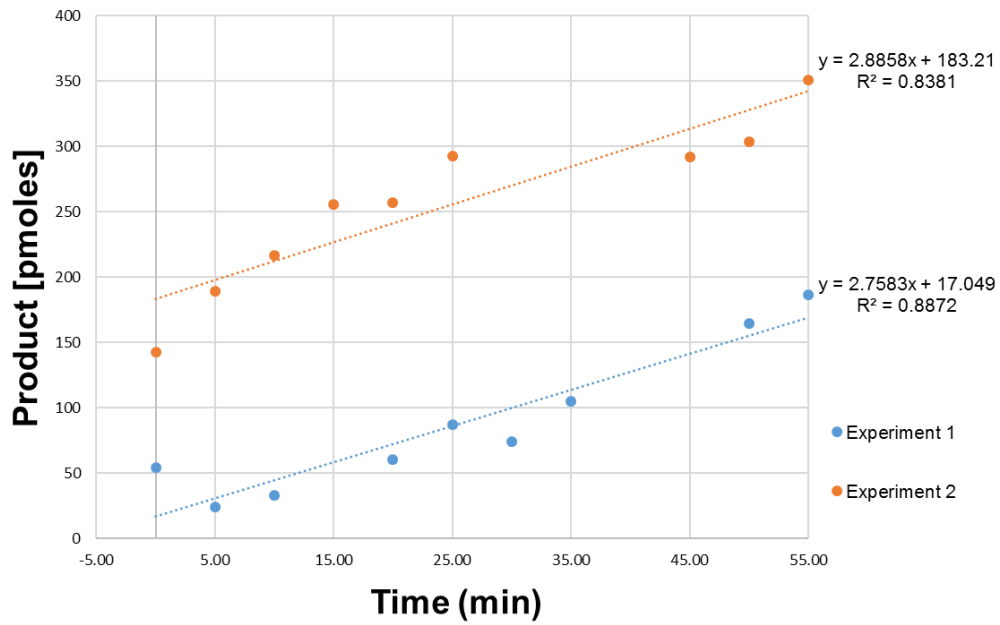


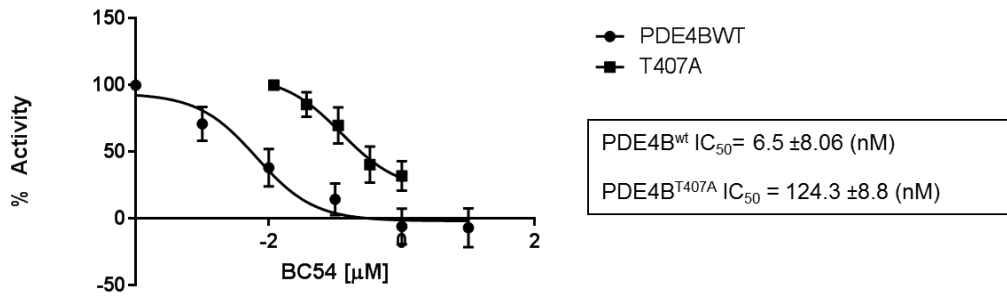
Table 3.2. Properties of enzyme kinetics for PDE4B2 and PDE4B2^{T407} enzymes

Enzymes	Vo=Vmax (pmol/min)	[E] µg/µL	Dilution used in the assay	Turnover (min⁻¹)	Efficiency (pmols/min -mg)
PDE4WT	5	0.65	1:10,000	80	1.91
	6.2			99.5	2.37
T407A	2.75	0.84	1:20,000	68.88	1.64
	2.88			71.4	1.7

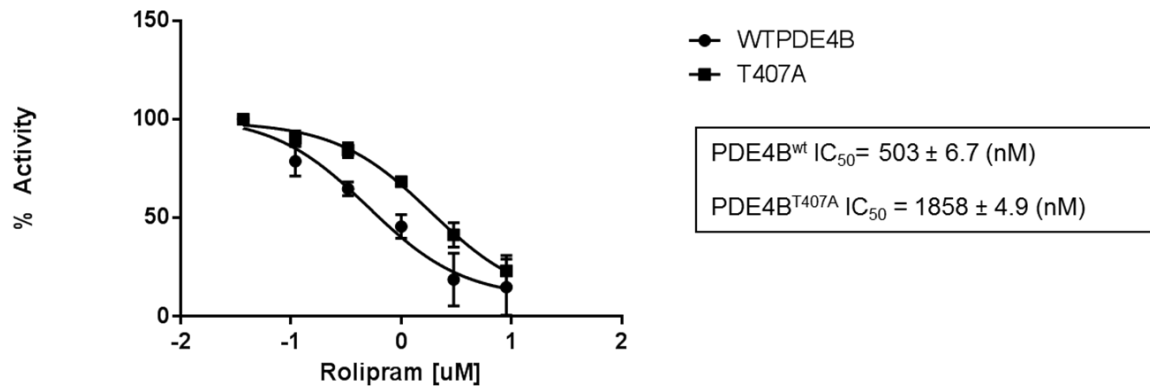
Figure 3.12. IC₅₀ assays. A) Inhibition of PDE4B^{wt} and PDE4B^{T407A} by BC54. B) Inhibition of PDE4B^{wt} and PDE4B^{T407A} by Rolipram.

Figure 3.12 IC₅₀ assays

A



B



CHAPTER FOUR

DEVELOPMENT OF A HIGH THROUGHPUT SCREEN FOR PDE ACTIVATORS

4.1 Development of a chemical screen for phosphodiesterase activators

Small molecule regulators of PDEs are important as chemical probes to study the roles of individual PDEs and as potential therapeutics. While there have been many efforts by both academia and industry to develop PDE inhibitors, relatively little work has been done to identify small molecule activators of PDEs. Therefore, I used a cell-based GFP assay to develop a HTS that is better-suited to detect small-molecule PDE activators that reduce PKA activity than a screen based on expression of the *fbp1-ura4* reporter that has been used to detect PDE inhibitors (Figure 2.2b) (de Medeiros et al., 2015). As a proof of concept for this screening platform, I carried out a 10,000 compound screen for small molecule activators of the human PDE4D3 enzyme. The screening strain (CHP1702) expresses PDE4D3 enzyme that possesses an N-terminal inhibitory domain, which displays less PDE activity than does a strain expressing PDE4D2 (CHP1742) that lacks this domain (Figure 1.3b). Due to lack of known PDE4 activators, we used CHP1742 as a control due to its higher PDE4D activity. Thus, CHP1742 produces a higher GFP signal in comparison to the screening strain (Figure 4.1a). Further, since the PKA level in a strain also affects its growth rate, GFP values have been normalized by OD₆₀₀ values (Figure 4.1b). The normalized values are summarized in Table 4.1.

Strains used in this screen (CHP1702 and CHP1742) were generated as previously described in section 3.1, but expressing the *fbp1-GFP* reporter (Table 2.1) (de Medeiros et al., 2015). By matching the level of cAMP synthesis in strains carrying various mutations affecting the fission yeast glucose/cAMP pathway with the activity of a target PDE, we are able to generate sensitized

strains that require more exogenous cAMP than strains lacking PDE expression to reduce GFP signal to 10 units. As seen in Figure 4.2 using strains for which exogenous cAMP is used to control PKA activity, a normalized GFP signal of 10 units reflects a level of PKA activity for which a further reduction should be detectable when treating PDE-expressing strains with small molecule activators of a given PDE. In order to keep the reporter off for proper assessment of compound hits for PDE4D3, exogenous cAMP was added to EMM medium during the growth of both experimental and control strains prior to initiating the GFP assay (Table 2.3).

4.2 Optimization of fission yeast HTS for PDE activators

The optimal conditions for a robust PDE activator HTS should provide a large difference in the fluorescence signal in cells that have been exposed to a PDE activator when compared to control cells exposed to the vehicle DMSO. In order to keep the well-to-well variability low, the fluorescent signal is normalized to the optical density (OD₆₀₀) of the cultures. The assay development involved 3 steps: (1) establishment of pre-assay growth conditions that repress the GFP reporter, which promotes proper assessment of activation of PDE in the presence of compound and comparison to fluorescence of control; (2) determination of an optimal initial cell density; (3) establishment of the type of readings taken at 0 and 48-h.

The best conditions for GFP assays with either PDE4D3- or PDE4D2 –expressing strains were the addition of 20mM cAMP in the pre-growth of cells in EMM medium, and three washes for complete removal of cAMP prior to the screening. The initial cell density of 4×10^6 cells/mL allows cells to grow to saturation (OD ~ 1) after 48h at 30° C. The GFP values are higher and OD₆₀₀ values are lower in the control strain versus the experimental strain as an indicative of low PKA activity in the control strain (Figure 4.1a, b).

Once the conditions for the HTS were established, a mock assay was performed to determine the Z'-factor, which is a statistical measurement of the robustness of the screen (Franz et al., 2007). In this screen, the Z'-factor corresponds to the difference between the positive control (genetic control

treated with DMSO) and the negative control (experimental strain treated with DMSO), based on the variation among data-points. A robust HTS produces Z'-factor values between 0.5 and 1 and is calculated using the following formula:

$$Z'\text{-factor} = \frac{1 - 3(\sigma_p + \sigma_n)}{(\mu_p - \mu_n)}$$

where σ and μ represent the standard deviation and the mean, respectively, for both positive (p) and negative (n) controls.

The appropriate conditions for data analyses were taken by collecting top and bottom readings of both GFP and OD₆₀₀ values. The bottom reading provides the most appropriate data assessment because the fluorescing cells are concentrated on the bottom of the well. GFP values are collected as described in section 2.2.12. In addition, GFP and OD₆₀₀ values were collected at 48h (prior to incubation) to identify fluorescent compounds. The GFP values at 0h and 48h (Figure 4.3a, b) and OD values (Figure 4.3c) can be visualized using the Vortex software.

4.3 Screen with a compound library

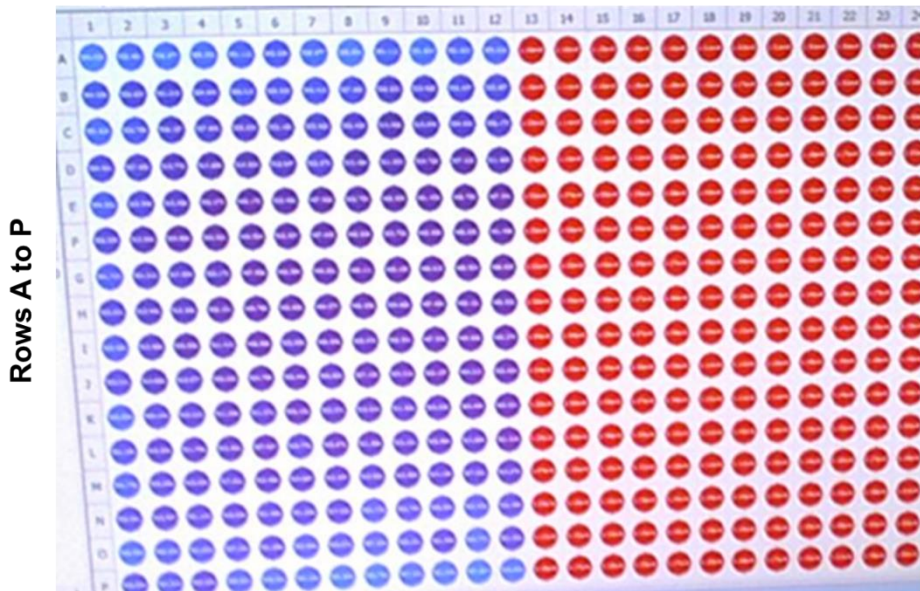
The HTS screen for PDE4D3 activators was performed at the ICCB-Longwood Screening Facility at Harvard Medical School. The Chembridge 3 library was chosen for this initial HTS for PDE4D3 activators and has a total of 10,560 compounds. The chemical screening, comprised of several steps, from delivery of the cells to pinning of compounds, data collection and analyses (Figure 4.4a). In the initial step, 30 μ L of cells in EMM were delivered into 384-well plates in duplicates and 100nL of compounds from the library plates were pinned into the wells followed by incubation for 48h at 30° C. The compound stock solutions from Chembridge were generally at ~5mg/mL as the initial concentration with a final concentration of ~30 μ M. The controls were included in every screening plate in column 23 (negative controls) and column 24 (positive controls) (Figure 4.4b). Fluorescence and OD₆₀₀ values were initially assessed with the use of the Vortex software (Figure 4.3) and followed by calculation of Z-factor and Z-scores as previously described (sections 2.2.11.1

Figure 4.1. Heatmap displaying reproducibility of GFP and OD values from screening and control strains. A) Heatmap of fluorescence readings. B) Heatmap of OD₆₀₀ readings. Screening strain CHP1702 was delivered in columns 1 to 12. Positive control strain CHP1742 was delivered in columns 13 to 24. Blue indicates low GFP (400,000 units) or OD values (below 0.5). Red indicates high GFP (Above 800,000 units) or OD values (~1.0). This assay was used to estimate the robustness of the assay (Z' -factor; see Table 4.1). Readings were taken after a 48h incubation at 30°C.

Figure 4.1 Heatmap displaying reproducibility of GFP and OD values from screening and control strains.

A

Columns 1 to 12 (CHP1702) Columns 13 to 24 (Positive control)



B

Columns 1 to 12 (CHP1702) Columns 13 to 24 (Positive control)

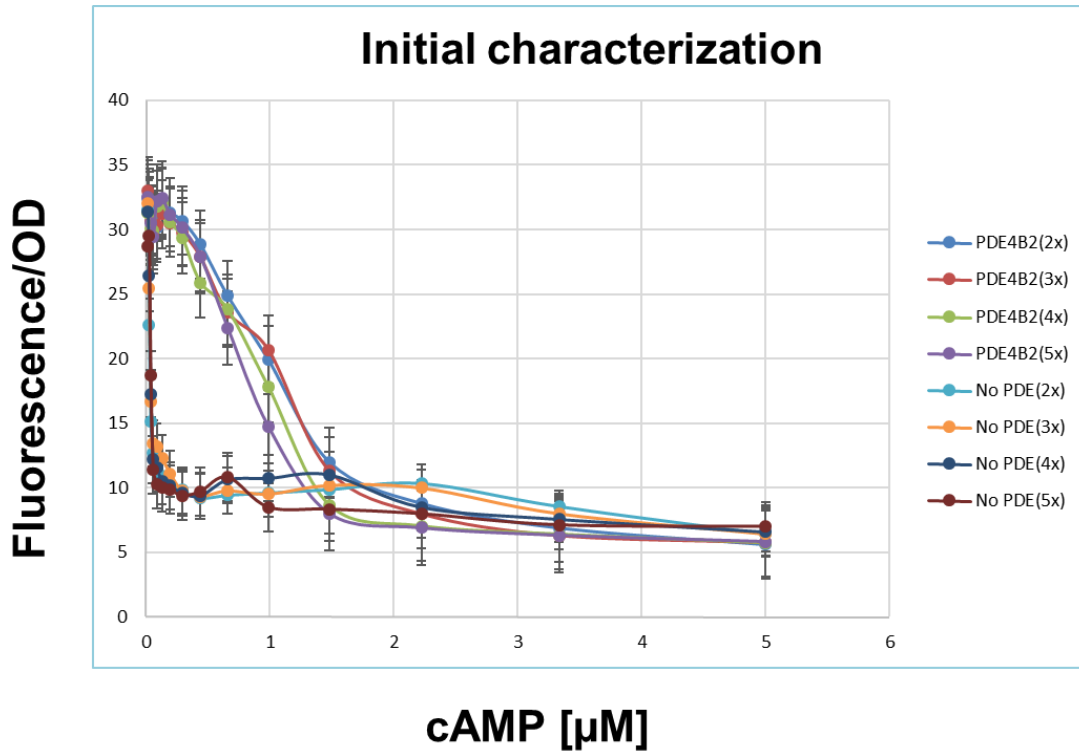


Table 4.1. Normalized Fluorescence of optimized HTS

Strain	Mean (plate 1)	Mean (plate 2)	Standard Deviation (Plate 1)	Standard Deviation (Plate 2)	Z' factor (Plate 1)	Z' -factor (Plate 2)
CHP1702	678455	654289	55868.80085	73793	0.675	0.47
CHP1742	2138139	2078457	102347	282535		

Figure 4.2. Cells expressing PDE4B require more exogenous cAMP than a strain lacking PDE activity to repress GFP reporter. In cells lacking AC activity, the amount of exogenous cAMP needed to reduce the GFP fluorescence is a reflection of PDE activity. In this experiment, the GFP fluorescence (normalized to the OD₆₀₀) was compared between a strain lacking PDE activity and strains expressing different PDEs. These results are consistent through a range of initial cell densities (2×10^6 to 5×10^6 cells/ml) and show that PDE4B2 activity can hydrolyze some of the exogenous cAMP to increase GFP expression. It also shows that for strains that have an intact AC enzyme, a value of ~ 10 units represents a level of PKA activity for which a further reduction in activity would likely cause a detectable elevation in the GFP signal.

Figure 4.2 Cells expressing PDE4B require more exogenous cAMP than a strain lacking PDE activity to repress GFP reporter.



and 4.2). Variations of raw GFP and OD values were analyzed by Vortex software (Figure 4.5). These variations are generally due to fluorescence, well-to-well variation, and temperature changes during incubation.

For each compound, a Z-score was calculated. Z-scores represent the number of standard deviations above or below from the mean of the negative controls wells. Z-scores above 6 are considered “hits” and compounds that produce the highest Z-scores in both duplicates are selected for a Cherry-Pick for further validation as long as they do not appear to be fluorescent or toxic. In this screen, the classification of Z-scores was required for a better selection of hits. The classification is listed in Table 4.2.

4.4 Validation of primary screen Hits

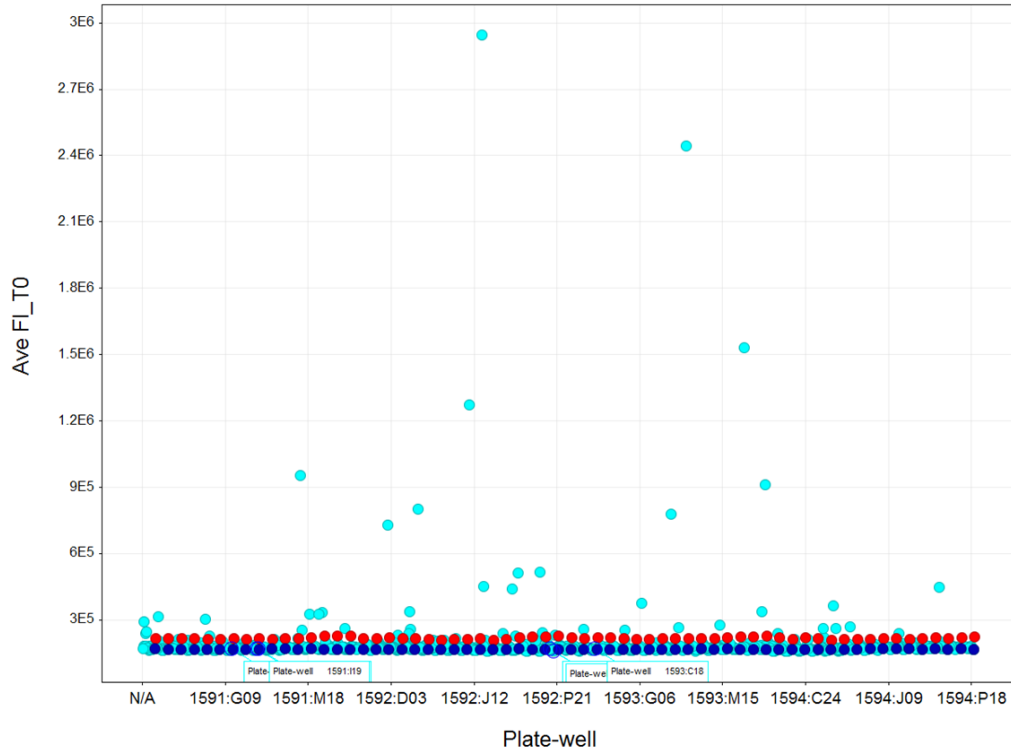
4.4.1 Selection of compounds for cherry-pick experiments

At the end of the primary screening, 1,015 compounds were identified as candidate hits, however 963 compounds could be eliminated as either fluorescent or toxic compounds that would produce a false positive value in this assay. The first step to reconfirm the remaining hits is to analyze the Z-scores, as mentioned in Table 4.2, to create a list of candidate hits for cherry pick. Typically, only 0.3% of the total library tested can be rescreened in the Cherry-pick assays. However, as this was our first effort using this new HTS for PDE activators, 52 compounds were selected for validation in the Cherry-pick assays (Figure 4.6). This selection was based on their Z-score values. The compound candidate hits were rescreened against the PDE4D3-expressing strain and against yeast strains expressing a combination of mammalian AC4 and PDE4D3 (CHP1807) or mammalian AC4 only (CHP1812). The rationale for choosing these strains is that a PDE activator will be a hit in strains that express the PDE4D3 enzyme, while false positives will appear to act on CHP1812 as well. After the screening, false positive compounds for PDE4D3 were eliminated. These compounds were increasing fluorescence by hitting targets other than our enzyme of interest,

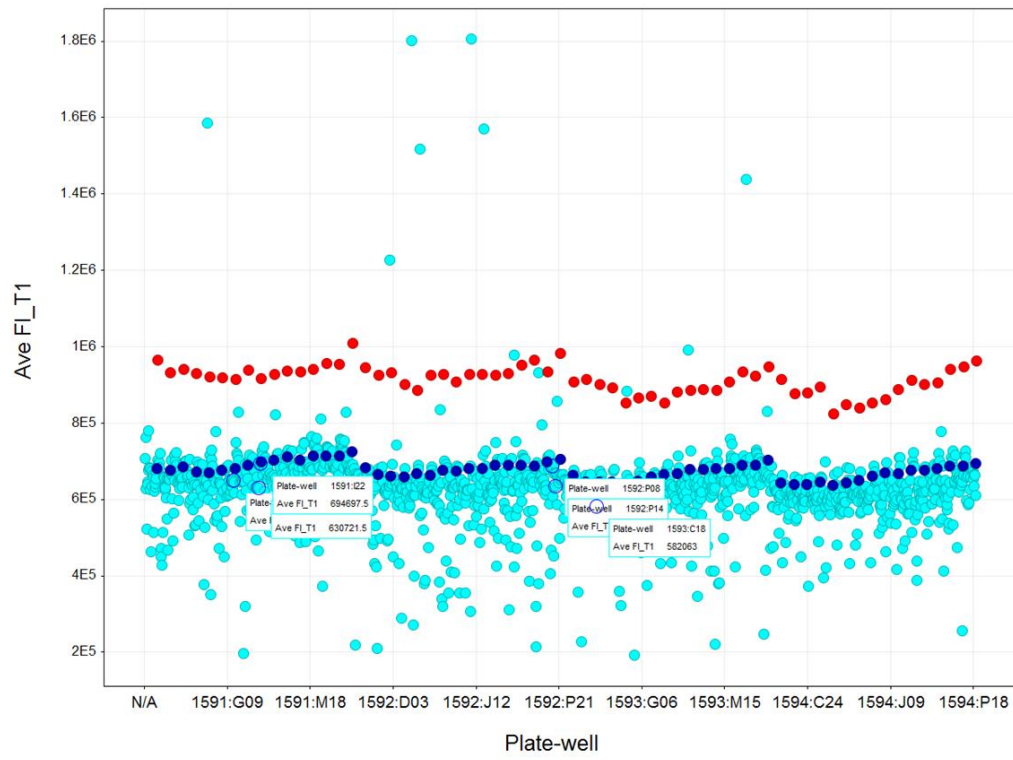
Figure 4.3. Qualitative data overview of 10,000 compound screen. A) Average of fluorescence at time zero. B) Average of Fluorescence at 48h. C) Average of OD₆₀₀ at 48h. Data analyses was performed using Vortex Software. Color coding: Cyan= Experimental sample; Dark blue= Negative controls; Red= Positive controls. This experiment was performed in duplicates. The Y-axis indicates the average values of either fluorescence or OD. The X-axis indicates the plate and well of each compound treatment.

Figure 4.3 Qualitative data overview of 10,000 compound screen

A



B



C

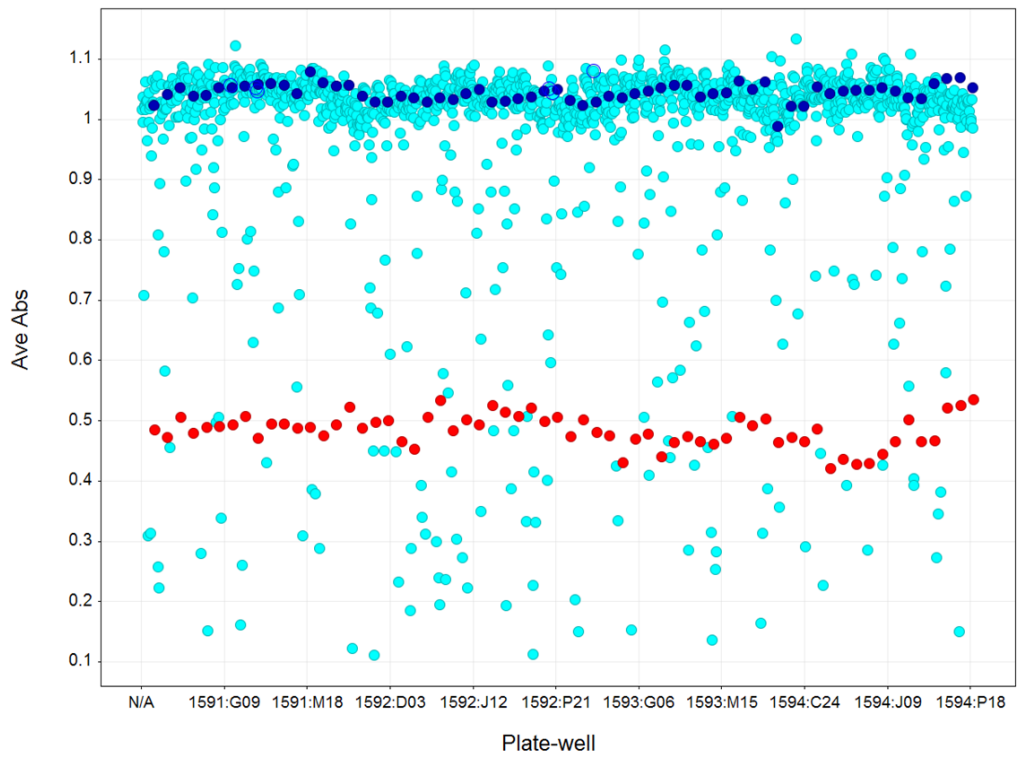
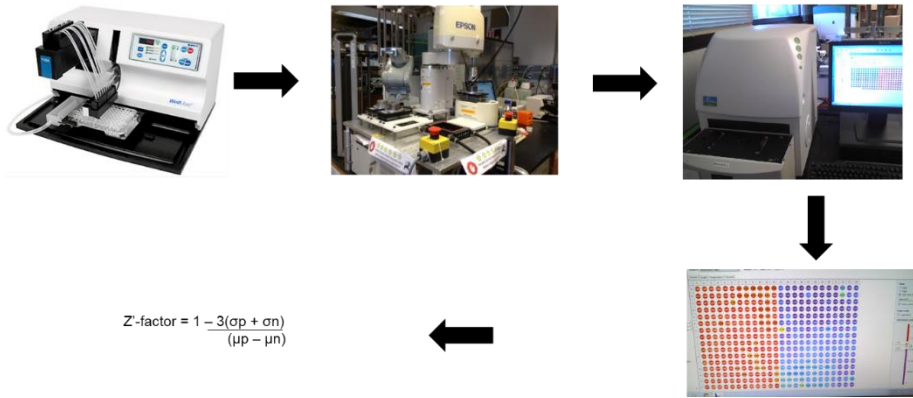


Figure 4.4. High throughput screen for PDE4D3 activators. A) HTS steps are composed of delivery of the cells using a cell dispenser to pinning of compounds using a robot, followed by data collection using Envision which produces a heatmap as it reads each plate followed by data analysis by calculating Z' -factor for quality of assay and further progress of the HTS. B) Example of a screening plate readout. The column 23 and 24 contain negative (CHP1702 treated with DMSO) and positive controls (CHP1742 treated with DMSO), respectively. The colors of wells represent their fluorescence values, increasing from blue to red. Hit compounds were identified based on the higher normalized GFP of the cultures.

Figure 4.4. High throughput screen for PDE4D3 activators

A



B



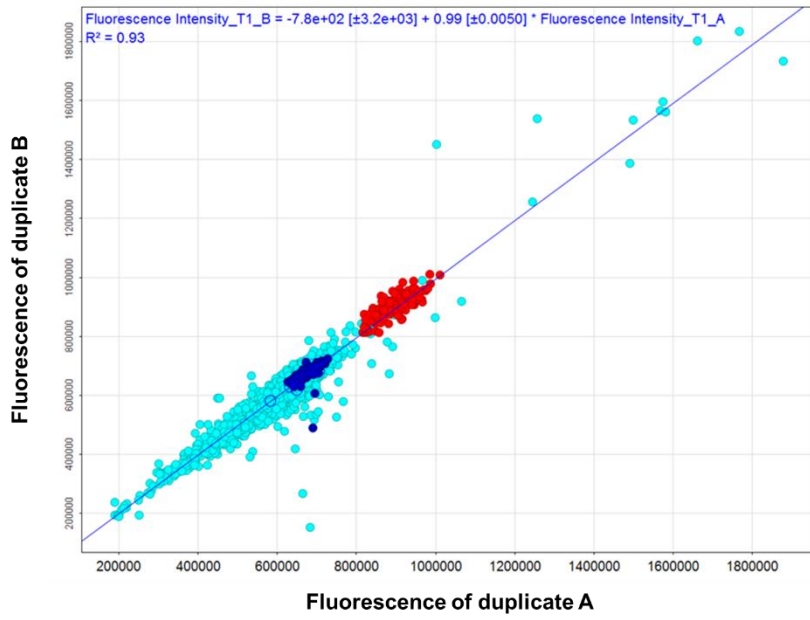
Table 4.2. Classification of Hits according to Z-scores of duplicates

S=both Z scores are >25
M= both Z scores are >15, but not >25
W= both Z scores are >7.6, but not >15
OD's <0.6
Fluorescence at T0 > 200000 units

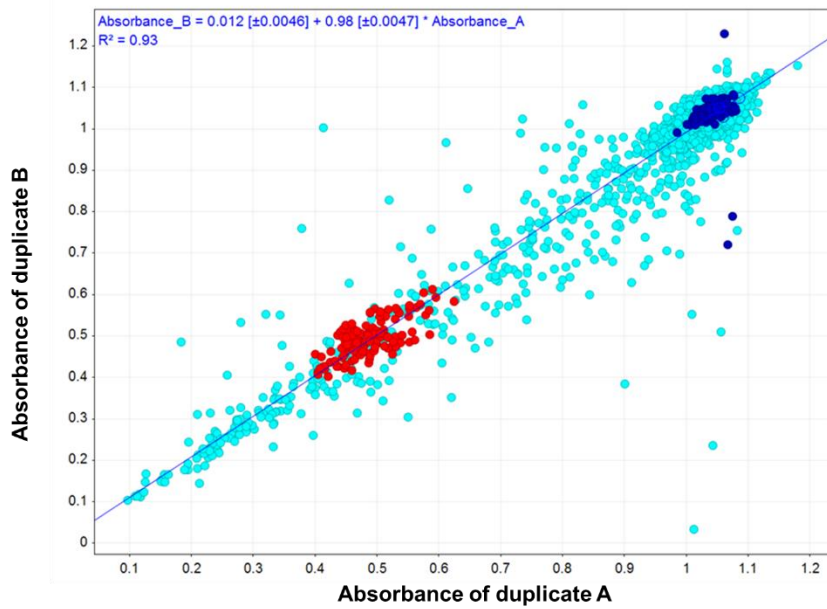
Figure 4.5. Results of the HTS. A) Scatter plot representing fluorescence values for duplicate wells pinned with 100nL of compounds or DMSO. B) Scatter plot representing OD values for duplicate wells pinned with 100nL of compounds or DMSO. Values along the X and Y axis represent the results from each of a pair of duplicate plates. Experimental samples treated with compounds are depicted in cyan circles. Negative controls treated with DMSO are depicted in dark blue circles. Positive controls treated with DMSO are depicted in red circles.

Figure 4.5. Results of the HTS

A



B



PDE4D3. A total of 20 compounds were selected for counter-screen assays at Boston College (Table 4.3).

4.4.2 Counter-screen assays

The 20 candidate PDE4D3 activators were subjected to counter-screen assays in an effort to confirm their putative activity. I used GFP assays to evaluate candidate hits and eliminate false-positive or non-selective candidates. The same strains used for the Cherry-pick assays were used for the GFP assays (Figure 4.7a, b, c). To simplify nomenclature, the candidate compounds were named A1 to A20. The rationale was to quickly eliminate compounds that were targeting proteins other than PDE4D3. Based on this GFP assessment, compounds A2, A4 and A14 were eliminated due to increase in fluorescence in treatment with strain CHP1812 that does not express PDE4D3 (Figure 4.7c). To better visualize treatment of compounds with the three chosen strains, two candidates will be shown (Figure 4.8a, b).

Both the A11 and A17 compounds promoted an increase of GFP fluorescence in the strains expressing PDE4D3 (Figure 4.8a, b). The strain expressing the fission yeast AC has a slight increase in fluorescence compared to the strain expressing mammalian AC, which reflects the stronger AC activity in fission yeast in comparison to the mammalian AC. Both compounds had no effect in the strain CHP1812, which lacks PDE activity (Figure 4.8a, b). Furthermore, neither compound was validated as I was unable to demonstrate a decrease in cAMP levels using cAMP assays (data not shown). The summary of the HTS is depicted in Table 4.4. Although, there were no confirmed candidate PDE4D3 activators, our yeast –based HTS successfully shows that we can successfully detect increased GFP, but that it may not reflect a change in PKA activity.

The lack of validation of the potential hits points out a potential issue with the assay or may be difficult to detect fluorescence levels that are associated with PDE activity. Therefore, if one wants to find compounds that act by reducing PKA activity, it may be easier to detect AC inhibitors than it is to find PDE activators, as the decrease in production of cAMP and consequent of PKA activity

Figure 4.6. Pie-chart of candidate hit compounds. A total of 1,015 candidate hits were identified in the primary screen. After elimination of toxic and fluorescent compounds, 52 compounds were rescreened for validation. After that, 20 compounds were selected for further testing in counter-screens.

Figure 4.6 Pie-chart of candidate hit compounds

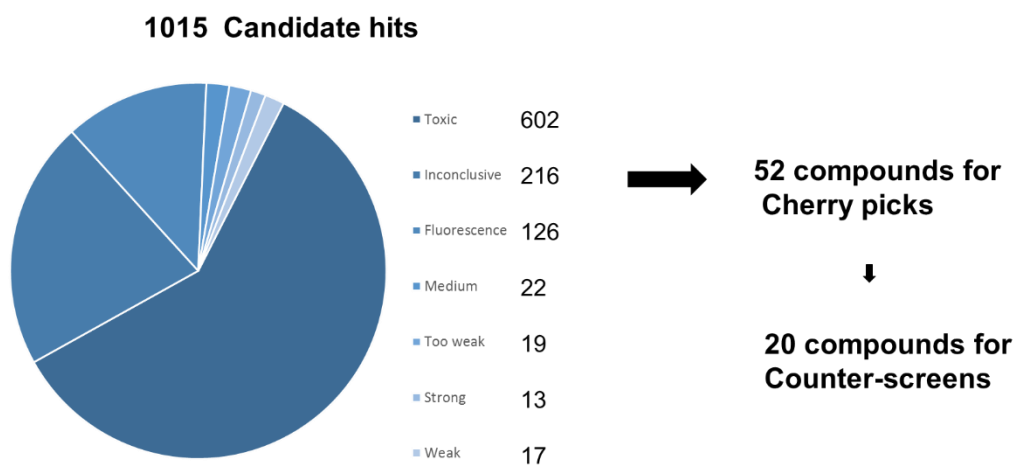


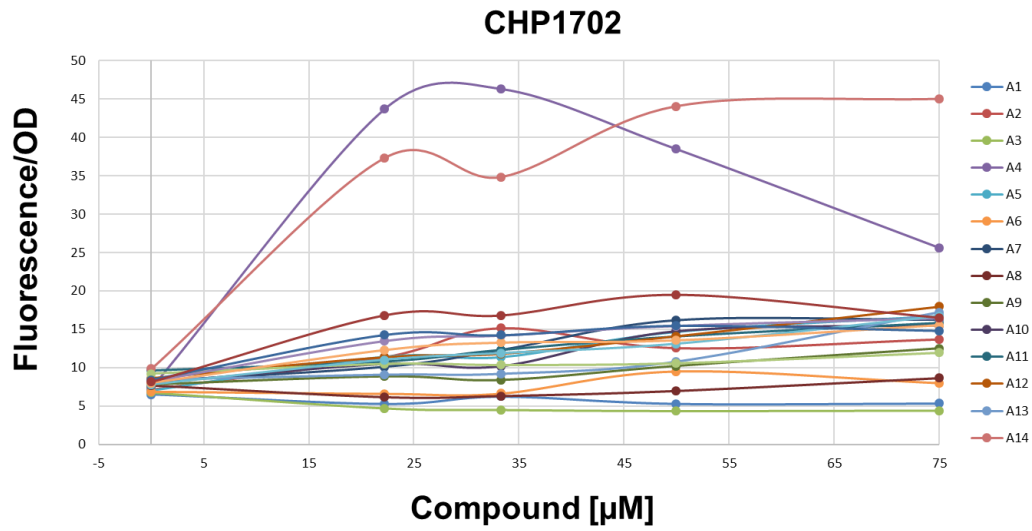
Table 4.3 List of Chembridge compounds selected for secondary screens

Compound Candidates	Catalog number
A1	5115325
A2	5115555
A3	5141013
A4	5248611
A5	5354034
A6	5457747
A7	5459675
A8	7395070
A9	7668702
A10	7904106
A11	7910193
A12	7926862
A13	7937708
A14	7962037
A15	9002075
A16	9024667
A17	9025694
A18	9031439
A19	9036941
A20	9040995

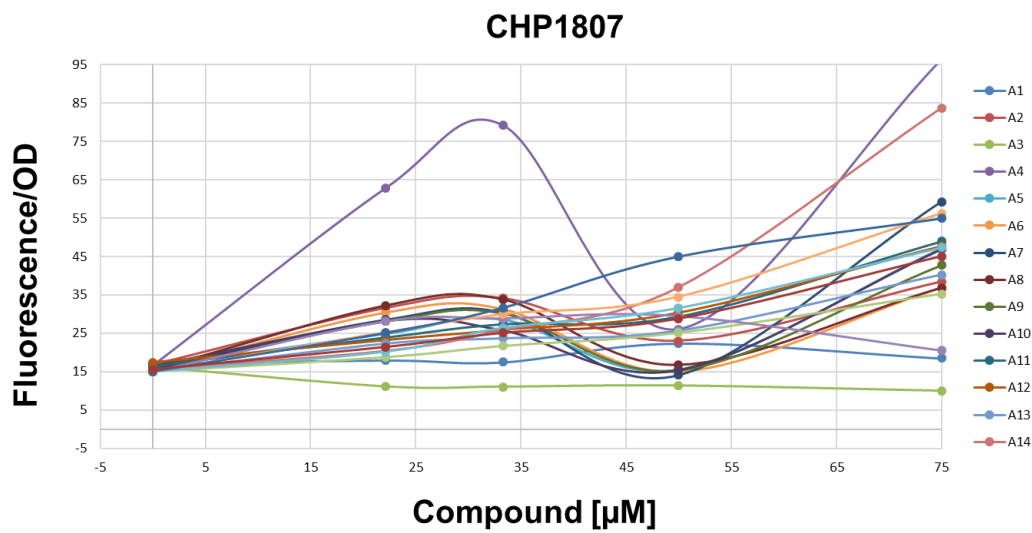
Figure 4.7. Counter-screen of compounds A1 to A20. A) Strain CHP1702 treated with compounds. B) Strain CHP1807 treated with compounds. C) Strain CHP1812 treated with compounds. This screen was carried out with strains that express either fission yeast AC (1702) or mammalian AC (1807) along with PDE4D3 or expressing only mammalian AC with no PDE (1812). All strains were treated with all 20 candidate hits. Experiments were performed in quadruplicates. All plates were incubated for 48h at 30°C.

Figure 4.7 Counter-screen of compounds A1 to A20

A



B



C

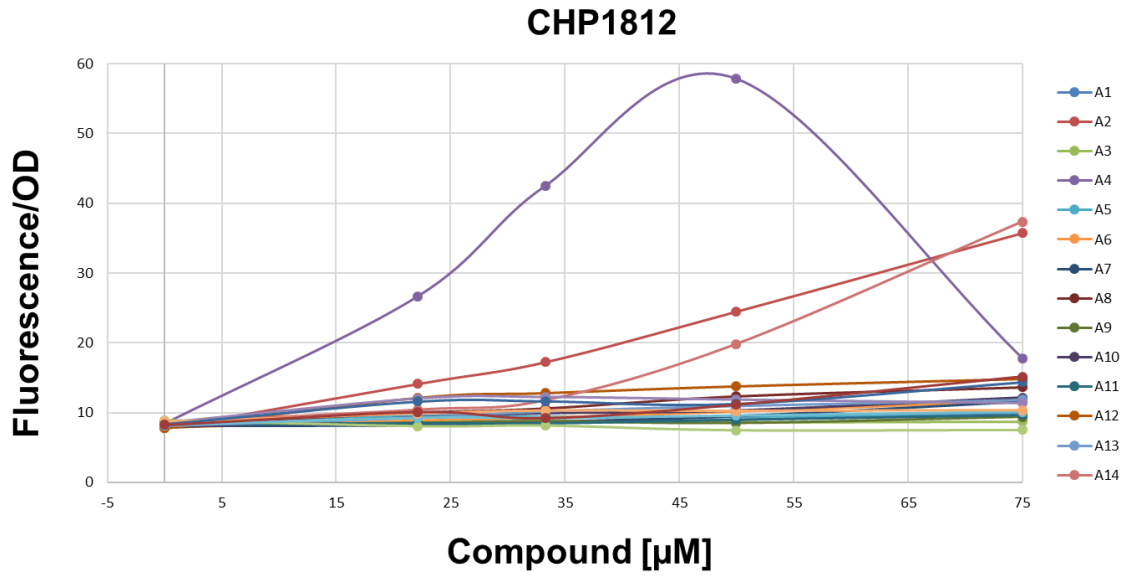
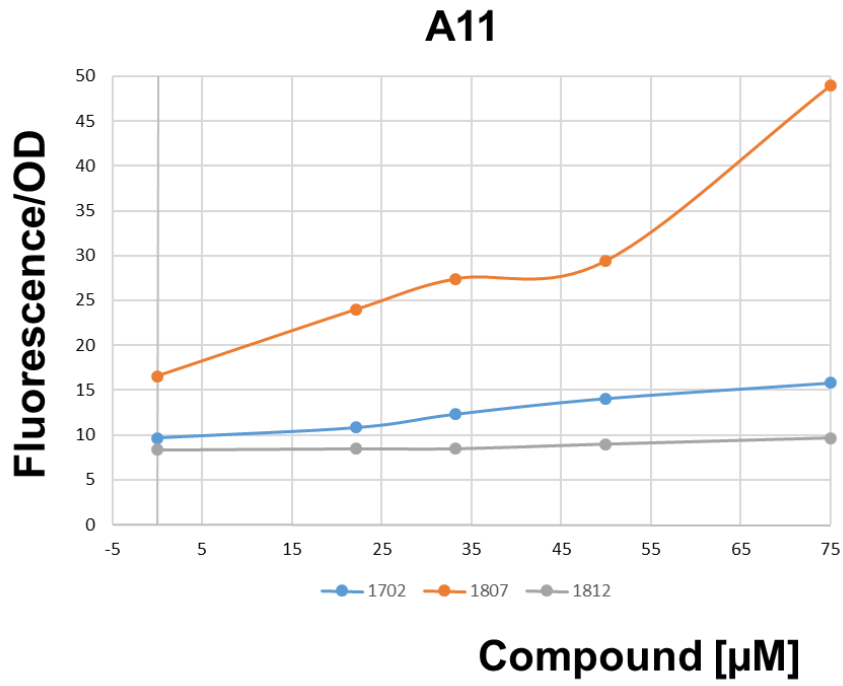


Figure 4.8. Counter-screen of compounds A11 and A17. A) Counter-screen of compound A11 and B) Counter-screen of compound A17 with three strains. This screen was carried out with strains that express either fission yeast AC (1702) or mammalian AC (1807) along with PDE4D3 or expressing only mammalian AC with no PDE (1812).

Figure 4.8. Counter-screen of compounds A11 and A17

A



B

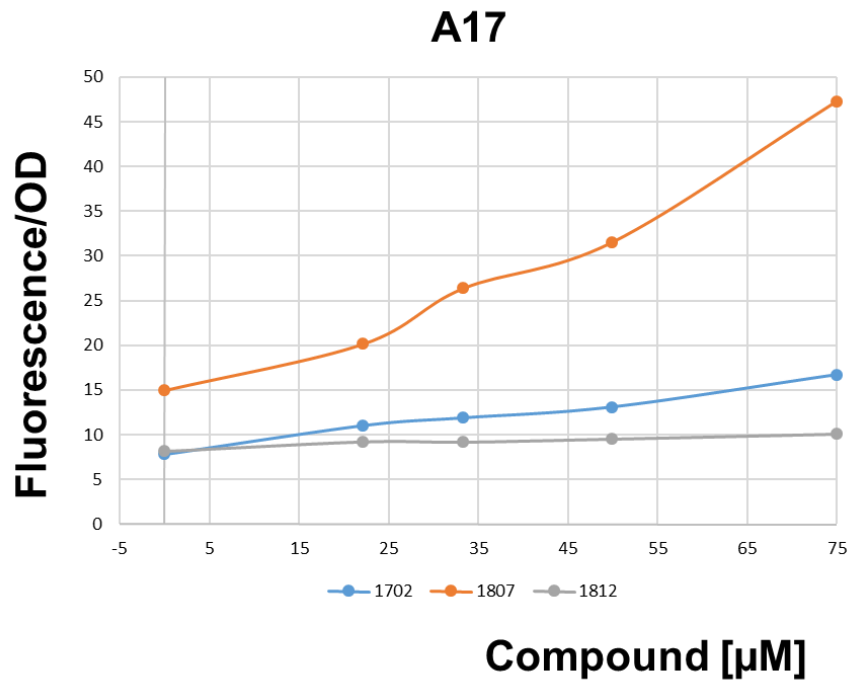


Table 4.4. Characterization of candidate PDE4D3 candidates

Screened	Acquired	Confirmed
10,560 compounds	20 candidates	0

can be greater than inhibiting its regulator responsible for its destruction. In an effort to diminish potential problems with the assay and identify AC inhibitors, the next step is to expand HTS screening two strains in parallel to identify AC and GNAS1 inhibitors along with PDE activators.

4.5 Conclusion

There has been a remarkable effort to understand PDE structure, regulation and function. In the past few years, many inhibitors have been designed and placed into clinical trials. To fully understand PDE regulation is important to know not only what happens when enzyme activity is inhibited, but what happens when the enzyme activity is increased. Despite the need, there are no known small molecule activators of PDE4 enzymes. Therefore, I developed a HTS screen to identify PDE activators. Using a yeast HTS screen, I was able to detect candidate hits based on increased fluorescence. However, the potential hits were not validated. To exclude the possibility of technical issues with the assay itself or with the difficulty to screen for PDE activators, I suggest to expand the HTS comparing two strains along with the inclusion of AC inhibitor screening in future experiments.

CHAPTER FIVE

HIGH THROUGHPUT SCREEN FOR PDE ACTIVATORS OR AC/GNAS1 INHIBITORS

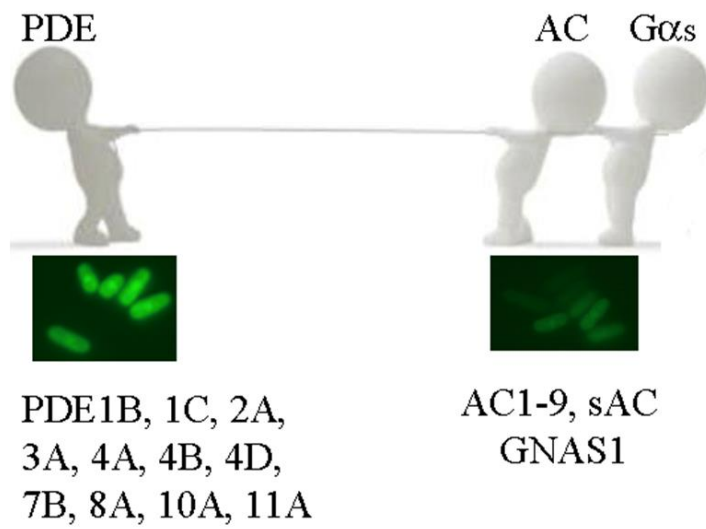
5.1 HTS for small molecules that reduce PKA activity using commercial libraries

The data presented in chapter 4 demonstrate that the *fbp1- GFP* reporter can be used for a robust assay detecting small molecules that increase fluorescence. However, I have not completely eliminated problems with false positives. In this chapter, I have expanded the screen for compounds that reduce PKA activity to include target proteins involved in cAMP production and made two changes from the chapter 4 screen that are designed to increase the likelihood of success: the inclusion of a counter-screen strain and the expansion of the screen to 100,000 compounds.

I used the 10,000 HTS as a proof of concept to develop a HTS that is better-suited to detect small-molecules that reduce PKA activity, which would include PDE activators and AC or GNAS1 inhibitors (Figure 5.1). This screen was HTS performed at ICCB- Longwood Screening Facility at Harvard Medical school. The screening process was similar to that described in Chapter 4, however fluorescence at T=0 was not determined since I used a counter-screen strain in parallel to the screening strain that should identify false positives due to fluorescence. For this HTS, I used two strains (CHP1823 and CHP1882) along with the positive control strain (CHP1742). These strains have basal GFP values that are somewhat similar and were in a level that are great for screening. The screening strain (CHP1823) expresses PDE4D3 enzyme that possesses an N-terminal inhibitory domain, as mentioned in Chapter 4. Strain CHP1882 was used as the counter-screen to help eliminate nonselective hits and false positives. In addition to the expression of different PDEs, the screening strain expresses AC5 and the counter-screen expresses AC1 (Table 2.1). The lack of validation for the potential hits described in Chapter 4, raised concerns to both a technical problem

Figure 5.1. HTS for compounds that reduce PKA activity. HTS with two strains in parallel targeting five mammalian genes (PDE4D3 and AC5 or PDE7B1, AC1 and GNAS1). Small molecules of interest will increase the GFP signal (Figure acquired from Dr. Hoffman).

Figure 5.1 HTS for compounds that reduce PKA activity



Pilot 100,000 compound screen against:
PDE4D3 vs. AC5 and PDE7B1 vs. AC1+GNAS1

with the assay and/or difficulty in screening PDE activators. Therefore, I decided to perform a HTS with two strains in parallel and screen for AC inhibitors as well.

I screened 100,000 compounds in duplicate from commercial libraries against the PDE4D3- and AC5- expressing strain (CHP1823) and the PDE7B1-, AC1- and GNAS1- expressing strain (CHP1882). The library collections used are listed in Table 5.1. In order to consider a compound a hit for the screening strain, the Z-score was calculated to individual wells as described in Chapter 2. In the 10,000 HTS, I calculated the Z-scores using mean and standard deviations as the statistic response to the negative controls wells. In the screen described in this chapter, I initially employed the same statistical analysis. However, the standard deviations were so low that it created a large number of candidate hits, defeating the purposes of the screen to find few but specific small molecules. For this reason, I decided to calculate the Z-scores using median and median absolute deviation (MAD) of the experimental samples, which gave a more conservative estimate of hit compounds. In Table 5.2, I list two examples that the change in the Z-scores analyses helped us eliminate false positives. Both small molecules were initially considered hits for the screening strain with Z-scores equal or above 12 (Table 5.2), but were eliminated once Z-scores were calculated taking into account variation of the experimental samples instead of the negative controls. Each compound was tested in duplicate wells.

In the analyses of the GFP and OD₆₀₀ values, variations were observed on different experiments, as demonstrated by differences of fluorescence and absorbance seen in experiments performed in different days. These variations usually are likely due to three main factors: GFP variation from well-to-well (possibly reflecting fluorescent compounds with poor solubility such that they are not reproducibly delivered to each well), temperature fluctuations during incubation and cell behavior in the presence of different compounds. However, in this screening the main factor for fluorescence variation was due to changes in the instrument used for data collection. It is important to note that these variations affected the screening, counter-screen and positive control strains equally. In addition, fluorescence values of the duplicates were normalized by the absorbance to decrease these

Table 5.1. List of commercial libraries screened at ICCB – Longwood Screening Facility*

Library	N_o of compounds	Plates	Plate N_o
IF Lab 2	292	1	1459
Mixed commercial	268	1	1520
Enamine2a	352	1	3153
Maybridge 5	3212	10	1661-1670
Life Chemicals 1	3893	12	1649-1660
NIH clinical 1	446	2	357-3578
NIH clinical 2	281	1	3392
ChemBridge 3	10560	30	1577-1606
Maybridge 3	7639	22	1431-1452
ChemDiv 3	16544	47	1473-1519
Enamine 1	6004	18	1394-1411
Enamine 2	6295	18	1716-1733
ChemDiv 6	6295	18	1795-1919
Total	99786	288	

*List is presented in screened order in HTS

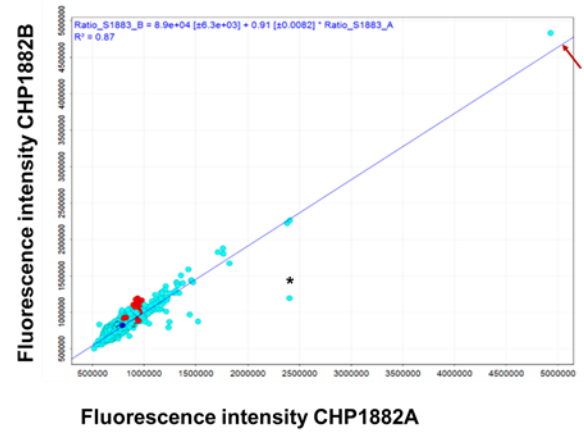
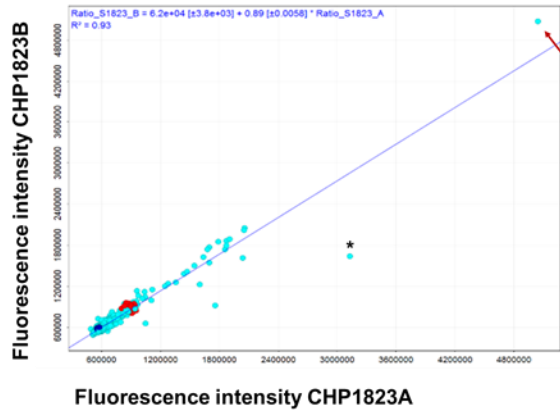
Table 5.2 Analyses of duplicate Z-scores to eliminate false-positives*

Compound	GFP AC5+PDE4D3		GFP AC1+GNAS1+PDE7B1		Z score by average and SD			Z score by median and MAD			
	716185	692948	789215	785914	14.0	12.0	2.0	3.0	4.5	2.0	1.8
1662 O02	712470	710579	687503	678284	17.0	12.0	-3.0	-3.0	4.0	-0.1	-0.2

Z scores based on average and standard deviation (SD) from DMSO treated wells. Z scores based on median and MAD of experimental samples. All values were analyzed from duplicate wells.

Figure 5.2. Scatter plot of normalized fluorescence. The scatter plot represents the fluorescence intensity in duplicates for screening strain CHP1823 (left) and counter-screen strain CHP1882 (right). Cyan circles represent experimental samples treated with small molecules. Dark blue circles represent negative controls. Red circles represent positive controls. Red arrow indicates a fluorescent and nonselective hit.

Figure 5.2 Scatter plot of normalized fluorescence



variations (Figure 5.2).

From the libraries used, a total of 2,176 compounds were annotated as hits, but only 727 of those hits were annotated for our screening strain. Most of the potential compound hits for the screening strain were eliminated due to various reasons, such as: fluorescence, toxicity, counter-screen hits, high LogP (a measurement for compound solubility) or a combination of at least two of these characteristics (Figure 5.3). The analyses for elimination of five out of eight potential hits are listed in Table 5.3.

5.2 Evaluation of the Primary screen

The first analysis of a pin appointment is to determine the quality of the library plate against the screening and counter-screen strains based on Z' -factor described in Chapters 2 and 4. The qualitative analyses are done with the Vortex software provided by the ICCB screening facility. Scatter plots can depict both the average fluorescence and average absorbance by plate-well for each strain (Figure 5.4). In this type of analysis, the screener can assess which compounds are specific or nonselective hits that appear in the scatter plots of both strains, respectively (Figure 5.4 a and b, red arrow). In addition, compounds can be eliminated on the basis of low OD values, which indicate toxicity (Figure 5.4 c and d). It can also indicate technical problems such as edge effects, which can cause the samples to form a smile shape on the grid (Figure 5.4 c and d, black arrows). Furthermore, it allows one to correlate the normalized fluorescence of the replicates for the respective strains, to identify wells with spikes in counts that may indicate auto-fluorescent compounds or to identify non-selective compounds (Figures 5.2 and 5.4a and b, red arrows), and to visualize potential hits for each strain as highlighted with asterisks in Figures 5.2 and 5.4.

The edge effects or well bias as seen in Figure 5.4 can also be analyzed by the scatter by size of signal per well (data not shown). No edge effect was observed in the majority of the pin appointments. In addition, variations caused by edge effect or temperature fluctuations can be seen in a 3D histogram that analyzes the average of the normalized fluorescence in each well for

Figure 5.3. Potential candidate hits in the Primary screen. The top pie chart represents the total number of hits and their distribution for the Primary HTS. The bottom pie chart represents the number of hits for the screening strain and elimination of hits due to fluorescence, toxicity, potential solubility issues (high Log P), or a combination thereof. The total of small molecules selected for cherry pick experiments is depicted in the bottom pie chart in light green.

Figure 5.3 Potential candidate hits in the Primary screen

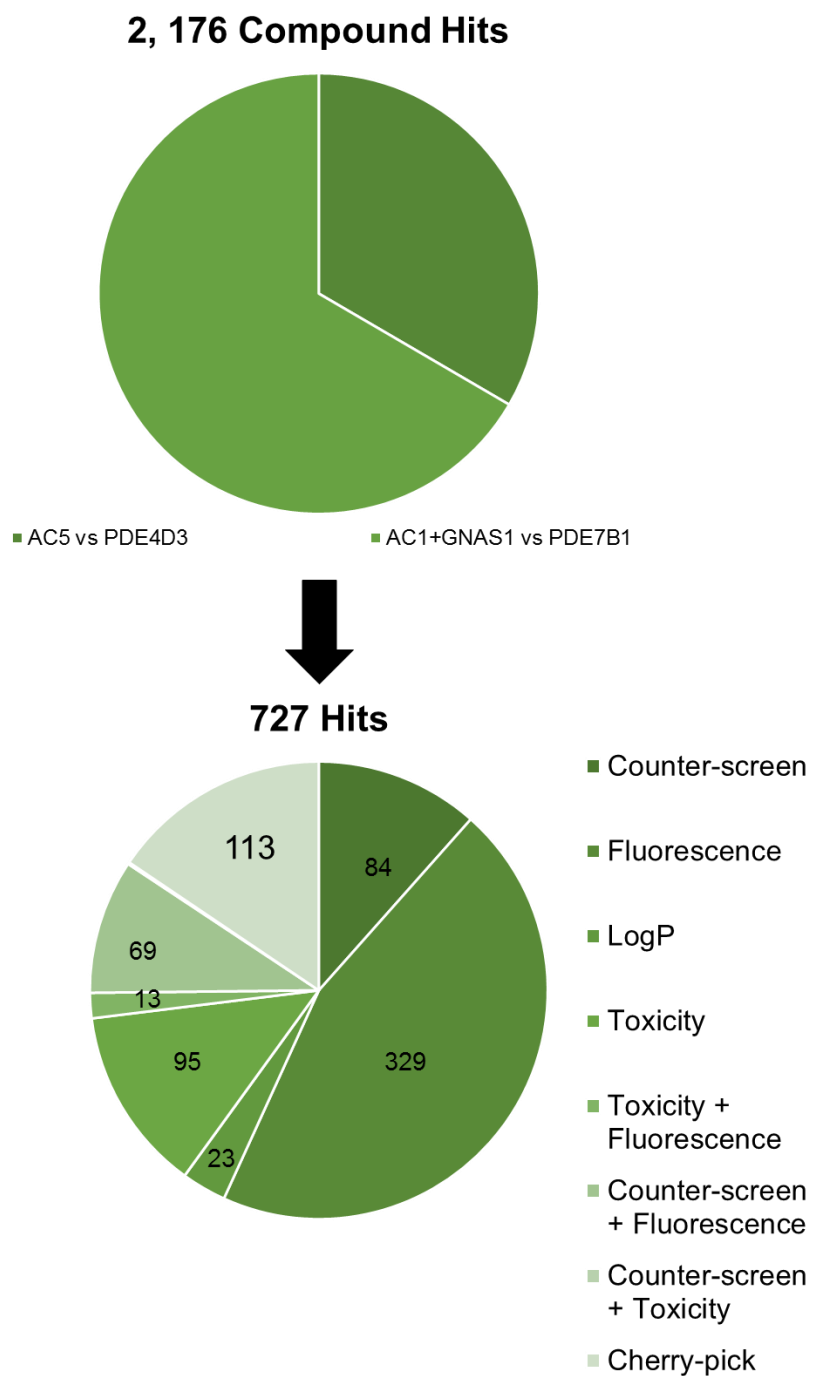


Table 5.3. Elimination of potential candidate hits*

Plate	Well	Type	Hit	GFP				OD				Normalized		Normalized		Normalized		Normalized		1823A Zscore	1823B Zscore	T	F	LogP> 5	Counter -screen
				1823_A	1823_B	1883_A	1883_B	1823_A	1823_B	1883_A	1883_B	1823_A	1823_B	1883_A	1883_B	1823A	1823B								
1437	J10	C	M	402239	370811	364206	335311	1.152	1.126	1.24	1.24	349166	329317	293715	270412	19.18	14.85								
1440	P04	C	W	312744	314525	276307	285199	1.155	1.167	1.17	1.201	270774	269516	236160	237468	6.11	7.89								
1394	A04	W	W	1176104	1107092	1081229	1075425	1.239	1.223	1.228	1.227	949236	905226	880480	876467	7.39	7.01							X	
1433	E01	M	M	343623	350705	477312	444495	1.198	1.195	1.288	1.301	286831	293477	370584	341656	10.23	10.39					F			
1434	H21	S	S	356246	369476	432093	263359	0.996	1.009	0.859	0.778	357677	366180	503019	338508	17.91	20.10					F			
1432	E04	M	M	90460	93354	75615	77129	0.265	0.277	0.17	0.191	341358	337018	444794	403817	14.51	19.01					T	F		
1396	N12	S	S	1252856	1324679	1174571	1120823	1.012	1.031	1.312	1.299	1238000	1284849	895252	862835	19.78	20.83							L	

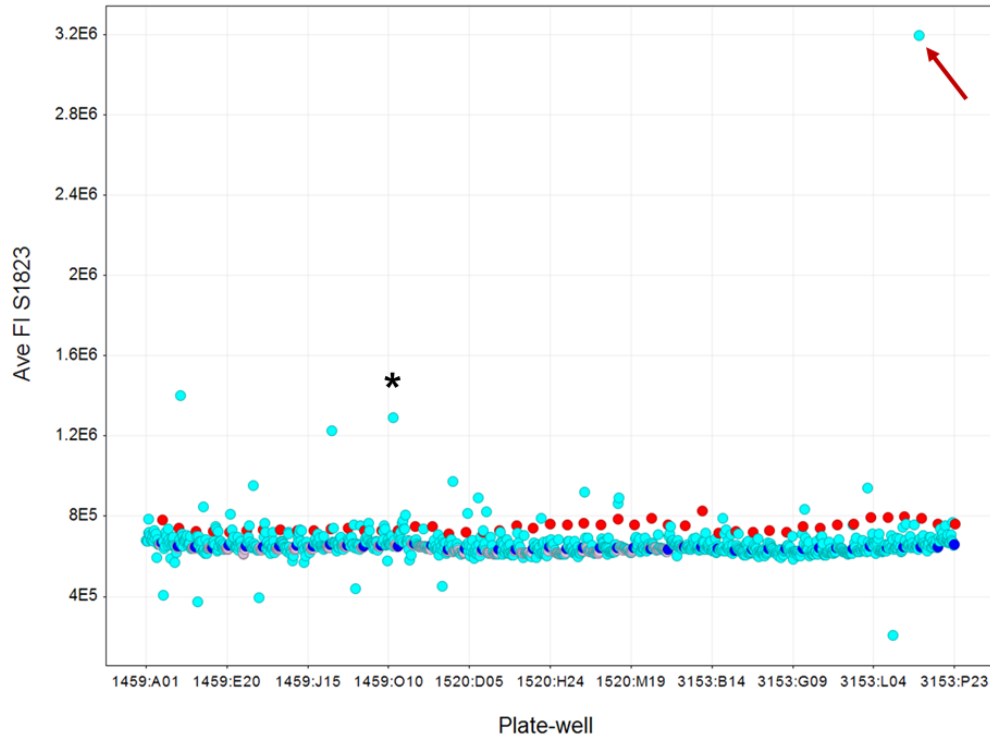
*Type represent the compounds that were cherry-picked (C). Hit are classified as strong (S), moderate (M) or weak (W)FA. OD are in conditional formatting from red (low OD) to green (high OD). Z-scores are color coded in pink from stronger (>15) to weak (<10) hits. Elimination due to Toxicity (T), to Fluorescence (F), to LogP (L) or counter-screen (X) are indicated.

Figure 5.4. Qualitative Data Overview. Average of Fluorescence for screening strain (CHP1823) after 48h (A). Average of Fluorescence of screening strain (CHP1882) after 48h (B). Average of OD₆₀₀ for screening strain (C) and counter-screen strain (D) after 48h. Data analysis was performed using Vortex Software. Color coding: Cyan= Experimental sample; Dark blue= Negative controls; Red= Positive controls. This experiment was performed in duplicate. Red arrows represent nonselective compounds (likely due to autofluorescence given the extremely high value). Black arrows represent the edge effect. Asterisks represent different small molecules that increase GFP values specifically for one strain.

Figure 5.4 Qualitative Data Overview

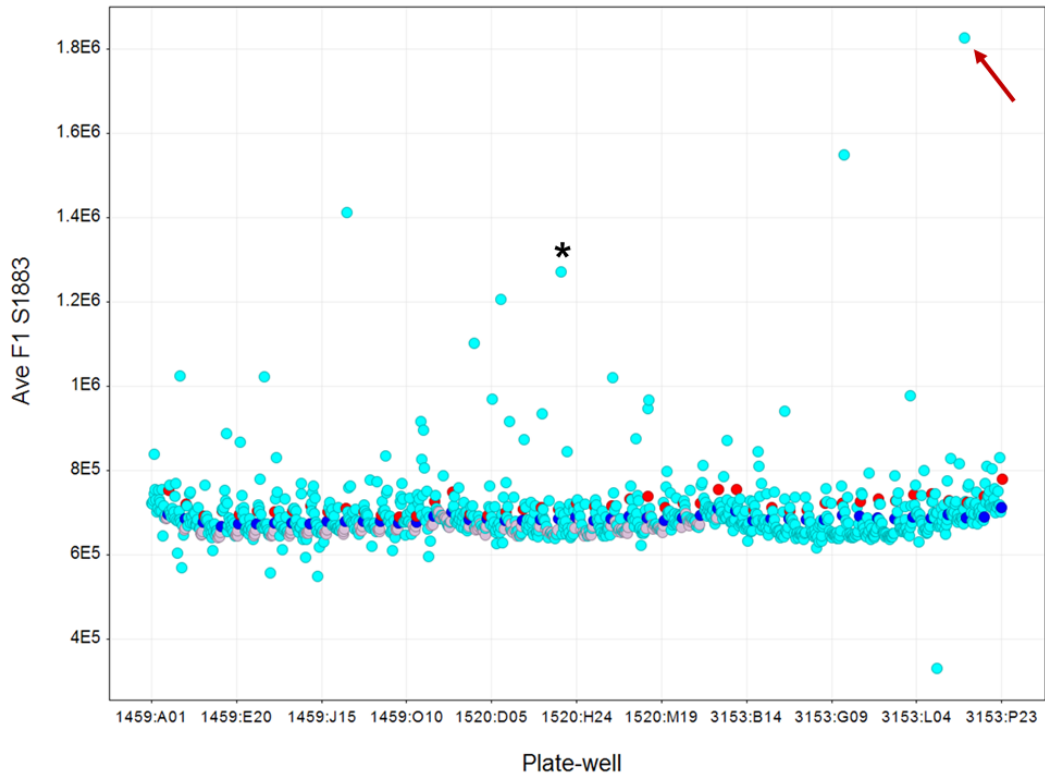
A

Fluorescence of AC5 vs PDE4D3



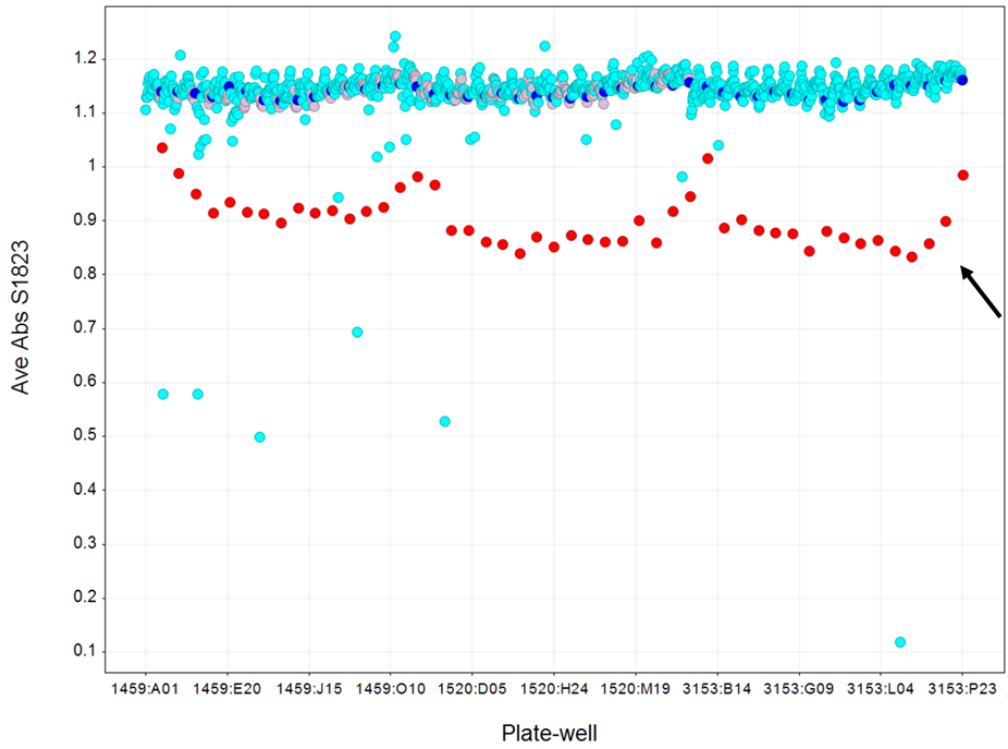
B

Fluorescence AC1+GNAS1 vs PDE7B



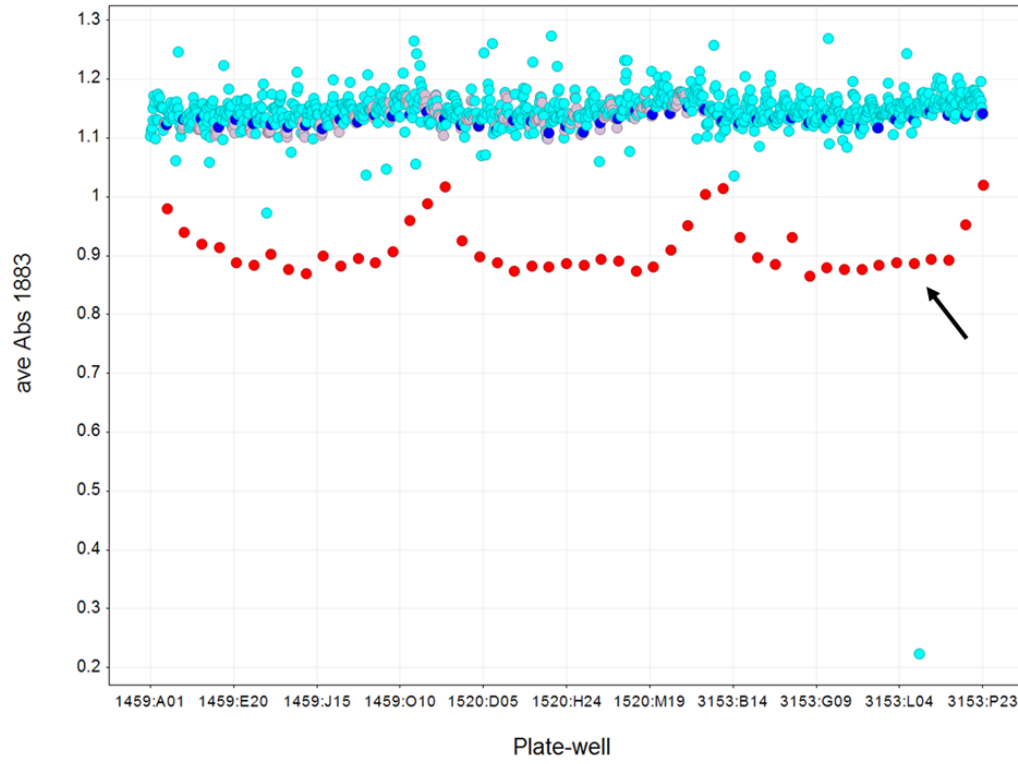
C

Absorbance of AC5 vs PDE4D3



D

Absorbance AC1+GNAS1 vs PDE7B



both replicates (Figure 5.5). Moreover, this type of map can indicate potential hits based on high fluorescence values. For instance, some wells have fluorescence above 800,000 GFP units/OD, which correspond to the positive control values (Figure 5.5). However, it is still possible that the positive hits will be eliminated due to reasons depicted on Figure 5.4.

In conclusion, a combination of qualitative (the data analyzed with the software) and quantitative (data analyzed by median and MAD) analyses were used to identify potential candidate hits using normalized Z-score values and GFP values for both duplicates of the screening strain. The counter-screen allowed us to eliminate fluorescent and nonselective hits (Figure 5.4, red arrows). At the end of the primary screen, I detected 113 potential candidate hits for the screening strain (Figure 5.4). The following sections described efforts to validate these potential candidates that were hits for the screening strain CHP1823 in more detail.

5.2.1 Selection of the Primary screen hits

As already mentioned, 727 compounds produced Z-scores of >6 in both replicates for the screening strain. From 727 compounds only 113 of those were annotated as hits for cherry pick assays (11 strong hits (Z-scores > 15), 22 moderate hits (Z-scores < 15 , but >10) and 80 weak hits (< 10 and > 6) (Figure 5.6). In addition, I compared the sum of the duplicate Z-scores for each strain defining a Z-score differential as the sum for the screening strain minus the sum for the counter-screen strain. We can observe that positive Z-score differentials above 12 indicate hits for the screening strain and negative Z-scores below 12 indicate hits for the counter-screen strain (see Table 5.4 for an example of how this analysis was carried out). Therefore, Z-differentials help the process for selection of hits to validate in the Cherry picks experiments.

5.2.2 Optimization for Cherry-pick experiments

I was concerned with the possibility that a hit compound could affect transcription of the target

Figure 5.5. 3D Histogram of normalized fluorescence. Variation of normalized fluorescence values can be observed in 3D. Dark blue columns indicate fluorescence above 600,000 GFP units/OD₆₀₀. The histogram is a representative of the average normalized fluorescence of both duplicates from a single library plate. Col Y represents Columns 1 to 24 and Row X represents rows A to P in a 384-well plate.

Figure 5.5 3D Histogram of normalized fluorescence

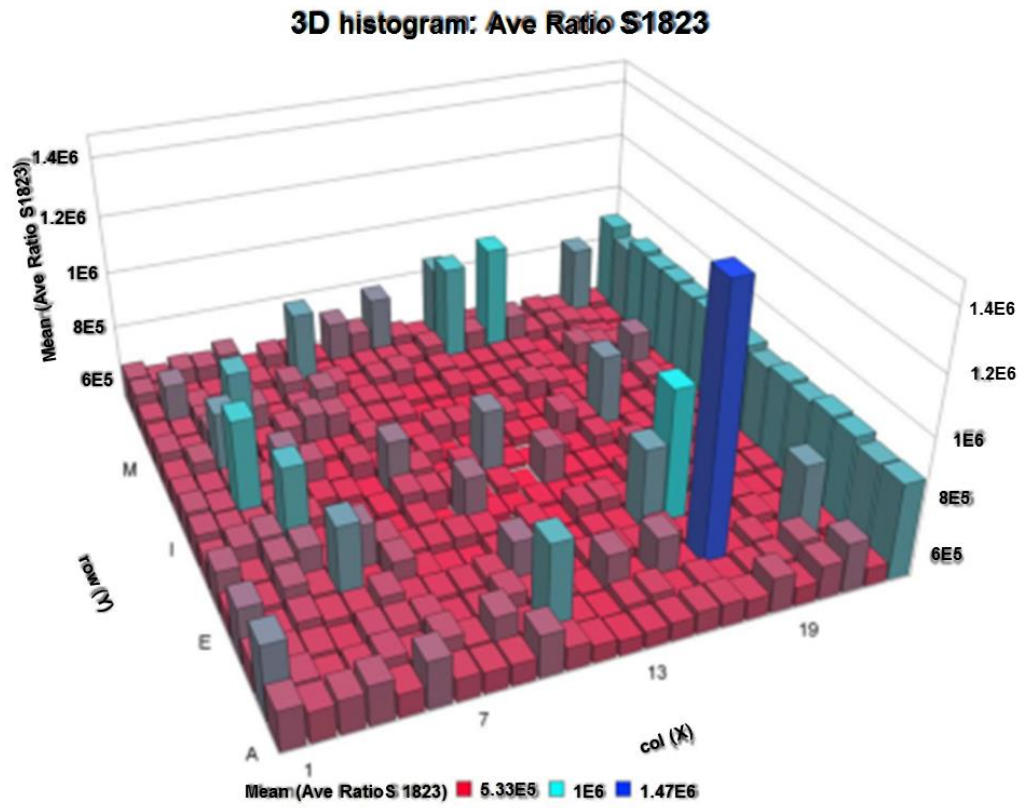


Figure 5.6. Selection of small molecules for cherry pick experiments. The pie chart on the left represents the total of compounds with Z-scores were above 6 in both duplicate in the screening strain. In addition, it depicts the number of the compounds eliminated. The part chart of the right represents the total compounds selected and classified as strong (>15), moderate (<15 and >10) and weak (<10 and >6).

Figure 5.6 Selection of small molecules for cherry pick experiments

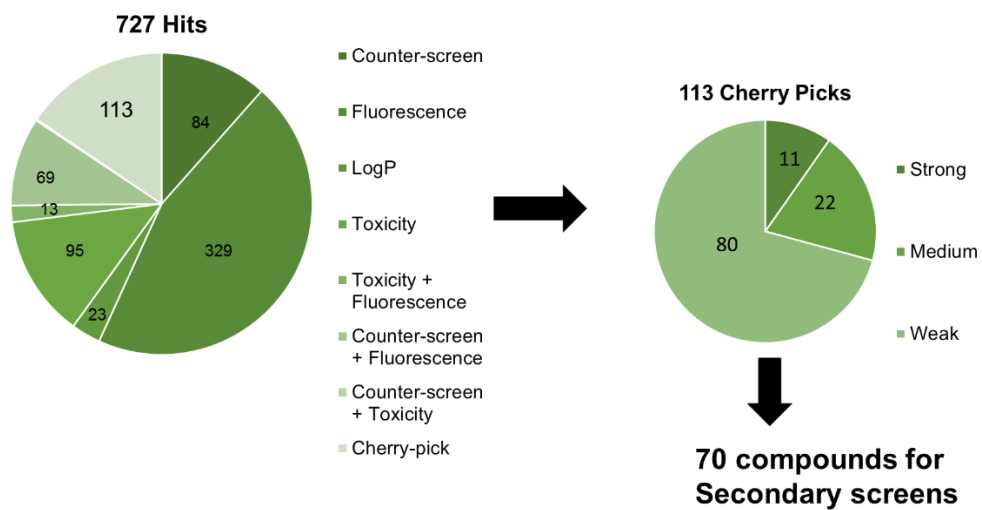


Table 5.4. Examples for the evaluation of potential hits based on Z-scores

Plate	Well	Normalized AC5 vs PDE4D3	Normalized AC5 vs PDE4D3	Normalized AC1+GNAS1 vs PDE7B1	Normalized AC1+GNAS1 vs PDE7B1	Z score AC5 vs PDE4D3	Z score AC5 vs PDE4D3	Z score AC1+GNAS1 vs PDE7B1	Z score AC1+GNAS1 vs PDE7B1	Zscore differential
1459	C02	1201608	1117424	579071	600965	25.8	30.4	-0.7	0.2	56.8
1459	O17	1059257	1020841	572138	598058	19.8	25.0	-1.0	0.0	45.8
1664	I09	1247410	1203543	870527	862425	25.8	25.1	3.1	2.4	45.3

gene instead of the enzyme activity. Therefore, I wanted to test strains that expressed the same enzyme from two different promoters. Depending on the strength of the promoter such as *adh1*, the AC or PDE expression can be stronger (Hoffman lab, unpublished). Therefore, the first step for optimization is to analyze if expression of PDE or AC was affected due to the compound targeting the promoter and not the protein of interest. These experiments were carried out at Boston College. For this first part, I wanted to determine if the compounds inhibit the *adh1* promoter. In this case, if there is a regulation of transcription, I will observe a minimal increase of 10% in GFP values in strains CHP1805, CHP1823 and CHP1962 in comparison to DMSO treatment. In addition, I wanted to select strains that can distinguish among the target proteins. I tested six different strains that expressed different combinations of AC with PDE to verify if selectivity can be determined (CHP1805, CHP1823, CHP1882, CHP1911, CHP1962 and CHP1966; Table 5.5) in the presence of compounds. Therefore, if compounds are targeting PDE4D3, the GFP values will increase in strains CHP1805, CHP1823 and CHP1911. If compounds are targeting AC5, GFP values will increase in strains CHP1823 and CHP1966. The rationale of this experiment is summarized in Table 5.5.

For these experiments, six compounds were purchased in advance for further testing at Boston College. I treated these strains with compounds we purchased based on their high GFP value in the primary screen (BC23 -4, -5, -6, -7, -8) along with a designed compound BC23-1 and Progesterone (a hit for the counter-screen) and DMSO as a control. Qualitative results for the pilot experiment are summarized in Table 5.6. Based on our data, compounds are not inhibiting the *adh1* promoter. In addition, strains CHP1911, CHP1962 and CHP1966 were eliminated due to lack of growth in the presence of compounds. Moreover, results suggest that BC23-4, -5, -7 and Progesterone are nonselective AC inhibitors (Table 5.6).

After the in-house pilot test, I tested three strains with the same compounds depicted in Table 5.6 using the cherry pick compounds and instrumentation from ICCB Screening facility. In the pilot test for the cherry pick, I chose two strains (CHP1805 and CHP1822) along with the screening

Table 5.5. Pilot experiment to evaluate candidate compounds prior to cherry-pick experiments

Strain	Target enzymes	Promoter AC	AC inhibitor	PDE4D3 activator	Adh1 inhibitor
CHP1805	PDE4D3 + AC1	adh	-	+	+
CHP1823	PDE4D3 + AC5	adh	+	+	+
CHP1882	PDE7B1 + AC1	pJV1	-	-	-
CHP1911	PDE4D3 + AC1	pJV1	-	+	-
CHP1962	PDE1C4 +AC6	pJV1(AC) kan- adh1(PDE)	-	-	+
CHP1966	PDE10A + AC5	pJV1(AC) pLEV(PDE)	+	-	-

(+) represents increase in GFP values in comparison to control; (-) represents decrease in GFP values in comparison to control.

Table 5.6. Results for pilot experiment

Strain	Target enzymes	Promoter driving AC/PDE expression	BC23-1	BC23-4	BC23-5	BC23-6	BC23-7	BC23-8	P	OD
CHP1805	PDE4D3 + AC1	adh (AC)	+	+	+	-	-	-	+	High
CHP1823	PDE4D3 + AC5	adh (AC)	-	+	+	-	+	-	+	High
CHP1882	PDE7B1 + AC1 + GNAS1	pJV	-	+	+	-	+	-	+	High
CHP1911	PDE4D3 + AC1	pJV	-	+	-	-	+	-	-	Low
CHP1962	PDE1C4 + AC6	adh (PDE)	-	+	+	-	+	-	-	Low
CHP1966	PDE10A + AC5	pJV	-	+	+	-	+	-	+	Both

(+) represents increase in GFP values in comparison to control; (-) represents decrease in GFP values in comparison to control; P represents Progesterone.

strain (CHP1823) (Table 5.7). All of the strains have the AC expression driven by the *adh1* promoter. The complete genotype of the strains used for optimization procedures are listed in Table 2.3. Based on our data, it seems that BC23-1/-6/-8 do not target any enzyme of interest and it suggests that BC23-4, -5, and -7 are non-selective AC inhibitors (Table 5.7). Unlike our in-house pilot experiment, BC23-1 and Progesterone failed to increase the GFP values in strains CHP1805 and CHP1823 (Table 5.7). These discrepancies will be discussed in Chapter 6. Overall, this experiment seems promising since it can distinctly identify compounds that are either targeting the screening strain expressing the proteins of interest or targeting in a non-selective manner. After these preliminary results, I moved forward with the cherry pick assays. To further eliminate non-selective compounds, I included the strains CHP2028 (PDE7B1- and AC6- expressing strain) in the cherry pick experiments.

5.2.3 Validation of potential candidate hits using Cherry-pick experiments

I performed a GFP assays testing 2.5-fold dilutions of compounds from 0.625 μM to 5 μM . In this way, I could test for potency of the compounds. I also used three strains along with the screening strain to test for selectivity. A total of 70 out of 113 compounds yielded at least a 10% increase in the normalized fluorescence values for the highest compound at the concentration tested (5 μM) for the screening strain.

Although 70 compounds were validated, only 17 compounds were used for further confirmation in the secondary screenings. A total of 49 potential hits were eliminated due to non-selectivity or likely fluorescence of the compounds. These compounds were selected on the basis of potency and to a certain level of selectivity. The data for each compound hit are summarized in Table 5.8. Most of the compounds were non-selective. However, the compounds that were selected for secondary assays promoted a greater increase in GFP values higher in the screening strain and/or in both AC5-expressing strains than in the other two strains. Compounds were eliminated if they produced an increase in fluorescence signal in only one of the duplicates or if there was too much variation

Table 5.7. Pilot test results of candidate hit compounds at ICCB

Strain	Target enzymes	BC23-1	BC23-4	BC23-5	BC23-6	BC23-7	BC23-8	P
		CHP1805	-	+	+	-	-/+	-
CHP1822	PDE7B1 + AC5	-	+	+	-	+	-	+
CHP1823	PDE4D3 + AC5	-	+	+	-	+	-	-

(+) represents increase in GFP values in comparison to DMSO control; (-) represents decrease in GFP values in comparison to control; P represents Progesterone.

Table 5.8. Compounds examined in cherry pick experiments with comments on cherry pick results

Library Name	Library Plate	Source Well	FA values	FB values	Z-score A	Z-score B	Primary screen	Comments based on GFP values for screening strain
Enamine1	1402	H01	1710672	1645175	6.4	10	W	20% increase in GFP values, seems selective
Enamine1	1404	O04	1580946	1612288	7.7	7.9	W	10-20% increase in GFP values, but non-selective
Enamine1	1406	A18	1643326	1546862	7.9	6.9	W	10% increase with GFP values only in one of the duplicates
Enamine1	1406	F05	1653592	1620818	8.2	8.5	W	10% increase with GFP values only in one of the duplicates
Maybridge3	1440	P04	270774	269515.9	6.1	7.9	W	20% increase in GFP values, but non-selective
Maybridge3	1440	P16	311770.9	267975.9	11.1	7.7	W	20% increase in GFP values, but non-selective
Maybridge3	1445	D06	276162.6	270761.6	7.5	6.3	W	20% increase with GFP values in AC5 expressing strains, but non-selective
IFLab2	1459	C02	1201608	1117424	25.8	30.4	S	Very potent, but non-selective (possible toxicity and/or fluorescence?)
ChemDiv3	1473	N17	482644	505711	6.3	7.3	W	10% increase with GFP values higher in AC1-expressing strain, but non-selective
ChemDiv3	1480	C03	624872.8	670735.3	13.2	17.5	W	15% increase in GFP values, but non-selective
ChemDiv3	1484	L14	468524.3	497988.2	8.5	9.3	W	30% increase with GFP values higher in AC1-expressing strain, but non-selective
ChemDiv3	1485	D01	441654.8	437346.3	8.2	8.3	W	Non-selective with variation of GFP values in duplicates
ChemDiv3	1489	P05	412858.8	422768.2	6.8	7.4	W	30% increase with GFP values higher in AC1-expressing strain, but non-selective
ChemDiv3	1490	C17	464678.4	464554.9	9.65	9.4	W	Non-selective, 15-30% increase with one AC5-expressing strain with higher GFP values
ChemDiv3	1490	N12	483271.7	474250.6	9.9	10.1	W	15% increase in GFP values, but non-selective
ChemDiv3	1499	B22	476189.2	488293.8	10.9	11.7	M	20% increase with GFP values in AC5 expressing strains, but non-selective
ChemDiv3	1499	D11	520055.9	550037.1	13.8	15.7	M	20% increase with GFP values in AC5 expressing strains, but non-selective
ChemDiv3	1499	D21	424631.2	432805.2	7.5	8.1	W	25% increase with GFP values in AC5 expressing strains, but non-selective
ChemDiv3	1499	K05	527632.4	574166.7	14.2	17.3	M	Potent, but non selective
ChemDiv3	1499	K07	447540.3	455716.6	9	9.6	W	10% increase with GFP values only in one of the duplicates
ChemDiv3	1499	O09	487699.1	475694.9	11.6	10.9	M	10% increase in GFP values, but non-selective
ChemDiv3	1517	H04	639309.6	614310.6	12	11.5	M	10% increase in GFP values, but non-selective
Maybridge5	1664	I09	1247410	1203543	25.8	25.1	S	Very potent, but non-selective (possible toxicity and/or fluorescence?)

Enamine2	1729	D11	1337302	1125595	16	12.2	M	Non-selective, but had 30% increase in the GFP values for screening strain
Enamine2	1729	F22	1441230	1265737	19.6	18	S	Non-selective, with variation of GFP values between duplicates
Enamine2	1729	O13	1334610	1194314	15.9	15	S	Non-selective, with variation of GFP values between duplicates
Enamine2	1730	B17	1054483	1021402	7.1	7.9	W	Non-selective, with variation of GFP values between duplicates
Enamine2	1730	G06	1049966	1017384	6.9	7.8	W	Non-selective, with variation of GFP values between duplicates
Enamine2	1730	G16	1067488	1033229	7.5	8.4	W	Non-selective
Enamine2	1730	M20	1074331	1032686	7.8	8.3	W	Non-selective
Enamine2	1732	K02	15.37191	16.78282	15.4	16.8	S	Non-selective
Enamine2	1733	H11	970194	970161.2	9	8.1	W	Non-selective with 10% increase in GFP values
ChemDiv6	1801	K22	1140466	1120694	12.8	12	M	Non-selective with 10% increase in GFP values
ChemDiv6	1804	M19	962411.6	876931.1	17.8	14.6	M	Very potent, but non-selective (fluorescence?)
ChemDiv6	1816	F01	1010632	912347.1	14.6	13.1	M	Non-selective
ChemDiv6	1816	F05	1088379	834564.6	18	9	W	Non-selective
ChemDiv6	1816	F22	1242120	1168835	24.5	26.3	S	Non-selective, with variation of GFP values between duplicates
ChemDiv6	1826	F17	748862.5	818171.4	8.8	10.1	W	Non-selective
ChemDiv6	1829	D04	685480.9	743725.5	8	10.8	W	Non-selective
ChemDiv6	1832	J05	626965.7	665205.5	6.4	6.2	W	Non-selective
ChemDiv6	1832	P09	689151.7	715520.4	10.1	8.8	W	Non-selective
ChemDiv6	1834	F03	1.12	612669	7.5	12.3	W	Non-selective
ChemDiv6	1835	C19	707520.6	723344.7	8.7	10	W	Non-selective, but had 30% increase in the GFP values for screening strain
ChemDiv6	1837	E21	719498.7	677212.5	10.6	7.5	W	Non-selective
ChemDiv6	1852	J20	843114.2	849576.4	7.9	7.3	W	Non-selective

ChemDiv6	1852	L05	844064.8	823139.5	8	6.3	W	Non-selective
ChemDiv6	1852	N05	872577.4	869394.4	9.2	8.14637 2	W	20% increase in GFP values, but non-selective
ChemDiv6	1852	P18	812009.2	834786.6	6.5	6.7	W	20% increase in GFP values for both AC5-expressing strains, but non-selective
ChemDiv6	1853	G01	853622.5	873138.7	9.2	8.3	W	Non-selective
ChemDiv6	1857	G05	755289.1	741421.2	11.9	7.2	W	Non-selective
ChemDiv6	1857	M05	737712.2	729558.9	10.4	6.5	W	Non-selective
ChemDiv6	1857	N07	754631.3	755606.1	11.8	8	W	Non-selective
ChemDiv6	1858	F03	823342	826705.9	8.6	9.4	W	Non-selective
ChemDiv6	1858	J03	808953.4	779357.3	7.9	6.9	W	Non-selective
ChemDiv6	1859	H08	874824.8	873790.4	7.5	6.2	W	Non-selective
ChemDiv6	1859	H22	930701.1	980738.8	9.4	9.8	W	Potent, but non-selective
ChemDiv6	1859	L06	832733.3	926895.8	6	8	W	Potent, but non-selective
ChemDiv6	1860	B10	810442.3	807561.8	7.9	7	W	Potent, but non-selective with too much variation between duplicates for screening strain
ChemDiv6	1860	F22	827974.1	822806.6	8.7	7.8	W	Non-selective with too much variation between duplicates for screening strain
ChemDiv6	1860	J16	819370.4	864116.5	8.3	9.6	W	30% increase in GFP values for both AC5-expressing strains
ChemDiv6	1860	L14	798799.7	805602	7.3	7	W	Non-selective with too much variation between duplicates for screening strain
ChemDiv6	1861	F16	807385.3	833798.5	7.9	8.5	W	Non-selective
ChemDiv6	1865	C14	891045.7	859773.3	9.4	7.7	W	10% increase in GFP values in only one duplicate
ChemDiv6	1867	C19	939813.5	909684.6	9	6.5	W	20-26% increase in GFP values, but non-selective
ChemDiv6	1874	L09	970184.5	900872.6	12.2	10.3	W	Non-selective with too much variation between duplicates for screening strain
ChemDiv6	1875	A04	913916.5	898534.8	7.1	6.7	W	Non-selective
ChemDiv6	1875	G04	983881.7	991869.9	9.6	10	W	Non-selective
ChemDiv6	1876	P15	891605.5	944298.7	7.5	7.7	W	Non-selective
ChemDiv6	1912	D19	709298.1	698977.5	9.1	6.8	W	Non-selective
ChemDiv6	1912	F19	728625.2	743851.5	10.6	9.7	W	Non-selective

between both duplicates in comparison to DMSO control. It is worth to note that no toxicity was detected in the cherry pick experiments (data not shown). Overall, testing against three additional strains helped eliminate 63 compounds out of 113. In addition to the 17 compounds, 8 compounds (7 hits from the Primary screen and I designed compound BC23-1) were included in the counter-screen experiments. A summary of the 25 candidate hits selected for the counter-screens is listed in Table 5.9.

5.3 Secondary assays to confirm potential candidates as final hits

To characterize the 17 lead compounds along with 8 compounds purchased by us due to their performance in the primary screen, I used cAMP and GFP assays, as described in Chapter 2. The data were not reproducible in either assay (data not shown). For example, the cAMP levels appeared to drop upon compound treatment in some assays, but not upon repeating the experiment. Therefore, no compounds could be validated using the screening strain with these assays since they seemed to target the different proteins expressed in screening and counter-screen strains giving similar GFP values. Conversely, non-target proteins expressing strain (CHP2053), genotype listed on Table 2.3, confirmed that most of these compounds have no effect in *S. pombe* strain expressing non-target proteins. The GFP values for strain CHP2053 treated with 25 compounds are depicted in Figure 5.7. The majority of the compounds had GFP values below 11 units/OD at the highest concentration tested. However, compounds BC23-6,-8,-10, -12, -13 and -19 had values above 13 units/OD at the highest concentration (Figure 5.7). Although, use of counter-screen would reduce technical issues, I believe that these elevations are artifacts, which could explain why they appear as hits in the primary screen. Moreover, the treatment of CHP2053 strain with compounds BC23-5 and -19 yielded OD values below 0.35 (data not shown), which suggests a possible toxicity effect that was not previously identified. Conversely, the treatment of CHP2053 strain with compounds BC23-6, -8 and -13 yielded high OD values, but it is possible these compounds are fluorescent. In summary, these experiments indicate that these compounds are having an effect against strains with

candidate target proteins, as our previous analyses demonstrated. Moreover, our analyses are supported by experiments where the compounds fail to increase fluorescence in a strain not expressing target proteins. However, the GFP results clearly demonstrate that the assay cannot validate any of candidate hits against the screening strain and assessment of potency and selectivity could not be made either.

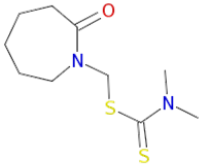
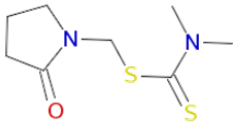
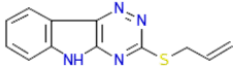
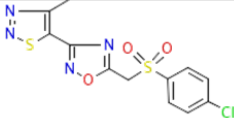
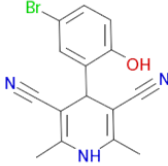
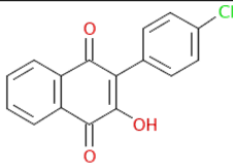
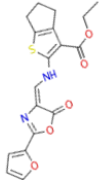
There are multiple reasons that artifacts as toxicity have not been previously detected. One caveat, it is the different methods used to deliver the compounds as followed: the pin transfer was used in the primary screen; the transfer from cassette to wells by vibration was used in the cherry picks; and transfer was used multichannel pipettes for the secondary assays. Another caveat that may have affected is the compound source. The compounds used at ICCB have been thawed many times and after many rounds of thawing, it is possible that I was using derivatives of the original compound tested. In the cherry pick, compounds are from the libraries at ICCB, but they are prepared exclusively from stocks. For in-house testing, the compounds were directly purchased from the companies. Therefore, I believe I am testing the potential hit and assessing its chemical activity fully.

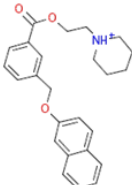
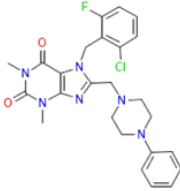
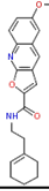
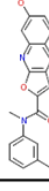
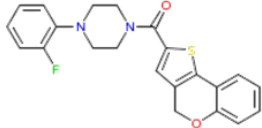
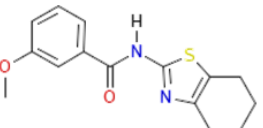
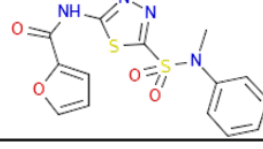
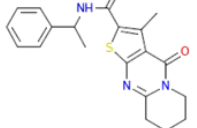
Due to inconsistent data for the screening strain in both GFP and cAMP assays, I decided to perform KCl assays as the secondary assay. In this assay, I can assess PKA activity independent from the use of *fbpI-GFP* construct expressed in the screening strain (Stiefel et al., 2004). The goal of this assay is to test whether a compound can confer KCl-sensitivity upon a strain that is KCl resistant due to high PKA activity. These assays were performed in both solid and liquid media.

5.3.1 Secondary screens for assessment of PKA activity in liquid medium

The purpose of this assay is to validate compounds that reduce PKA but independent from the PKA-repressible reporter carried in our strains. In salt stress conditions, strains expressing high PKA activity will present a KCl - resistance growth. Conversely, strains expressing low PKA activity will present a KCl - sensitivity growth. Therefore, I need to validate compounds against

Table 5.9. Small molecules selected for secondary assays

Compound ID	Structure	Library Plate	Source Well	Primary screen hits
BC23-1	Similar to BC23-2 and BC23-3	N/A	N/A	N/A
BC23-2		1459	C02	S
BC23-3		1459	O17	S
BC23-4		1664	I09	S
BC23-5		1662	I09	W
BC23-6		1665	E03	W
BC23-7		1582	E19	W
BC23-8, but pick for solubility		1589	G19	M

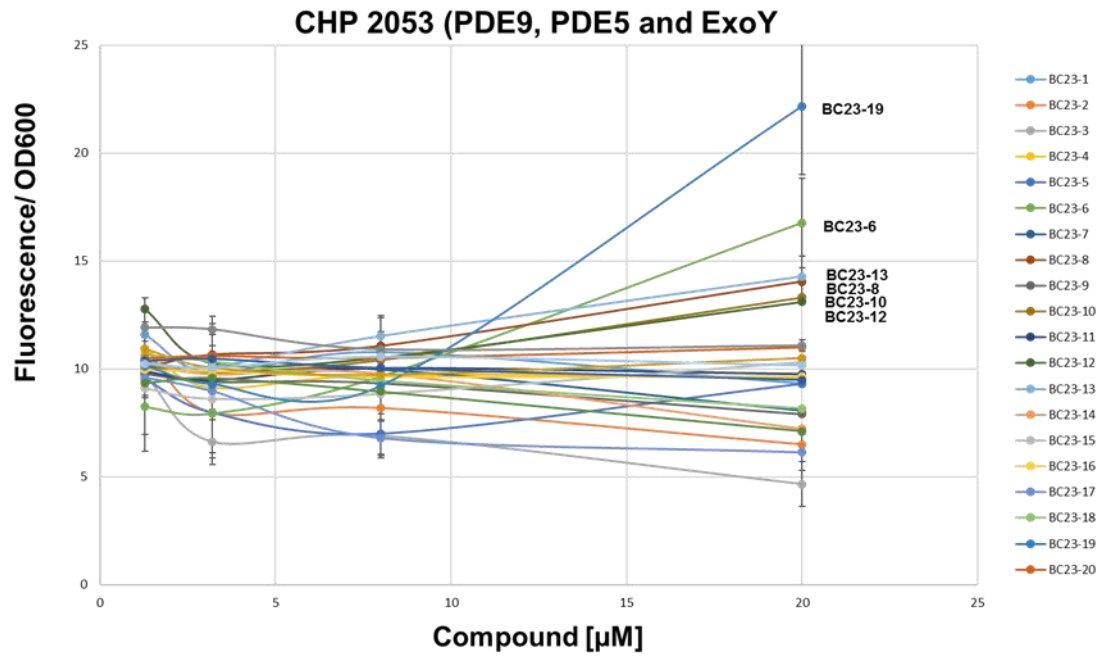
BC23-9		1490	C17	W
BC23-10		1499	B22	M
BC23-11		1499	K05	M
BC23-12		1499	O09	M
BC23-13		1835	C19	W
BC23-14		1852	P18	W
BC23-15		1859	H22	W
BC23-16		1859	L06	W
BC23-17		1860	J16	W

BC23-18		1867	C19	W
BC23-19		1400	N07	M
BC23-20		1402	H01	W
BC23-21		1404	O04	W
BC23-22		1406	A18	W
BC23-23		1406	F05	W
BC23-24		1729	D11	M
BC23-25		1445	D06	W

Bolded compounds were either not screened (BC23-1) or were hits for the Primary screen only or was not validated in the cherry-pick assays (BC23-19).

Figure 5.7. GFP assay to validate candidate hits. CHP2053 strain was treated with 25 compounds four series of 2.5-fold a serial dilution where the first concentration was 20 μ M for each compound. This is a representative of a single experiment. Experiment was performed in quadruplicate. Plate was incubated for 48h at 30°C. Error bars represent standard errors.

Figure 5.7 GFP assay to validate candidate hits



strains that have high PKA activity and, consequently, have a KCl-resistance phenotype. In order to identify the most suitable strain for the KCl assays in liquid medium, I tested the following strains: the screening strain (CHP1823), the counter-screen (CHP1882), the PDE4B2 expressing strain (CHP1641) and the PDE4D2-, AC5- and GNAS1- expressing strain (CHP1852). These strains were treated at different concentrations of KCl.

The screening and the counter-screen strains behaved similarly to strain that expresses PDE4B2 only under KCl stress (Figure 5.8). The PDE4D2-, AC5- and GNAS1- expressing strain (CHP1852) presents the most distinct KCl-resistance growth phenotype. In this strain, more than 1.25M KCl is needed to confer KCl – sensitivity growth (Figure 5.8). However, due to variability with control values, I could not assess the effect of the compounds in the KCl assay in liquid media (data not shown).

5.3.2 Secondary screens for assessment of PKA activity in solid medium

In this assay, I chose strains that display a growth resistance phenotype in the presence of KCl in solid medium. Thus, if a compound has an effect, it will reduce PKA activity, which in turn will confer KCl sensitivity and a halo of inhibition will form. Twelve strains were used for this assay (Table 5.10). These strains express either the *S. pombe* AC (Git2), no AC with PDE4D3, or one of the ten mammalian AC, respectively. In these experiments, compounds BC23-18 and -21 have an effect in strains expressing group I (AC1 and AC8), group II (AC2 and 4), group III (AC1 and AC8) and group IV (AC9). BC23-5 inhibits groups I(AC8), group III (AC5 and AC6) and group IV (AC9) (top panel). Further, BC23-22 seems to strongly inhibit all ACs from group I along with a moderate inhibition of AC9 and weak inhibition of AC5 and AC6. BC23-7 clearly shows no effect in solid medium, while compound BC23-19 is toxic as it inhibits growth of all strains (Figure 5.9, top panel). Most of the other compounds behaved like BC23-7 and produced no halos. However, these compounds deserve further testing as the sensitivity of the assay varies somewhat

depending on the density of the cells plated so that it is possible that a halo would be observed on plates receiving fewer cells.

5.4 Conclusion

I developed and optimized a high-throughput screen for PDE activators and AC/GNAS1 inhibitors. In this HTS, I used a screening strain expressing PDE4D3 (long form of PDE4D that possesses an N-terminal inhibitory domain) and AC5 enzymes. The conditions for this assay produced Z-factors above 6 with MAD values around 4%. A total of 100,000 compounds from commercial libraries were screened and 727 hits were identified. Cherry pick assays with the candidate hits from primary screened were performed and 70 compounds were confirmed. However, 49 were eliminated due to non-selectivity. Based on our assessment of the potency and selectivity of the cherry-picked candidates, 17 candidate hits along with 8 additional compounds were purchased for further analyses. Preliminary data suggest that compound BC23-19 is toxic, inhibiting growth on YES+KCl for all strains tested. Most compounds were like BC23-7 that they make any halos in solid medium (Figure 5.9). In addition, BC23-18 and BC23-21 inhibit the same ACs in a similar manner. BC23-22 appears to inhibit group 1 ACs strongly followed by moderate and weak inhibitions of groups 4 and 3, respectively. Thus, it appears that I have identified broad specificity AC inhibitors, but not ones that only act on AC5. Further investigations are underway. In the future, enzymatic assays will need to be performed to determine enzyme affinity and potency of compounds.

Figure 5.8. Optimization of KCl assays. Assay was performed with various KCl concentrations against four yeast strains. This is a representative of a single experiment. The experiment was performed in quadruplicates. Plate was incubated for 48h at 30°C. Error bars indicate standard errors.

Figure 5.8 Optimization of KCl assays

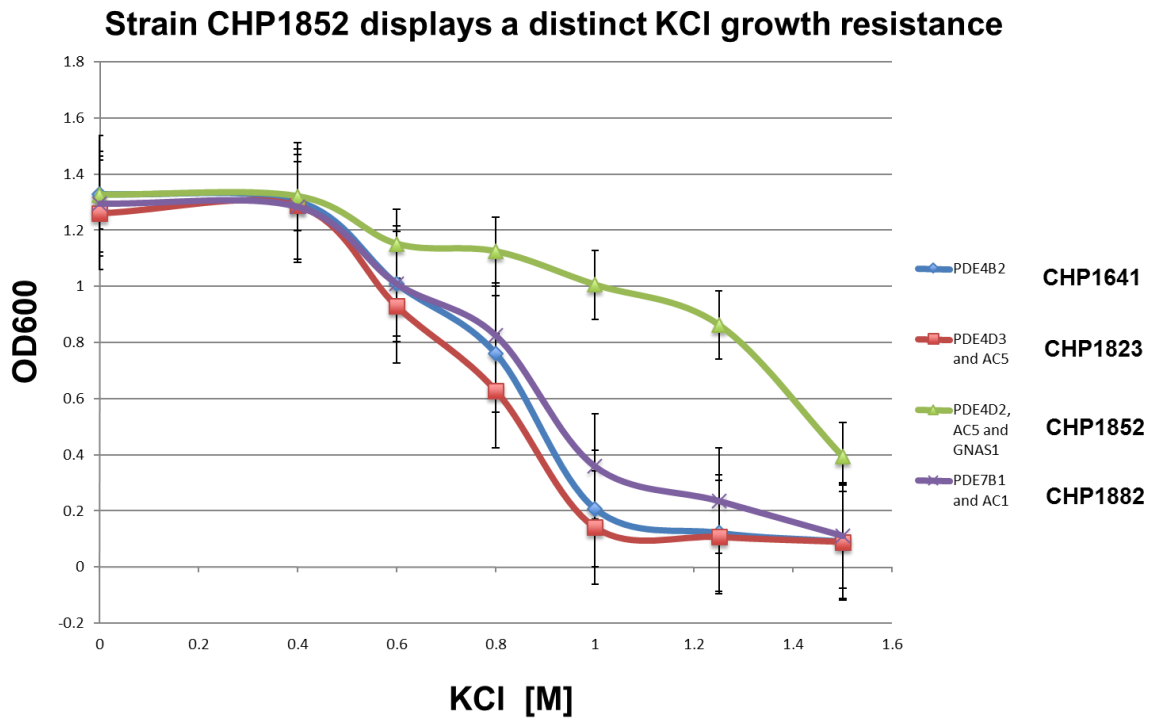


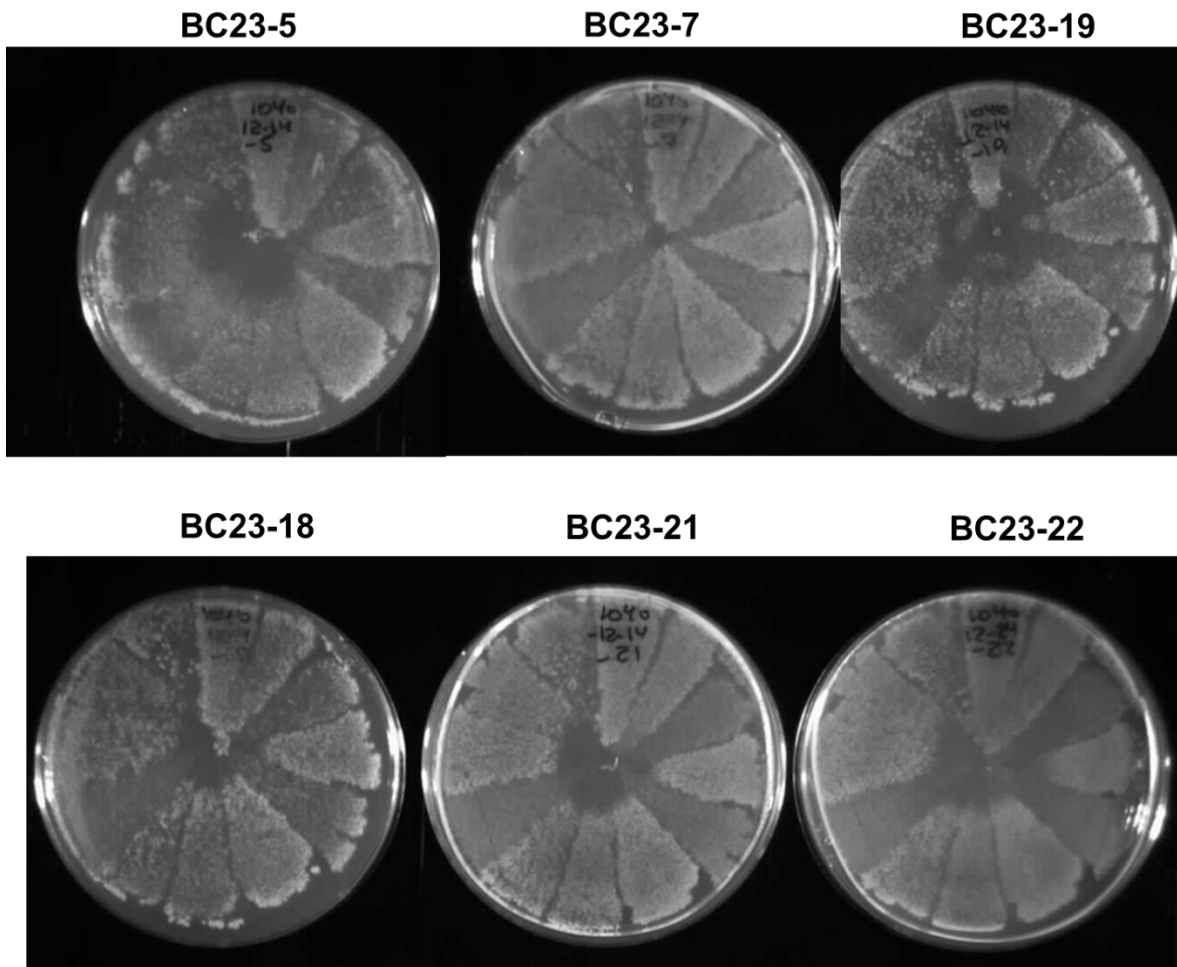
Table 5.10. List of strains used for KCl assays in solid medium

Strains	Mammalian PDE assessed	Mammalian AC assessed	Mammalian Gα (GNAS1) assessed
CHP1040	–	–	–
CHP1167	PDE4D3	–	–
CHP1811	–	AC1	–
CHP2016	–	AC2	–
CHP1990	–	AC3	GNAS1
CHP1812	–	AC4	–
CHP1731	–	AC5	GNAS1
CHP1981	–	AC6	–
CHP1813	–	AC7	–
CHP2015	–	AC8	–
CHP2024	–	AC9	–
CHP2017	–	sAC	–

N-terminal inhibitory domain) and AC5 enzymes. The conditions for this assay produced Z-factors above 6 with MAD values around 4%. A total of 100,000 compounds from commercial libraries were screened and 727 hits were identified. Cherry pick assays with the candidate hits from primary

Figure 5.9. KCl assay in solid medium. Twelve strains were treated with six compounds. AC inhibition is characterized by formation of zone of inhibition in KCl solid medium. Strains were streaked in a clockwise direction following the strain order listed in the Table 5.10

Figure 5.9 KCl assays in solid medium



CHAPTER SIX

DISCUSSION AND FUTURE DIRECTIONS

Small molecules can be used as research tools to understand the biological roles of specific target proteins. They can also be developed into drugs via medicinal chemistry. Our lab is interested in studying the modulation of key components of the cAMP pathway and have previously conducted screens for chemical inhibitors of cyclic nucleotide phosphodiesterases (PDEs). In this thesis, I wanted to address two distinct goals, as follows: 1) To have a better understanding of a promising PDE4/7 inhibitor, and 2) to try to develop a screen that would identify novel tool compounds that, rather than elevating cAMP signaling as would be the effect of a PDE inhibitor, would reduce cAMP signaling.

Currently, there are several ongoing clinical trials of PDE inhibitors related to many pathologies from immune to central nervous system diseases (Maurice et al., 2014). Conversely, there are few ongoing trials in targeting ACs for disease related purposes, such as the AC6 gene transfer clinical trial (Hammond, 2015). It is possible that the difficulty in assessing the effectiveness of AC inhibitors *in vivo* has created barriers for the discovery and further testing of specific compounds. Although there has been a remarkable effort from both academia and industry to identify and characterize PDE inhibitors, there are no known PDE4 activators to date. The lack of PDE activators and assessment of AC inhibitors in cells have limited our understanding of their function and their potential as therapeutic targets. The aim of this study was to develop research tools that allow us to better investigate the roles that PDEs and ACs play in various biological processes. In this section, I will summarize and discuss the findings from my research.

6.1 Development of a genetic screen to identify BC54-resistant PDE alleles

BC54 is a dual specificity PDE4/PDE7 compound discovered by our lab using a fission yeast HTS system. Both enzymes (PDE4 and PDE7) are involved in inflammatory response (Keravis and Lugnier, 2012). BC54 outperformed rolipram in mammalian cultures by reducing TNF α and IL-2 with a 3-fold difference (Hoffman lab, unpublished). Thus, supporting BC54 anti-inflammatory role.

I have developed a genetic screen to generate and characterize mammalian *PDE4* and *PDE7* mutant alleles that are resistant to BC54 (dual specificity PDE4/7 inhibitor). The purpose of this screen was to identify single amino acid changes in PDE4 and PDE7 that confer resistance to BC54. Mutant alleles were identified by growth in SC-Ura medium within the zone of inhibition of BC54 as the retention of PDE activity leads to an increase in expression of the PKA-repressed *fbp1-ura4* reporter.

Both stationary phase survival and growth on SC-Ura medium are phenotypes that can reflect the presence of PDE activity. A rapid loss of viability in stationary phase is associated with deletions in the *cgs1* (PKA regulatory subunit) and *cgs2/pde1* (PDE) genes that lead to hyperactive PKA (Mochizuki and Yamamoto, 1992; DeVoti et al., 1991). In order to carry out a genetic screen for mutant PDEs, I had to choose the appropriate strain to assess the phenotype. The ideal host strain is the one that produces high intracellular cAMP levels that lead to high PKA activity, such that expression of a functional PDE could lower PKA activity to alter its growth behavior. In addition, the strain can be differentiated when expressing either wild-type or mutant PDEs by the failure (the wild type phenotype) or ability (the mutant phenotype) to enter stationary phase in the presence of compound. To determine the conditions, I tested six strains that produce different levels of cAMP. Strain CHP1346 has a disrupted *cgs2* PDE gene that can be replaced by a plasmid expressing PDE4B or PDE7B. In addition, CHP1346 was the only strain tested that I could differentiate failure to enter stationary when expressing either a wild-type or compound-resistant mutant 1 for both PDE4 and PDE7. In the most diluted samples, a PDE4B-expressing transformant displayed a 10-fold decrease in survival, which reflects an increase in PKA activity (Figure 3.3). As described in

the following section, these results allowed me to enrich for rare transformants that express compound-resistant *PDE* alleles so that I would be better able to detect them when screening for colony formation on a plate.

6.1.1 Enrichment is important to screen compound resistant transformants

It was a reasonable assumption that the compound-resistant alleles I was screening for would be rare within the population of PCR-generated alleles. Therefore, an enrichment step in the procedure was used to increase the percent of cells among the transformants that carry alleles of interest. Pilot experiments demonstrated that loss of survival of cells expressing PDEs occurred rapidly (Figures 3.3 and 3.4), which it made more difficult to assess growth of PDE transformants in the halo of inhibition in the SC-ura medium depicted in Figure 3.4. After enrichment, I identified two mutant *PDE4B* alleles that have an altered behavior in the presence of BC54: *PDE4*^{Y233H} and *PDE4*^{T407A}. After different attempts to identify compound-resistant PDE alleles, I can confirm that the enrichment was an important step to identify the mutants of interests. The enrichment killed off cells that failed to express an active PDE, which would include ones that fail to express PDE activity under any condition or ones that express a PDE that is sensitive to a PDE inhibitor that is added to the growth medium. Even after enrichment, relatively few of the transformants formed colonies on SC-ura with the BC54 zone of inhibition, suggesting that the percent of cells carrying plasmids of interest must have been very low after the original gap repair transformation.

6.1.2 Screening for compound-resistant alleles identifies important residues in target PDEs

PKA activity is associated with several phenotypes. Initially, I screened for mutants with an altered behavior in the presence of inhibitors assessing the mating phenotype (Appendix A). Although, the altered phenotype was detected, the compound did not necessarily affect all the cells within a colony. Thus, the sensitivity of the assay was relatively low. In contrast, the SC-ura phenotype

starts with individual cells on a plate. Therefore, if a compound fails to inhibit growth, the difference in colony size is noticeable.

The SC-ura growth phenotype was the best choice for the screen, but it required the enrichment step looking at survival in the presence of BC54 compound. The identification of mutant PDE alleles based on growth in SC-ura was the best approach in comparison to the mating phenotype, since growth within the zone of inhibition demonstrates that the transformant colony expresses a PDE enzyme with reduced sensitivity to BC54. Thus, this phenotype is not only associated with PKA activity, but with PDE activity. In the past, colony formation in SC-ura was used to isolate *git* mutants that had *fbp1* constitutive expression and low PKA activity (Hoffman and Winston, 1990). Therefore, it increased the chances of successful identification and characterization of mutants. After optimization and development of the screen, I identified two transformants expressing mutant alleles of *PDE4B* as previously mentioned. The plasmids expressing these mutant alleles were isolated and integrated as a single copy plasmid into the chromosome, which can be used for further characterization of PDE being expressed by a single plasmid to confirm the initial altered phenotype. I confirmed both mutant alleles of PDE4B conferred altered behavior in the presence of BC54 in cell-based assays.

In a previous work from our lab, mutant alleles were stably incorporated into a genome by disruption of *git2* locus with *ura4⁺* marker for selection (Ivey and Hoffman, 2004). This approach was employed to generate mutants that helped identify the binding site of Git2 that promotes activation of Gpa2 using a two-hybrid screen (Gα – subunit) (Ivey and Hoffman, 2004). In this study, I used a different approach, which was to integrate the entire plasmid. While this method could have been problematic as it creates a direct repeat flanking the gene of interest, such that a second recombination event might remove the gene from the genome, I did not obtain any results that suggested this method created unstable strains.

In the screen described in Chapter 3, I used PCR and gap repair to generate and clone mutant PDE alleles in *S. pombe* (Kostrub et al., 1998). Critical to the success of this procedure was the

optimization of the mutagenic PCR such that the mutant proteins I detected only possessed a single amino acid change. In the previous genetic screen (Appendix A), the mutant alleles identified carried more than one missense mutation, which made it difficult to re-confirm the initial altered mutant for mating phenotype in the presence of PDE inhibitor. Therefore, I optimized the mutagenic PCR by decreasing the number of cycles of amplification and using only buffers B, C, J and L from the Failsafe PCR kit (Chapter 2) that were previously shown to promote a low level of transition and transversion mutations (Hoffman lab, unpublished). This reduced the amount of mutagenesis, which allowed me to identify mutant alleles carrying single point mutations in the screen carried out in Chapter 3.

Although there are other options to screen for mutant alleles such as changes in the mating phenotype (Appendix A), I believe the combination of enriching for mutant alleles of interest via stationary phase survival and screening for compound resistance by colony formation on SC-Ura has been the best approach to follow. The enrichment for cell survival allowed rare transformants of interest to increase their relative numbers within the cells to be screened. Growth on SC-Ura in the presence of compound is an effective phenotype to identify transformant colonies carrying mutations that allow the PDE to remain active.

6.1.3 The value of knowing the mutants that display BC54-resistance

Over the years, crystal structure studies have helped clarify the amino acid interactions with each other in the PDE catalytic site (Xu et al., 2000; Houslay and Adams, 2003). According to crystal structure studies of PDE4B2, the two residues altered in our mutant alleles (*PDE4B*^{Y233H} and *PDE4B*^{T407A}) have been proposed to play roles in substrate binding and/or rolipram binding (Xu et al., 2000; Houslay and Adams, 2003). Moreover, the early structural models suggest that interactions of other amino acids with Tyr233 are important for stabilization of the hydrogen bond network. Meanwhile, Thr407 contacts the nucleotide base directly, which could be associated with substrate specificity for cAMP along with Thr403 playing a role in orienting Glu443 residue (Xu

et al., 2000, Houslay and Adams, 2003). To confirm and better understand these mutant forms of PDE4B, I have characterized their activity using both cell-based and *in vitro* approaches.

Cell-based assays developed in our lab have been very useful to better understand the sensitivity of PDE proteins to specific inhibitors (Demirbas et al., 2013; Ceyhan et al., 2012; Ivey et al., 2008). In the present study, I used two cell-based assays that assess PDE activity, as the inhibition of PDE activity would either increase growth in 5FOA medium or decrease the fluorescent signal. In both assays, PDE4B –expressing mutant strains were resistant or partially resistant to both BC54 and rolipram. Although PDE4B^{Y233H} –expressing strain displayed resistance to both inhibitors, it was observed this mutant strain expressed a weak PDE. In the screen that identified the mutant alleles, transformants expressed PDE4B from a multi-copy autonomously-replicating plasmid. However, once integrated, only a single-copy plasmid expressed PDE4B^{Y233H}, which revealed its weak activity that made it unsuitable for biochemical characterization. The screen using autonomous multicopy plasmids is probably the reason this weak PDE was initially detectable.

Since the T407A mutation confers reduced sensitivity both rolipram and BC54, one way to screen for possible allosteric inhibitors of PDE4B would be to use a strain expressing the PDE4B^{T407A}. It should display resistance to compounds that act through the cAMP-binding site as do rolipram and BC54, but remain sensitive to compounds that act through other sites. Once these compounds have been identified, one could then carry out a screen for alleles of *PDE4B* that are resistant to these compounds as a way of identifying the allosteric site or sites.

The findings from the cell-based assays suggested that PDE4B^{T407A} is potentially involved in direct binding of inhibitors, such that the mutant protein has a lower affinity for BC54. However, it was possible that this mutant is resistant due to an increase in affinity for cAMP. For this reason, I performed *in vitro* assays to examine the enzyme kinetics and determine IC₅₀ values for both BC54 and rolipram.

To assess enzyme activity, I optimized the conditions to test for V_{max}, enzyme efficiency and turnover number. Before going over the results, it is important to remember that PDE4B^{Y233H} had

such a weak activity that none of *in vitro* assays with PDE4B^{Y233H} were reproducible. Interestingly, this tyrosine residue is known to stabilize the interactions in the hydrogen-bonding network responsible for cAMP hydrolysis (Houslay and Adams, 2003; Xu et al., 2000). In *in vitro* assays, the PDE4B^{T407A} mutant enzyme was less active than the PDE4B^{wt} enzyme, which is in contrast to results from the GFP assay suggesting that PDE4B^{T407A} mutant strain was slightly more active than wild-type PDE4B (Figure 3.8). There are three possible explanations for this discrepancy between cell-based and *in vitro* assays, as followed: (1): the mutant enzyme may be more stable inside the cell than it is in the *in vitro* conditions; (2) the mutant enzyme may perform better in the cell cytoplasm versus in the *in vitro* environment; (3) I assess the full-length size of the mutant enzyme in the cell-based assay and only assessed the catalytic domain in the *in vitro* assays and it is possible that the full-length mutant enzyme may perform differently under *in vitro* conditions in comparison with its short form.

As I previously mentioned, PDE4B^{T407A} was less active than the Wild type PDE4B under *in vitro* conditions. The V_{max} for PDE4B^{T407A} was two-fold lower than that of the wild-type PDE4B under saturated conditions. This decrease in V_{max} also reflected the decrease in enzyme efficiency of the mutant protein. The mutant enzyme's ability to convert cAMP molecules into 5'AMP per minute also decreased in comparison to the wild type PDE4B enzyme. These results suggest that the altered behavior in the presence of compounds is not be due to an increase in affinity for cAMP since the efficiency and V_{max} of the mutant enzyme is less than that of the wild type enzyme.

Thr407 residue has previously been implicated in rolipram binding (Houslay and Adams, 2003). To verify that PDE4B^{T407A} mutant protein is altered in its sensitivity to these inhibitors, I performed *in vitro* enzyme assays to determine the IC₅₀ values for BC54 and rolipram. Consistent with the cell-based assays, I observed an almost 20-fold reduction in inhibition by BC54 against the mutant protein in comparison to the wild-type protein. In addition, there was an almost four-fold reduction in the IC₅₀ for rolipram against PDE4B^{T407A} in comparison to the wild-type PDE4B. This less dramatic decrease in inhibition by rolipram may be misleading and due to the use of just the

catalytic domain in this assay. As described earlier, monomeric forms of PDE4s display a low affinity for rolipram representing a conformation known as LARBS (Houslay and Adams., 2003). Thus the IC₅₀ for rolipram against the catalytic domain of the wild type enzyme may be artificially high, which would lessen the observed effect of the mutation in this assay (Figure 3.12). One may see a greater effect of the mutation in assays that use the full-length enzyme with and without the altered residue.

In future studies it will be interesting to introduce both Y233H and T407 mutations in PDE7 enzymes and verify if there is a loss of sensitivity by BC54 in *in vitro* assays and resistant phenotype in cell-based assays. Tyr233 is a conserved residue in PDE4B2 (NP_001032416.1), PDE7A (NP_001229247.1) and PDE7B (NP_061818.1). The conservation is supported by PDE4B2 crystal structure studies that suggest Tyr233 role in stabilization the hydrogen bond network, which is important for its hydrolytic activity (Xu et al., 2000). The loss of activity seen in PDE4B^{T233H} our cell-based assay supports Tyr233 role in hydrolytic activity. Thr407, on the other hand, is somewhat conserved. In PDE7 enzymes, there is a serine in place of the threonine. However, since both amino acids belong to the same biochemical group (nonpolar). By substituting the Ser for an Ala, PDE7 enzymes we may understand if this change in residues dramatic affect the mode of inhibition of BC54 and, perhaps help elucidate differences in BC54 inhibition between PDE4 and PDE7 enzymes.

Overall, these findings suggest that these mutations are directly involved in inhibitor affinity to PDE4B as our results suggest that the altered response of the mutant PDEs to BC54 is not associated with an increase in affinity for cAMP. In addition, studies of compounds related to BC54, described below, have identified some pharmacophores within BC54 that appear to be important for its activity. Taken together, this information can help to develop a model of how BC54 binds to PDE4B. Such a model would be useful in medicinal chemistry to design other dual specificity PDE4/7 inhibitors that are structurally-related to BC54.

6.1.4 BC54 analogs have different chemical groups that are important for activity against PDE4B2

As already mentioned, the knowledge about PDE structure helped understand amino acid interactions with each other in the catalytic site and their binding to inhibitors. In addition, many studies used PDE crystal structures to design PDE inhibitors. Therefore, I decided to examine the structure activity relationship (SAR) of BC54 using a series of related compounds. For this study, I profiled the potency of twelve compounds, which are structurally similar to BC54, in both a 5FOA-growth assay (where PDE inhibition stimulates growth) and an SC-ura halo assay (where PDE inhibition prevents growth), as shown in Appendix B. The purpose of these experiments was to identify chemical groups associated with changes in potency and selectivity.

Five out of 12 BC54 derivatives showed some activity using strains expressing PDE7B and PDE4B, and the pattern of inhibition was consistent between the 5FOA growth assay and the SC-ura halo assay. BC54 itself shows some preference for PDE4B over PDE7B, consistent with a lower IC_{50} for PDE4 (6.5nM; Chapter 3) than for PDE7 (140nM; Doug Ivey, unpublished data). Of the two most effective derivatives, BC54-8 shows a preference for PDE4B, while BC54-6 shows a preference for PDE7B, although neither is as effective as BC54 itself. The absence of a cyclohexyl group attached to the nitrogen of the pyrimidine ring in both analogs is one of the two main structural differences from BC54. In place of this group, BC54-8 has an isobutyl group and BC54-6 has an isopropyl group. Since BC54-6 shows a preference for PDE7B over PDE4B, while BC54 and BC54-8 show a preference for PDE4B over PDE7B, it can be inferred that these side-groups attached to the nitrogen of the pyrimidine ring are directly contacting the target enzymes. The second structural difference is in the acetylimino group attached to the carbon in the 2' position of the pyrimidine ring. The double bond connecting this carbon to the nitrogen of the acetylimino group blocks the rotation of the acetylimino group. In both BC54-6 and -8 the acetylimino orientation is locked in one direction that distinct from the orientation in BC54. The same orientation of the acetylimino group of BC54 is seen in analogs -5, -7, -9 through -12. Although

these data are preliminary, these findings suggest that both the cyclohexyl side group and the orientation of the acetylimino group may be important for BC54 activity. Furthermore, three BC54 analogs display moderate activity. These compounds are BC54-1, -3 and -11. BC54-1 and BC54-3 also seem to have a stronger inhibition on a strain expressing PDE4B as compared to PDE7B, while BC54-11 seems to display the opposite preference. BC54-1 and BC54-3 lack the acetylimino group and replace this group with a double bond to NH (imino group). Also, BC54-3 has a methylcarboxyl group instead of the ethylcarboxyl group present in BC54 and BC54-1. In addition, BC54-11 has a methylfuran in place of the cyclohexyl group. The absence or substitution of the cyclohexyl group of BC54 may affect not only specificity, but cause a strong reduction in potency. These findings suggest that the cyclohexyl group is the most effective side-group in this position of those that have been tested, although it leaves open the possibility of identifying an even more effective group for this position. However, these data are preliminary and required enzyme assays to confirm our initial findings.

Overall, all the compounds that had no effect against PDE4B- and PDE7B either 1) lack the cyclohexyl group, 2) lack the ethylcarboxyl group and/or 3) lack the acetylimino group. For example, BC54-5 is identical to BC54 with the exception of having only a methyl group in place of the cyclohexyl group. In addition, some compounds such as BC54-2 and BC54-7 possess additional atoms that may either abolish inhibition or prevent the compound from entering the cells. One could distinguish between these two possibilities by carrying out *in vitro* enzyme assays to determine IC₅₀s for the various compounds. Overall, the BC54 derivative data along with the findings about PDE4B^{T407A} mutant can help to validate docking models of BC54 bound to PDE4 and PDE7 enzymes. This information can then guide efforts to design a new generation of more potent and soluble PDE inhibitors based on the BC54 structure.

6.1.5 Conclusion

In the current study, both PDE4B^{Y233H} and PDE4B^{T407A} mutant strains display an altered response to either BC54 or rolipram in cell-based assays. In the *in vitro* assays, the point mutation in the PDE4B^{T407A} decreases its efficiency in hydrolyzing the substrate and decreases its affinity to the inhibitors. The decrease in the interaction with the substrate, can be seen in the decrease in V_{max}, enzyme efficiency and turnover number. Based on the *in vitro* assay data, it seems that Thr407 is an important residue for both PDE4B enzymatic activity and for inhibition by BC54. Further, profiling of BC54 derivatives suggests that the acetylrimino and cyclohexyl are important for potency and selectivity, respectively. The work performed with BC54 analogs was limited by what compounds currently exist in the collections of compound companies. Therefore, relatively few regions of the structure were varied. In the future, a project in collaboration with a chemist might allow us to look at portions of the compound that are the same in all these derivatives, but are identified as being important based on the T407A mutant.

As the T407A substitution was only assessed in the context of the PDE4B2 enzyme, it will be interesting to introduce this change to the long forms of PDE4 to see if produces a more dramatic loss of sensitivity to rolipram than seen in our study. In addition, it will be important to introduce the T407A mutation into the PDE7 enzyme to investigate if a mutant PDE7 is resistant to BC54 as well, since the interaction between BC54 and PDE4 does not necessarily mimic that of the interaction between BC54 and PDE7. We have previously observed that a compound, BC8-15, that inhibits both PDE4 and PDE8 enzymes appears to interact with enzymes of these two families in significantly different orientations (Demirbas et al., 2013). Due to this difference, many related compounds completely lost activity against PDE8, while retaining activity against PDE4.

Finally, these studies demonstrate that BC54 and rolipram act by contacting residues in the active site of these PDEs. Therefore, we are in a position to test our collection of PDE4 inhibitors against a strain expressing PDE4B^{T407A} as a way of identifying compounds that act at a site other than the cAMP-binding site. These would likely be allosteric inhibitors, which could then be used to isolate compound-resistant PDE4 alleles in an effort to identify their site(s) or action.

In conclusion, we confirmed residues that affect PDE4B inhibitor binding and affinity for the dual specificity BC54 inhibitor. Furthermore, the results of BC54 derivatives help us understand that substituting side groups in the pyrimidine ring and/or in the ethylcarboxyl, and changing the orientation of the acetylimino group may enhance the inhibitors when designing the next generation of PDE4/7 inhibitors. Taken together, these findings help us to better understand the interaction between PDE4 and BC54, and will be useful to guide efforts to generate inhibitors with enhanced activity in medicinal chemistry. In the future, it might be possible to design drugs using the knowledge gained about BC54 to treat autoimmune conditions.

6.2 The 10,000 HTS screen can identify compounds that reduce PKA activity

I developed a HTS that was designed to identify compounds that reduce PKA activity by stimulating PDE activity. The stimulation of PDE activity is reflected by an increase of the GFP signal.

6.2.1 Failure to validate compounds points out to technical issues

While the screen identified a number of compounds that appeared to elevate the GFP signal, we were unable to confirm that any of the cherry-picked compounds were authentic PDE activators. There are different reasons that can explain the lack of compound validation. For example, it is possible that the active compounds are breakdown products of the compounds supposedly present in the wells of interest. For the primary screen, we use library plates that have been frozen and thawed a few times. These freeze-thaw cycles may degrade the compound to create new compounds. It is possible that it is the effect of the derivative and not the compound that led to the initial positive result in the primary screen. In the cherry pick assays, we use compounds prepared from the original stocks. These compounds may lack the breakdown products and therefore not retest as hits. In the counter screen assays, we purchase new compounds directly from the companies. When dissolving these compounds, we observe solubility issues or color changes that

can be an indication of fluorescence (Meanwell, 2011; Turek Etienne et al., 2003), which may suggest that they were false positives in the primary screen. These observations cannot be fully addressed using the compounds from the screening facility.

A third reason why validation may have failed is that the cell delivery methods were completely different. In the primary screen, I used pin transfer. In the cherry pick assays, I used pocket tips that can fail to deliver the compounds properly, especially ones that fall out of solution in an aqueous medium. In the counter screens, we use multichannel pipettes for the assays. Multichannel pipettes can have problems delivering compounds due to not fully dispensing the compounds or formation of bubbles. It is worth noting that similar problems for validation were encountered in the screens for PDE inhibitors.

For future screens, it will be important to use a method for cherry pick assays that gives us more information about the compounds' potency and selectivity. A good alternative would be to perform a dose response against strains that express the initial target protein as well as nontarget proteins that carry out the same function. This way, we can separate selectivity versus potency before purchasing the compounds for in-house assay. Moreover, it is also important to expand the HTS. Finding PDE activators might be a rare event. Thus, a 10,000 HTS may not be sufficient to find a PDE activator. Furthermore, it will be good to perform future screens targeting different PDEs in parallel to decrease false-positives.

6.2.2 Conclusion

In conclusion, I have developed a HTS for small molecules that activate PDE activity. To our knowledge, this is the first HST developed with the effort to identify such compounds. For further optimization and validation of candidate hits, it will be important to expand the HTS using strains that express other PDEs. As an effort to identify PDE activators is to increase the number of compound libraries tested, which can help decreasing technical issues in the validation process.

Therefore, it might help find and characterize stronger hits versus weak hits using different strains expressing other PDE against a larger library screen.

6.3 Development of a HTS for PDE activators and AC/GNAS1 inhibitors

While the 10,000 compound screen for PDE activators showed promise, it suffered from two issues. In the absence of a counter-screen strain, we could not differentiate between PDE activators and compounds that elevated the GFP/OD₆₀₀ signal because they were either partially toxic or fluorescent. In addition, the relatively small number of compounds screened meant that it was possible there simply was not a PDE4 activator in this library. The HTS described in Chapter 5 addressed both of these issues by using a counter-screen strain and expanding the compound libraries.

The main goal of the larger HTS screen is to find compounds that reduce PKA activity by either activating PDE or inhibiting AC/GNAS1. We have recently developed the ability to express mammalian ACs along with the GNAS1 G α S that stimulates the tmACs, which allowed us to construct strains that expressed multiple target proteins to enhance the ability to find novel chemical regulators of mammalian cAMP signaling. In addition, a combination of targeting AC inhibitors and PDE activators can help decreasing technical issues in the validation process. It is possible that AC inhibition promotes a greater increase in GFP signal in comparison to PDE activation.

As already mentioned, I carried out this HTS with two strains simultaneously. The use of two strains aims to decrease the number of false positives due to fluorescence and toxicity as we would expect such compounds to show up as hits for both strains. The screening strain expresses PDE4D3 and AC5 and the counter-screen strain expresses PDE7B1, AC1 and GNAS1. Both strains were chosen because they have similar basal levels of GFP signal. Thus, any changes in GFP signal for one but not for the other strain indicates a specific compound reducing PKA activity for that particular strain. In chapter 5, I described the HTS to screen 100,000 small molecules that might identify compounds that either activate PDEs or inhibit ACs/GNAS1.

After the primary screen, 727 compounds were confirmed as hits for the screening strain. The hits were calculated by measuring the median and MAD for the experimental samples (i.e., the compound-treated wells). I changed the method to calculate Z-scores during the screening process due to concerns raised by the ICCB facility staff when we noticed that we have many likely false-positives due to the extremely low SDs of the negative controls. Such small SDs allowed for compounds to appear as a hit on only one strain due to slight differences in the MAD/median ratio. Once I changed the Z-scores analyses, I reached a reasonable and more realistic number of hits. For the cherry pick experiments, I selected 113 compounds that displayed either strong (above 15), moderate (10-15) or weak (6-10) Z-score values for both duplicates.

To validate these compounds, I tested various doses of compounds in a GFP assay against four different strains, which included the screening strain. These strains expressed different combinations of PDEs with ACs and/or GNAS1. The goal was to verify specificity and potency. From the 113 cherry pick hits, 70 were reconfirmed as targeting the screening strain. However, 49 compounds were eliminated on the basis of insufficient selectivity and potency and 17 were acquired for in house testing (along with 8 compounds obtained based on the primary screen alone).

6.3.1 Methods to validate candidate hit compounds

The 17 hit compounds that were reconfirmed in the cherry picks were purchased for further testing in secondary assays. In addition, we purchased six compounds (BC23-2, -3, -5, -6, -7,-8,-19) that were highly active hits in the primary screen along with a compound (BC23-1) that was designed based on structure similarity to both BC23-2 and BC23-3. A combination of cAMP and GFP assays were performed, but results were not reproducible. One possibility is that compounds failed to enter the cells using both methods. Another possibility is that the cAMP levels in the screening and counter-screen strains are already low that any further reduction in cAMP may not be readily detectable. One more possibility is that we validated false positives that have either fluorescence or solubility issues that were not detected earlier.

Although, I encountered technical issues with the GFP assays, I was able to confirm that most of these compounds have no effect on non-target proteins by treating a yeast strain (CHP2053) expressing ExoY (*Pseudomonas aeruginosa* cyclase) with PDE5A and PDE9A (Figure 5.8).

After cAMP and GFP assays, I performed a KCl assay. As mentioned in Chapter 1, strains with low PKA activity display KCl sensitive growth stress and strains with high PKA activity display a KCl resistant growth (Stiefel et al., 2004). The purpose of this experiment was to validate the compound hits independently from the *fbpI*-GFP reporter. In the KCl assays, I used strains that display KCl-growth resistance due to their relatively high level of PKA activity. These strains would become KCl-sensitive if a compound could reduce PKA activity. I confirmed that BC23-19 is a toxic compound in the KCl assay (Figure 5.9). In addition, most of the candidate hits, as demonstrated with BC23-7 in Chapter 5, had no effect in the strains tested in KCl assay (Figure 5.9). However, the data seemed less conclusive because it is possible that these compounds do not diffuse in solid medium and may still be able to either inhibit ACs or activate PDE4D3. Moreover, I confirmed that compounds BC23-18, -21 and -22 are AC5 inhibitors. However, these inhibitors are not AC5-specific inhibitors, as they display a broad AC specificity.

6.3.2 Difficulty in detecting PDE activators may be related to the limitation in increasing the enzyme activity

Although PDE activators have yet to be validated, it could be related to the fact that the increase in GFP signal due to an increase in PDE activity may have a low threshold effect. This, in turn, would lead us to prioritize PDE activators below AC inhibitors. An inhibitor can fully inhibit an enzyme activity, but an activator may be limited to no more than doubling the enzyme activity. The majority of compounds re-confirmed in the cherry pick assays were considered weak due to Z-scores values below 10 in duplicate wells. Therefore, it is possible that compounds that produce a slight increase in GFP signal may not be confirmed in the cherry pick experiments or counter-screen assays.

6.3.3 Progesterone is an AC inhibitor

The use of two strains simultaneously allowed for detection of specific hits for each strain. The most potent candidate hit for the counter-screen was Progesterone (work to be continued in the Hoffman lab). Interestingly catechol estrogens, structurally related to Progesterone, inhibited mammalian AC1, AC2, AC5 expressed in membrane preparations of insect cells and inhibited AC7 in an *in vitro* assay (Steebhorn et al., 2005). Moreover, this study confirmed that catechol estrogens act as non-competitive AC inhibitors binding to a pocket near the active site (Steebhorn et al., 2005). Another study demonstrated that Progesterone inhibits adenylyl cyclase expressed in *Xenopus* oocytes (Sadler et al., 1984). Although there is evidence that Progesterone is an AC inhibitor, its specificity is unknown. In our study, Progesterone was initially identified as a hit for the counter-screen that expresses AC1. Following counter-screen experiments in our lab, it seems that Progesterone may be a broad specificity AC inhibitor. Therefore, I can conclude the use of our yeast HTS system can not only detect AC inhibitors, but can identify AC inhibitors with broad specificity. However, this characterization is not complete.

6.3.4 Using non-selective compounds to understand the mechanism of AC regulation

I have confirmed BC23-18, -21 and -22 are AC inhibitors using KCl assays. All these compounds seem to target AC5, one of the proteins of interest expressed in the screening strain. However, they also target other ACs. However, further testing needs to be performed for further characterization of potency and specificity.

Most of the current AC inhibitors were designed based on tmAC structure, mainly targeting the catalytic site (Seifert et al., 2011; Pavan et al, 2009). However, it is difficult to develop AC inhibitors due to the fact that the target protein is an integral membrane protein that creates challenges for *in vitro* enzyme assays, which generally rely on purified targets. Furthermore, many, but not all, inhibitors have low potency inside the cells with the use of concentrations greater than 100 μ M to elicit any effect, but with that comes the possibility of off-target effects (Seifert et al.,

2011). Our screen assessed AC inhibitors inside the cells in a much lower concentration depending on the method of compound delivery (below 25 μ M for Primary screen and 5 μ M and lower concentrations for cherry picks). In addition, several studies failed to assess their action inside the cell due to their hydrophilic nature. To our knowledge, this is the first time a research group has identified AC5 inhibitors using a yeast system for a large HTS, instead of design of compounds, and assessment of the inhibitor activity inside the cell. The only other AC inhibitor screen I am aware of was a small compound screen by Conley and colleagues (2013) for AC2 inhibitors using mammalian cell culture.

The validated AC5 inhibitors display a broad inhibition targeting different ACs. BC23-18 and BC23-21 inhibit AC1 and AC8 (group I), AC2 and AC4 (group II), AC5 and AC6 (group III), and AC9 (group IV). However, BC23-21 appears to inhibit AC5 and AC6 more strongly than BC23-18 as judged by an increased zone of inhibition on KCl plates. BC23-22 inhibits more strongly AC7, AC8 and AC9, while inhibiting weakly AC4, AC5 and AC6. Although the preliminary data are encouraging, IC_{50} assays will be required to quantitate potency and selectivity. In the future, this broad specificity may be useful as certain ACs have similar tissue distribution even if they do not belong to the same group (Seifert et al, 2009). In addition, subsequent screens of this collection using strains that express other mammalian ACs or cyclases from other organisms should allow us to identify compounds that were overlooked in this screen as being ones worthy of further examination.

When I started the HTS, we looked for compounds that selectively affected only one of the two strains that were screened. We may have set our sights too high in expecting highly selective hits. It is possible we overlooked some of the best AC inhibitors by requiring them to distinguish between AC1 and AC5. Non-selective AC inhibitors can be used to make a collection of related compounds and screening them for increased potency and selectivity. This was the approach initially used by the PDE scientific community using theophylline, a non-selective inhibitor, to design family-specific compounds that could be used in cell-based assays to investigate the roles

of specific ACs just as PDE inhibitors are used to study individual PDE isoforms (Houslay et al., 2005).

The discovery of non-selective AC inhibitors allows me to question our analyses for the Primary screen. At this stage, I believe that finding AC inhibitors is the best approach to understand the biological consequence of AC inhibition inside the cells. Further, due to detection of broad specificity AC inhibitors one can infer the need to reassess the primary screen candidate hits list since we might have eliminated stronger AC inhibitors that were also hits for the counter-screen. Perhaps, I may have eliminated compounds that have either more potency and/ or display specificity for fewer ACs.

6.3.5 Conclusion and Future directions

In summary, I developed a HTS for PDE activators and AC/GNAS1 inhibitors. Overall, I was able to identify compounds that appeared to be specific to the screening strain based on the increase in GFP levels, a function of reduction in PKA activity. I confirmed and validated three AC5 inhibitors using cell-based assays. These inhibitors have somewhat a broad AC inhibition, but they can specifically inhibit members from groups I, II, III, and IV of tmACs. This is a very promising finding for the development of specific AC inhibitors, but further characterization is required. If I were to continue working on this project, I would probably perform counter-screens in some of the compounds hits that were eliminated in the primary screen. Clearly, the future direction of this project is to expand the HTS using strains express other tmACs and other PDE4 isoforms. By having more data on the effects of these compounds using a collection of strains, we can identify AC inhibitors that act on more than one AC as well as PDE activators that may have only a moderate impact on the GFP signal. This approach will increase our knowledge about potency and specificity of these small molecules and help us optimize the conditions to validate the candidate hits. This HTS will also serve as a database for future HTS conducted in our lab for small molecules that reduce PKA activity.

LITERATURE CITED

Alaamery, M.A., Wyman, A.R., Ivey, F.D., et al. (2010). New classes of PDE7 inhibitors identified by a fission yeast-based HTS. *J. Biomol. Screen.* 15, 359–367.

Ariga, M., Neitzert, B., Nakae, S., et al. (2004). Nonredundant function of Phosphodiesterases 4D and 4B in neutrophil recruitment to the site of inflammation. *J Immunol.*, **173**:7531–7538.

Atienza, J.M. and Colicelli, J. (1998). Yeast model system for study of mammalian phosphodiesterases. *Methods*, 14 (1):35-42.

Bahler, J. and Wood, V. (2004). In Egel, R. (ed.). *The molecular Biology of Schizosaccharomyces pombe: The genome and beyond*. Berlin: Springer, 13-25.

Bahler, J., Wu, J.Q., Longtine, M.S., et al. (1998). Heterologous modules for efficient and versatile PCR-based gene targeting in *Schizosaccharomyces pombe*. *Yeast*, 14(10):943-51.

Beavo, J.A. and Conti, M. (2007). Biochemistry and physiology of cyclic nucleotide phosphodiesterases: essential components in cyclic nucleotide signaling. *Annu. Rev. Biochem.* **76**, 481–511.

Bender, A.T., and Beavo, J.A. (2006). Cyclic nucleotide phosphodiesterases: molecular regulation to clinical use. *Pharmacol. Rev.* **58**, 488–520.

Bischoff, J.R., Casso, D., Beach, D. (1992). Human p53 inhibits growth in *Schizosaccharomyces pombe*. *Mol Cell Biol.*, **12**:1405–1411.

Burgin, A.B., Olafur, T., Magnusson, O.T., et al. (2010). Design of phosphodiesterase 4D (PDE4D) allosteric modulators for enhancing cognition with improved safety. *Nature Biotechnology*, **28**:63–70.

Calverley, P.M., Sanchez-Toril, F., McIvor, A., et al. (2007). Effect of 1-year treatment with roflumilast in severe chronic obstructive pulmonary disease. *Am J Respir Crit Care Med* **176**: 154–161.

Card, G.L., England, B.P., Suzuki, Y., et al. (2004). Structural basis for the activity of drugs that inhibit phosphodiesterases. *Structure* **12**: 2233–2247.

Castro, A., Jerez, M.J., Gil, C., Martinez, A. (2005). Cyclic nucleotide phosphodiesterases and their role in immunomodulatory responses: advances in the development of specific phosphodiesterase inhibitors. *Med. Res. Rev.* **25**: 229–244.

Ceyhan, O., Birsoy, K., Hoffman, C.S. (2012). Identification of Biologically Active PDE11-Selective Inhibitors Using a Yeast-Based High-Throughput Screen. *Chemistry and Biology*, **19**:155–163.

Chen, D., Toone, W.M., Mata, J., et al. (2003). Global transcriptional responses of fission yeast to environmental stress. *Mol Biol Cell.* **14**:214–29.

Clontech. (2001). Diversify PCR Random Mutagenesis Kit. Clontech Laboratories, Inc., 1-19.

Conley, J.M., Brand, C.S., Bogard, A.S., et al. (2013). Development of a High-Throughput Screening Paradigm for the Discovery of Small-Molecule Modulators of Adenylyl Cyclase: Identification of an Adenylyl Cyclase 2 Inhibitor. *J Pharmacol Exp Ther* **347**:276–287.

Conn, P.J., Christopoulos, A., and Lindsley, C.W. (2009). Allosteric modulators of GCPRs: a novel approach for the treatment of CNS disorders. *Nat.Rev.Drug Discov.*, 8(1):41-54.

Copeland, R. A. (2000). *Enzymes- A practical introduction to structure, mechanism, and data analysis: Reversible inhibitors*. Wiley-VCH., Inc. 2nd Ed.

Colicelli, J., Birchmeier, C., Michaeli, T., et al. (1989). Isolation and characterization of a mammalian gene encoding a high-affinity cAMP phosphodiesterase. *Proc. Natl. Acad. Sci.*, 86(10):3599-3603.

Colicelli, J., Nicolette, C., Birchmeier, C. et al. (1991). Expression of three mammalian cDNAs that interfere with RAS function in *Saccharomyces cerevisiae*. *Proc. Natl. Acad. Sci.*, 88(7):2913-2917.

de Medeiros, A.S., Kwak, G., Vanderhooff, J., et al. (2015). Fission yeast-based high-throughput screens for PKA pathway inhibitors and activators. *Methods Mol Biol.*, **1263**:77-91.

de Medeiros, A.S., Magee, A., Nelson, K., et al (2013). Use of PKA-mediated phenotypes for genetic and small-molecule screens in *Schizosaccharomyces pombe*. *Biochem Soc Trans.*, **1**(6):1692-5.

Demirbas, D., Ceyhan, O., Wyman, A.R., and Hoffman, C.S. (2011a). A fission yeast-based platform for phosphodiesterase inhibitor HTSs and analyses of phosphodiesterase activity. *Handb. Exp. Pharmacol.* 204, 135–149.

Demirbas, D., Ceyhan, O., Wyman, A.R., et al. (2011b). Use of a *Schizosaccharomyces pombe* PKA-repressible reporter to study cGMP metabolising phosphodiesterases. *Cell. Signal.*, 23:594–601.

Demirbas, D., Wyman, A.R., Shimizu-Albergine, M., et al (2013). A yeast-based chemical screen identifies a PDE inhibitor that elevates steroidogenesis in mouse leydig cells via PDE8 and PDE4 inhibition. *PLOS ONE* , 8 (8), e71279.

DeVoti, J. Seydoux, G, Beach, D, and McLeod, M. (1991). Interaction between ran1+ protein kinase and cAMP dependent protein kinase as negative regulators of fission yeast meiosis. *EMBO J.*, 10(12):3759-68.

Fabbri L.M., Calverley P.M., Izquierdo-Alonso J.L., et al. (2009). Roflumilast in moderate-to-severe chronic obstructive pulmonary disease treated with long acting bronchodilators: two randomized clinical trials. *Lancet.* 2009, 374:695–703.

FDA (2011) http://www.accessdata.fda.gov/drugsatfda_docs/label/2015/022522s006lbl.pdf

FDA (2014) http://www.accessdata.fda.gov/scripts/cder/ob/docs/obdetail.cfm?Appl_No=205437&TABLE1=OB_Rx

Fortin, M., D'Anjou, H., Higgins, M. E., et al. (2009). A multi-target antisense approach against PDE4 and PDE7 reduces smoke- induced lung inflammation in mice, *Respiratory Research*, **10** (39), 1-14.

Franz, A.K., Dreyfuss, P.D., Schreiber, S.L. (2007). Synthesis and cellular profiling of diverse organosilicon small molecules. *J Am Chem Soc.*; **129**(5):1020–1.

Gancedo, J.M. (2013). Biological roles of cAMP: variations on a theme in the different kingdoms of life. *Biol. Rev*, **88**:645–668.

Gardner, C., Robas, N., Cawkill, D., and Fidock, M. (2000). Cloning and characterization of the human and mouse PDE7B, a novel cAMP-specific cyclic nucleotide phosphodiesterase. *Biochem. Biophys. Res. Commun.*, **272**:186–192.

Giembycz, M.A. and Smith, S.J. (2006). Phosphodiesterase 7A: a new therapeutic target for alleviating chronic inflammation? *Curr. Pharm. Des.*, **12**(25):3207–20.

Grange, M., Sette, C., Cuomo, M., et al (2000). The cAMP-specific Phosphodiesterase PDE4D3 is regulated by phosphatidic Acid binding:Consequences for cAMP signaling pathway and characterization of a Phosphatidic acid binding site. *J. Bio. Chem.*, **275**:33379-33387.

Hammond, H.K. (2015). [https://clinicaltrials.gov/ct2/show/NCT00787059?term=AC+6++gene+transfer &rank=1](https://clinicaltrials.gov/ct2/show/NCT00787059?term=AC+6++gene+transfer&rank=1)

Hanoune, J., Defer, N. (2001). Regulation and role of adenylyl cyclase isoforms. *Annu Rev Pharmacol.Toxicol.*, **41**:145–174.

Hanoune, J., Pouille, Y., Tzavara, E., et al. (1997). Adenylyl cyclases: structure, regulation and function in an enzyme superfamily. *Mol Cell Endocrinol*, **128**:179–94.

Hartwig, C., Bähre, H., Wolter, S., et al (2014). cAMP, cGMP, cCMP and cUMP concentrations across the tree of life: High cCMP and cUMP levels in astrocytes. *NeuroscienceLetters*, **579**(2014):183–187.

Hatanaka, M. and Shimoda, C. (2001). The cyclic AMP/PKA signal pathway is required for initiation of spore germination in *Schizosaccharomyces pombe*. *Yeast*, **18**: 207-217.

Hayles, J. and Nurse, P. (1992). Genetics of the fission yeast *Schizosaccharomyces pombe*. *Annu.Rev.Genet.*, 26:373-402.

Hetman, J.M., Soderling, S.H., Glavas, N.A., and Beavo, J.A. (2000). Cloning and characterization of PDE7B, a cAMP-specific phosphodiesterase, *Proc. Natl. Acad. Sci*, 97:472-476.

Ho, D., Yan, L., Iwatsubo, K., et al. (2010). Modulation of beta-adrenergic receptor signaling in heart failure and longevity: targeting adenylyl cyclase type 5. *Heart Fail Rev* **15**: 495–512.

Hoffman, C.S. (2005a). Except in every detail: Comparing and contrasting G protein signaling in *Saccharomyces cerevisiae* and *Schizosaccharomyces pombe*. *Eukaryotic Cell*, 4:495-503.

Hoffman, C.S. (2005b). Glucose sensing via the protein kinase A pathway in *Schizosaccharomyces pombe*. *Biochem Soc Trans*, 33(1):257-260.

Hoffman, C.S. and Winston, F. (1987). A ten-minute DNA preparation from yeast efficiently releases autonomous plasmids for transformation of *Escherichia coli*. *Gene*, 57:267-272.

Hoffman, C.S., and Winston, F. (1990). Isolation and characterization of mutants constitutive for expression of the *fbp1* gene of *Schizosaccharomyces pombe*. *Genetics*, 124:807–816.

Hoffman, C.S., and Winston, F., (1991). Glucose repression of transcription of the *Schizosaccharomyces pombe fbp1* gene occurs by a cAMP signaling pathway. *Genes Dev.*, 5:561–571.

Houslay, M.D., and Adams, D.R. (2003). PDE4 cAMP phosphodiesterases: modular enzymes that orchestrate signalling cross-talk, desensitization and compartmentalization. *Biochem. J.* **370**: 1-18.

Houslay, M.D., Schafer, P. and Zhang, K.Y.J. (2005). Keynote review: Phosphodiesterase-4- as a therapeutic target. *DDT*,**10** (22): 1503-1519.

Isshiki, T., Mochizuki, N., Maeda, T., and Yamamoto, M. (1992). Characterization of a fission yeast gene, *gpa2*, that encodes a G alpha subunit involved in the monitoring of nutrition. *Genes Dev.* 6:2455–2462.

Ivey, F.D., Wang, L., Demirbas, D., et al. (2008). Development of a fission yeast-based high-throughput screen to identify chemical regulators of cAMP phosphodiesterases. *J. Biomol. Screen.*, 13:62–71. *J Clin Endocrinol Metab.*, **99**(8): E1476-81.

Jensterle M., Kocjan, T, Janez, A. (2014). Phosphodiesterase 4 inhibition as a potential new therapeutic target in obese women with polycystic ovary syndrome.

Jimenez, J.L., Punzón C., Navarro J., et al. (2001) Phosphodiesterase 4 inhibitors prevent cytokine secretion by T lymphocytes by inhibiting nuclear factor-kappaB and nuclear factor of activated T cells activation. *J. Pharmacol. Exp. Ther.* **299**: 753–759.

Jin, M., Fujita, M., Culley, B.M, et al. (1995). *sck1*, a high copy number suppressor of defects in the cAMP-dependent protein kinase pathway in fission yeast, encodes a protein homologous to the *Saccharomyces cerevisiae* SCH9 kinase. *Genetics*, 1995.140(2): p457-67.

Jin, S.-L.C., Richard, F.J., Kuo, W.P., et al. (1999). Impaired growth and fertility of cAMP-specific phosphodiesterase PDE4D-deficient mice. *Proc Natl Acad Sci U S A.* 96, In press.

Kamenetsky, M., Middelhaufe, S., Bank, E.M., et al., (2006). Molecular Details of cAMP Generation in Mammalian Cells: A Tale of Two Systems. *J Mol Biol.*, **362**(4): 623–639.

Kao, R., Morreale, E., Wang, L., et al. (2006). *Schizosaccharomyces pombe* Git 1 is a C2- domain protein required for glucose activation of adenylate cyclase. *Genetics*, 173:49-61.

Ke, H., Wang, H., and Ye, M. (2011). Structural insight into the substrate specificity of Phosphodiesterases. *Handb Exp Pharmacol*, (204):121-34.

Keravis, T. and Lugnier, C. (2012). Cyclic nucleotide phosphodiesterase (PDE) isozymes as targets of the intracellular signaling network: benefits of PDE inhibitors in various diseases and perspectives for future therapeutic developments. *British Journal of Pharmacology* **165**:1288–1305.

Kostrub, C.F., Lei, E.P., and Enoch, T. (1998). Use of gap repair in fission yeast to obtain novel alleles of specific genes. *Nucleic Acids Research.*, **26** (20), 4783–4784.

Kumar, N., Goldminz A.M., Kim N. and Gottlieb, A.B. (2013). Phosphodiesterase 4-targeted treatments for autoimmune diseases. *BMC Med.*, **11**:96.

Landry, S. and Hoffman, C.S. (2001). The git5 Gbeta and git1l Ggamma Form an Atypical Gbetagamma Dimer Acting in the Fission Yeast Glucose/cAMP Pathway. *Genetics*, 157(3): 1159-68.

Landry, S., Pettit, M.T., Apolinario, E., and Hoffman, C.S. (2000). The fission yeast git5 gene encodes a G/3 subunit required for glucose-triggered adenylate cyclase activation. *Genetics*, 154(4):1463-1471.

Lee, R., Wolda, S., Moon, E., et al. (2002). PDE7A is expressed in human B lymphocytes and is up-regulated by elevation of intracellular cAMP. *Cell Signal.*, 14(3):277–84.

Lerner, A. and Epstein, P.M. (2006). Cyclic nucleotide phosphodiesterases as targets for treatment of haematological malignancies. *Biochem J*, 393(1):21-41.

Lin, D.-C., Xu, L., Ding, L.W., et al. (2013). Genomic and functional characterizations of phosphodiesterase subtype 4D in human cancers. *PNAS*, **110** (15), 6109–6114.

Linsong, L., Yee, C. and Beavo, J.A. (1999). CD3- and CD28-Dependent Induction of PDE7 Required for T Cell Activation. *Science*, 283:848-851.

Lipworth, B.J. (2005). Phosphodiesterase-4 inhibitors for asthma and chronic obstructive pulmonary disease. *Lancet* **365**:167–175.

Loukides, S., Bartziokas, K., Vestbo, J.R., Singh, D. (2013). Novel anti-inflammatory agents in COPD:targeting lung and systemic inflammation. *Curr Drug Targets.*, **14**:235–245.

Lugnier, C. (2006). Cyclic nucleotide phosphodiesterase (PDE) superfamily: A new target for the development of specific therapeutic agents. *Pharmacology & Therapeutics*, 109: 366-398.

Maeda, T., Watanabe, Y., Kunitomo, H., and Yamamoto, M. (1994). Cloning of the *pkal* gene encoding the catalytic subunit of the cAMP-dependent protein kinase in *Schizosaccharomyces pombe*. *J. Biol. Chem.* 269, 9632–9637.

Maurice, D.H., Ke, H., Ahmad, F., et al. (2014). Advances in targeting cyclic nucleotide phosphodiesterases. *Nat Rev Drug Discov.* **13**(4): 290–314.

Maurice, D.H., Palmer, D., Tilley, D.G., et al. (2003). Cyclic Nucleotides Phosphodiesterases Activity, Expression, and Targeting in Cells of the Cardiovascular System. *Mol.Pharm.* 64(3): 533-546.

Meanwell, N.A., (2011). Synopsis of Some Recent Tactical Application of Bioisosteres in Drug Design. *J. Med. Chem.*, **54** (8): 2529–2591.

Mehats, C., Andersen, C.B., Filopanti, M., et al. (2002). Cyclic nucleotide phosphodiesterases and their role in endocrine cell signaling. *Trends in End. & Metab.*, 13(1): 29-32.

Michaeli, T., Bloom, T.J., Martins, T., et al. (1993). Isolation and characterization of a previously undetected human cAMP phosphodiesterase by complementation of cAMP Phosphodiesterase-deficient *Saccharomyces cerevisiae*. *J. Bio. Chem.*, **17**:12925-12932.

Mochizuki, N., Yamamoto, M. (1992). Reduction in the intracellular cAMP level triggers initiation of sexual development in fission yeast. *Mol Gen Genet.*, **233**(1-2):17-24.

Nicol, X and Gaspar, P. (2014). Routes to cAMP: shaping neuronal connectivity with distinct adenylyl cyclases. *European Journal of Neuroscience*, **39**:1742–1751.

Nikawa, J., Cameron, S., Toda, T., et al. (1987a). Rigorous feedback control of cAMP levels in *Saccharomyces cerevisiae*. *Genes Dev.*, **1**(9):931-937.

Nikawa, J., Sass, P., and Wigler, M. (1987b). Cloning and characterization of the low-affinity cyclic AMP phosphodiesterase gene of *Saccharomyces cerevisiae*. *Mol. Cell Biol.*, **7**(10):3629-3636.

Nocero, M., T. Isshiki, M., Yamamoto, and Hoffman, C.S. (1994). Glucose repression of *fbpl* transcription of *Schizosaccharomyces pombe* is partially regulated by adenylyl cyclase activation by a G protein alpha subunit encoded by *gpa2* (*git8*). *Genetics*, **138**(1):39-45.

Offermanns, S. (2001). In vivo functions of heterotrimeric G α -proteins: studies in G-deficient mice. *Oncogene*, **20**:1635-1642.

Okumura S, Suzuki, S., Ishikawa, Y. (2009). New aspects for the treatment of cardiac diseases based on the diversity of functional controls on cardiac muscles: effects of targeted disruption of the type 5 adenylyl cyclase gene. *J Pharm Sci.*, **109**: 354–359.

Omori, K. and Kotera, J. (2007). Overview of PDEs and their regulation. *Circulation Research*, **100**(3):309-27.

Paterniti, I., Mazzon, E., Gil, C., et al. (2011). PDE7 inhibitors: New potential drugs for the therapy of spinal cord injury, *PLoS One*, 6 (1):1-15.

Pavan, B., Biondi, C., and Dalpiaz, A. (2009). Adenylyl cyclases as innovative therapeutic goals. *DDT*, **14**: 982-991.

Pillai, R., Kytle, K., Reyes, A., and Colicelli, J. (1993). Use of a yeast expression system for the isolation and analysis of drug-resistant mutants of a mammalian phosphodiesterase. *Proc. Natl. Acad. Sci.*, **90**(24):11970-11974.

Rall, T.W. and Sutherland, E.W. (1958) Formation of a cyclic adenine ribonucleotide by tissue particles. *J. Bio. Chem.*, **232**(2): p. 1065-76.

Richter, W. and Conti, M. (2004). The Oligomerization State Determines Regulatory Properties and Inhibitor Sensitivity of Type 4 cAMP-specific Phosphodiesterase. *J. Bio. Chem.*, **279** (29), 30338–30348.

Richter, W., Menniti, F.S., Zhang, H.-T., and Marco Conti, M. (2013). PDE4 as a target for cognition enhancement. *Expert Opin Ther Targets*, **17**(9): 1011–1027.

Robichaud, A., Stamatiou, P.B., Jin, S.L., et al. (2002). Deletion of phosphodiesterase 4D in mice shortens alpha (2)-adrenoceptor-mediated anesthesia, a behavioral correlate of emesis. *J. Clin. Invest.*, **110**:1045–1052.

Sadler, S.E., Maller, J.L., and Cooper, D.M. (1984). Progesterone inhibition of *Xenopus* oocyte adenylate cyclase is not mediated via the *Bordetella pertussis* toxin substrate. *Molecular Pharmacology*, **26** (3): 526-531.

Sasaki, T., Kotera, J., and Omori, K. (2002). Novel alternative splice variants of rat phosphodiesterase 7B showing unique tissue-specific expression and phosphorylation. *Biochem. J.*, **2**:211–220.

Sasaki, T., Kotera, J., and Omori, K. (2004). Transcriptional activation of phosphodiesterase 7B1 by dopamine D1 receptor stimulation through the cyclic AMP/cyclic AMP-dependent protein kinase/cyclic AMP-response element binding protein pathway in primary striatal neurons. *J. Neurochem.*, **89**:474–483.

Sasaki, T., Kotera, J., Yuasa, K., and Omori, K. (2000). Identification of human PDE7B, a cAMP-specific phosphodiesterase. *Biochem Biophys Res Commun.*, **271**:575–583.

Seifert, R., Lushington, G.H, Mou, T.-C., et al. (2012). Inhibitors of membranous adenylyl cyclases. *Trends in Pharmacological Sciences*, **33** (2):64-78.

Søberg, K., Jahnsen, T., Rognes, T., et al. (2013). Evolutionary paths of the cAMP-dependent protein kinase (PKA) catalytic subunits. *PLoS One*, **8**(4): e60935.

Soderling, S.H. and Beavo, J.A. (2000). Regulation of cAMP and cGMP signaling: new phosphodiesterases and new junctions. *Curr Opin Cell Biol.*, **12**(2):174-179.

Spina, D. (2008). PDE4 inhibitors: current status. *British Journal of Pharmacology*, **155**: 308–315.

Steegborn, C. (2014). Structure, mechanism, and regulation of soluble adenylyl cyclases - similarities and differences to transmembrane adenylyl cyclases. *Biochim Biophys Acta*. **1842**(12 Pt B):2535-47.

Steegborn, C., Litvin, T.N, Hess, K.C, et al. (2005). A Novel Mechanism for Adenylyl Cyclase Inhibition from the Crystal Structure of Its Complex with Catechol Estrogen. *J. Bio. Chem.*, **280**(36): 31754–31759.

Stiefel, J., Wang, L., David, A, et al., (2004). Suppressors of an Adenylate Cyclase Deletion in the Fission Yeast *Schizosaccharomyces pombe*. *Eukaryotic cell.*, **3** (3): 610–619.

Stratakis, C.A. (2012). Cyclic AMP, protein kinase A, and phosphodiesterases: proceedings of an international workshop. *Horm Metab Res*. **44**(10):713-5.

Sunahara, R.K., Dessauer, C.W., Gilman, A.G. (1996). Complexity and diversity of mammalian adenylyl cyclases. *Annu. Rev. Pharmacol. Toxicol.* **36**:461–480.

Turek-Etienne, T.C., Small, E.C., Soh, S.C., et al (2003). Evaluation of Fluorescent Compound Interference in 4 Fluorescence Polarization Assays: 2 Kinases, 1 Protease, and 1 Phosphatase. *Journal of Biomolecular Screening* **8**(2): 176-184.

US National Institutes of Health (2015). [www. ClinicalTrials.gov](http://www.ClinicalTrials.gov)

van Schalkwyk, E., Strydom, K., Williams, Z., et al. (2005). Roflumilast, an oral, once-daily phosphodiesterase 4 inhibitor, attenuates allergen-induced asthmatic reactions. *J. Allergy Clin. Immunol.* **116**: 292–298.

Vatner, S.F., Ishikawa, Y., Park, M., et al. (2013). Adenylyl cyclase type 5 in cardiac disease, metabolism, and aging. *Am J Physiol Heart Circ Physiol.*, **305**: H1–H8.

Wachtel H. (1982). Characteristic behavioural alterations in rats induced by rolipram and other selective adenosine cyclic 3', 5'-monophosphate phosphodiesterase inhibitors. *Psychopharmacology (Berl)*, **77**:309–16.

Wachtel, H. (1983). Potential antidepressant effects of rolipram and other selective PDE inhibitors. *Neuropharmacol.*; **22**:267–272.

Wang, H., Liu, Y., Chen, Y., et al. (2005a). Multiple elements jointly determine inhibitor selectivity of cyclic nucleotide phosphodiesterases 4 and 7. *J. Biol. Chem.*, **280**: 30949–30955.

Wang, H., Peng, M.-S., Chen, Y, et al., (2007). Structures of the four subfamilies of phosphodiesterase-4 provide insight into the selectivity of their inhibitors. *Biochem. J.*, **408** :193–20.

Wang, L., Griffiths, K. Jr., Zhang, Y.H., et al. (2005). *Schizosaccharomyces pombe* adenylate cyclase suppressor mutations suggest a role for cAMP phosphodiesterase regulation in feedback control of glucose/cAMP signaling. *Genetics*, **171**:1523-33.

Wang, P., Wu, P., Ohleth, K.M., et al. (1999). Phosphodiesterase 4B2 is the predominant phosphodiesterase species and undergoes differential regulation of gene expression in human monocytes and neutrophils. *Mol. Pharmacol.* **56**, 170–174.

Welton, R.M. and Hoffman, C.S. (2000). Glucose monitoring in fission yeast via the *gpa2* Ga, the *git5* G/3, and the *git3* putative glucose receptor. *Genetics*, 156:513-521.

Wood, V., Gwilliam, R., Rajandream, M.A., et al. (2002). The genome sequence of *Schizosaccharomyces pombe*. *Nature*, **415**:871-880.

Wood, V., Harris, M.A., McDowall, M.D., et al. (2012). PomBase: a comprehensive online resource of fission yeast. *Nuclei Acids res.*, **40**: D695-D699.

Xu, R.X., Hassell, A.M., Vanderwall, D., et al. (2000). Atomic Structure of PDE4: Insights into Phosphodiesterase Mechanism and Specificity. *Science*, **288**: 1822-1825.

Zeller, E., Stief, H.J., Pflug, B., and Sastre-y-Hernández M. (1984). Results of a phase II study of the antidepressant effect of rolipram. *Pharmacopsychiatry*, **17**:188–190.

Zhang, K.Y.J., Card, G.L., Suzuki, Y., et al. (2004). A glutamine switch mechanism for nucleotide selectivity by phosphodiesterases. *Mol. Cell*, **15**: 279–286.

Zhang, L., Murray, F., Zahno, A., et al. (2008). Cyclic nucleotide phosphodiesterase profiling reveals increased expression of phosphodiesterase 7B in chronic lymphocytic leukemia, *Proc. Natl. Acad. Sci.*, **105**:19532-19537.

APPENDIX A

DEVELOPMENT OF *S.POMBE* GENETIC SCREEN FOR - COMPOUND- RESISTANT PDE7 ALLELES

INTRODUCTION

As mentioned in Chapter 1, our lab has developed a cell-based platform to screen for PDE7 inhibitors using genetically engineered yeast strains. Currently, we have small molecules that inhibit many PDE proteins specifically. Here, we developed a genetic screen in an effort to characterize the interaction between PDE7 inhibitors, and the PDE7B enzyme by screening for compound-resistant mutant PDE7B alleles. Our approach takes advantage of the mating phenotype that is associated with low PKA activity as mentioned in Chapter 1. Mutant alleles of cAMP-specific PDE7 gene can be detected by their ability to increase mating in the presence of a specific PDE7 inhibitor. Thus, we have developed genetic screens for mutant alleles of mammalian PDE genes that are altered for their sensitivity to chemical inhibitors.

MATERIALS AND METHODS

A1. MATERIALS

A1.1 Growth media

Sensitivity to compound PDE inhibitors was determined in (5FOA) and SC-solid medium as described by Hoffman and Winston (1990).

A1.2 Yeast strains

The genotype of all yeast strains used in this study are listed in Table A1. The strains in this thesis carried either the *fbp1-ura4*⁺. Both constructs are translational fusions integrated at the *fbp1*⁺ locus, as previously described by Hoffman and Winston (1990) and de Medeiros et al. (2013), respectively. Strains were grown at 30°C.

A.1.3 Enzymes

Restriction endonuclease enzymes and their buffers were purchased from New England Biolabs (NEB, Ipswich, MA) and used according to NEB instructions. The enzymes used in this study were *HindIII*, *PvuII* and *XhoI* for D7

A2. Methods

A.2.1 Mutagenic PCR

Mutagenesis PCR was performed to clone either the mammalian PDE7B1 (Genbank accession number NM_018945) as described in section 2.2.2. PCR products were generated by FailSafe PCR kit already using "Premix" buffers A, B, E, F, K and L as described in section 2.2.2. The primers used were the *cgs2mut5*' and *cgs2mut3*' described in section 2.2.2. Mutant plasmid candidates were rescued out of yeast into *E. coli* by using the Smash and Grab method (Hoffman and Winston, 1987), and purified using a QIAquick PCR Purification kit, according to manufacturer's instructions (QIAGEN®, Valencia, CA) and sent out for sequencing.

A.2.2 Cloning and Plasmid construct

Mutant plasmid candidates were constructed as described in section 2.1. After sequencing, plasmids containing mutant candidate PDE7B1 alleles for the mating phenotype were integrated into the chromosome of a *S. pombe* strain (CHP1207) carrying the *cgs2-2* frameshift allele (no PDE activity) along with an adenyl cyclase deletion (*git2Δ*), carrying either the *fbp1-ura4*, as previously described (section 2.1.1).

Table A1. Strain list used in the genetic screen for mating

Strains	Genotypes
SP578	<i>h⁹⁰ fbp1-ura4⁺ ura4::fbp1-lacZ leu1-32 ade6-M216 cgs2-2</i>
CHP1440	<i>h⁹⁰ fbp1-ura4⁺ ura4::fbp1-lacZ leu1-32 pap1Δ cgs2-2 git2-2</i>
CHP1251	<i>h⁹⁰ fbp1-ura4⁺ ura4::fbp1-lacZ leu1-32 gpa2Δ pap1Δ</i>
CHP1501	<i>h^r fbp1-ura4⁺ ura4::fbp1-lacZ leu1-32 pap1Δ cgs2-2::pKG3-PDE7B:B1[LEU2] git2-2</i>
CHP1502	<i>h^r fbp1-ura4⁺ ura4::fbp1-lacZ leu1-32 pap1Δ cgs2-2::pKG3-PDE7B:C7[LEU2] git2-2</i>
CHP1503	<i>h^r fbp1-ura4⁺ ura4::fbp1-lacZ leu1-32 pap1Δ cgs2-2::pKG3-PDE7B:D7[LEU2] git2-2</i>
CHP1504	<i>h^r fbp1-ura4⁺ ura4::fbp1-lacZ leu1-32 pap1Δ cgs2-2::pKG3-PDE7B:G21[LEU2] git2-2</i>
CHP1505	<i>h^r fbp1-ura4⁺ ura4::fbp1-lacZ leu1-32 pap1Δ cgs2-2::pKG3-PDE7B:K19 (WT)[LEU2] git2-2</i>
CHP1506	<i>h^r fbp1-ura4⁺ ura4::fbp1-lacZ leu1-32 pap1Δ cgs2-2::pKG3-PDE7B:L1(WT)[LEU2] git2-2</i>
CHP1207	<i>h^r fbp1-ura4⁺ ura4::fbp1-lacZ leu1-32 git3Δ pap1Δ cgs2-2 git2-2</i>
CHP1209	<i>h^r fbp1-ura4⁺ ura4::fbp1-lacZ leu1-32 git3Δ pap1Δ cgs2::PDE7B1</i>
CHP1189	<i>h^t fbp1-ura4⁺ ura4::fbp1-lacZ leu1-32 gpa2Δ pap1Δ cgs2::PDE7A1</i>

A.2.3 DNA sequencing

The purified plasmids were sent out to Eurofins MWG Operon (Huntsville, Alabama) for DNA sequencing and confirmation of base-pair change. The following primers were used: cgsmut5' (5'TCATAGCATACTTCTTCACCAAGC3') and cgsmut3' (3'AAAGTGTCCGATGAGAAAAGCGTG).

A.2.4 Genetic Screen

A genetic screen was developed in the present study to identify and isolate compound-resistant PDE7B1 alleles by their ability to increase mating even in the presence of a PDE7 inhibitor (Figure A1). In the first phase of the screening, three strains were chosen where PDE activity can be detected by evaluating the cAMP levels required to confer growth response. The first step for the screen was to perform mutagenesis PCR to generate mutant candidates. Then, the *S. pombe* *cgs2* gene was replaced with human PDE7B1 gene, inserted it into a plasmid, and cotransformed them into three chosen strains (Table A1). The strain CHP1440 (no cAMP activity) had few transformants and strain CHP1251 (reduced cAMP levels) did not allow us to differentiate transformants from empty vector control, while strain SP578 (normal cAMP levels) produced a number of transformants amenable to this study. Therefore, strain SP578 was chosen for the continuation of the screen. After that, the mating phenotype was detected by utilizing iodine vapor (Egel, 1989). I screened for alleles that allow mating in the presence of the compound. The iodine staining was performed initially onto a plate. Initial stained cells were transferred to liquid medium for a second mating characterization where 220 colonies were identified. However, accuracy of mating can be masked in both staining procedures. In order to make a better assessment, each of the 220 colonies was verified under microscope. These colonies were then transferred to new medium in presence/absence of compounds and stained again. From 220 colonies screened, 10 candidate colonies were selected and plated to assess mating phenotype in solid medium in the presence/absence of compounds. Finally, 5 candidate colonies with mutant PDE7B alleles that were

obtained demonstrated altered patterns of iodine staining, where mating was either increased (G21, L1) or decreased (D7, F22) and no change was observed in colonies carrying the wild type PDE7B allele (K19) in the presence of the PDE7B inhibitor (BC12). These plasmids were rescued out of yeast into *E.coli* to be purified and sequenced.

A.2.5 Cell-based assays

Plasmids were integrated into CHP1207, as described in the previous section. Characterization of mutant PDE7B1 candidate alleles in the presence of exogenous cAMP and confirmation of altered behavior in the presence of PDE7B inhibitors (BC12, BC28, BC30 and BRL50481) were performed with 5FOA assays, as previously described (section 2.1.3.1).

A.2.6 Two- step PC to generate single missense mutations

In order to determine which mutation in each PDE7B mutant alleles was responsible for the initial altered behavior detected in the screen, the two-step PCR was used. This technique aimed to reproduce the point mutations near or close to the catalytic domain in the wild type human PDE7B1 gene (Genbank accession number NM_002603). The technique was performed as previously described (Mudge et al., 2012). The two sets of primers used for mutant C7 were: C7For 5'-CTCTTTGTAATCAATCCCTAGTATAC-3' and *cgs2mut3*'; C7Rev5'-GTATACTAGGGATTGTTACAAAGAG-3' and *cgs2mut5*'. The two sets of primers used for mutant D7 were: D7For 5'-GGGTCTGTGAAGAAGGCAAGGTGAAC-3' and *cgs2mut3*'; D7Rev5'-GTTACCTTGCCCTTCTTCACAGACCC-3 and *cgs2mut5*'. The primers *cgs2mut5*' and *cgs2mut3*' were described in section 2.2.2.

After that, PCR products were sent out for sequencing to confirm that each point mutations was introduced. The following sets of primers were used for both mutants: PDE7627F (TGCAGCAGCACACGATGTGG), PDE7B1199R (5' TCCGACAGGGTGCTGTTACC3'),

cgsmut5' and cgsmut3'. After that, 5FOA assays were performed to reconfirm the altered mating phenotype.

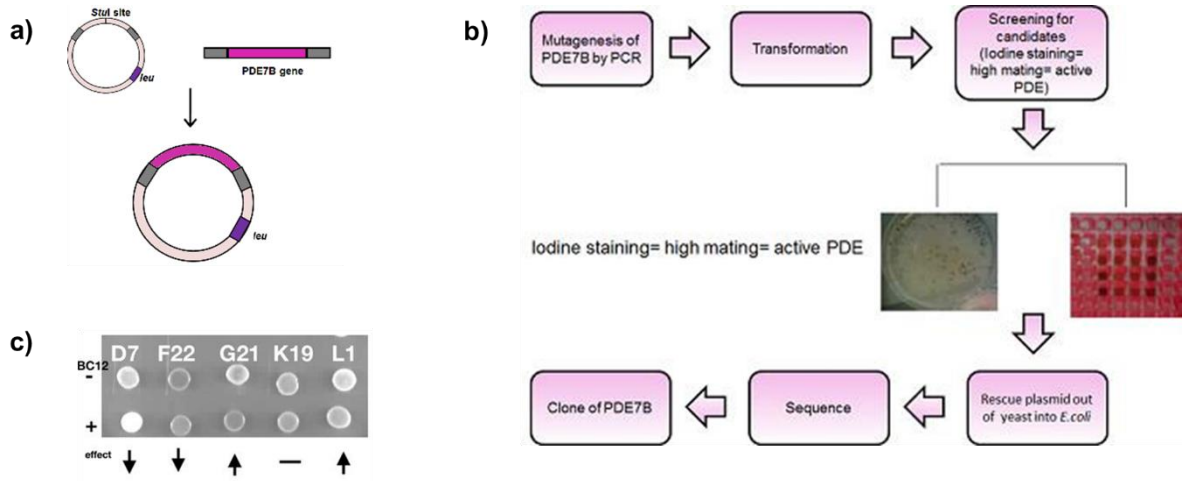
RESULTS

The candidate mutant plasmids were integrated into a strain carrying an adenylyl cyclase deletion (*git2Δ*) to better understand its behavior. A mutant strain (CHP1505) that has WT sequence was used as a control to determine the best growth conditions in which the mutant strains should be further tested in a 5FOA assay. The amount of exogenous cAMP needed to activate PKA and promote 5FOA growth is a reflection of PDE activity. It also identifies conditions where compound sensitivity can be examined. When the growth curve moves towards the right, the enzyme is more active, whereas when the growth curve moves towards the left, the enzyme is less active (Figure A2). In this experiment, two mutant PDE7B strains (CHP1503 and CHP1506) had lower enzyme activity when compared to the wild type PDE7B strain (CHP1505), while mutant PDE7B strain CHP1502 had similar PDE activity to the wild type PDE7B strain (CHP1505). In addition, two mutant PDE7B strains (CHP1501 and CHP1504) had a higher PDE activity in comparison to the wild type PDE7B strain. Also, the addition of 0.2 mM cAMP was found to be an optimal condition for the secondary screening assay (5FOA growth assay), promoting growth while PDE activity remained low (Figure A2).

After characterizing the optimal growth conditions in the cAMP dose response assay, a secondary screening assay was performed. Six candidate mutant strains (Table A1) were tested for sensitivity with PDE7B inhibitors (BC15, BC28, BC30 and BRL50481) in the 5FOA growth assay. The CHP1505 strain expressing wild-type PDE7B was used as the control. In comparison to the wild-type PDE7B strain, two PDE7B strains (CHP1502 and CHP1503) had altered response to compound BC12 and one PDE7B strain (1503) had no response to compound BC28. In addition, one PDE7B strain (CHP1503) was hypersensitive in the presence of compound BC30 and all

Figure A1. Development of a genetics screen. A) Gap repair was performed to clone mutagenic PDE7B PCR products into the plasmid. B) Genetic screen protocol. C) Screen using in mating analysis in presence (+) or absence (-) of compound BC12.

Figure A1



PDE7B strains had similar response to compound BRL50481, the commercially-available specific PDE7 inhibitor (Figure A3). Taking all data into account, I concluded that two mutant PDE proteins (strains CHP1502 and CHP1503) appeared to have an altered sensitivity to our compounds, but not to the commercially available PDE7 inhibitor (BRL50481). Further studies will be performed with these mutant PDE proteins.

Based on sequencing data, the two mutant candidate PDE7B plasmids, identified as C7 (inserted into strain CHP1502) and D7 (inserted into strain CHP1503) carry three and two candidate mutations, respectively (Figure A4). Therefore, I performed site-directed mutagenesis to isolate and investigate mutations that both mutant plasmids carry within/near the catalytic domain of PDE7B allele. The amino acid substitution of the D7 plasmid is from Phenylalanine to Leucine. While the C7 plasmid carries an amino acid substitution from Aspartic Acid to Glycine. After isolation of the mutations of interest, 5FOA assays were performed. However, the initial altered behavior from the screen was not confirmed (data not shown).

Figure A2. cAMP curve. 5FOA growth assays of strains expressing wild type PDE7B (CHP1505) and five candidate mutant PDE7B proteins (CHP1501, CHP1502, CHP1503, CHP1504 and CHP1506) in the presence of four PDE7 inhibitors (BC12, BC28, BC30, BRL50481). Values represent the average of $OD_{600} \pm$ standard error from one independent experiment. The values within each experiment represent an average of four replicate wells. Each experiment was incubated for a 48h growth at 30°C.

Figure A2 cAMP curve

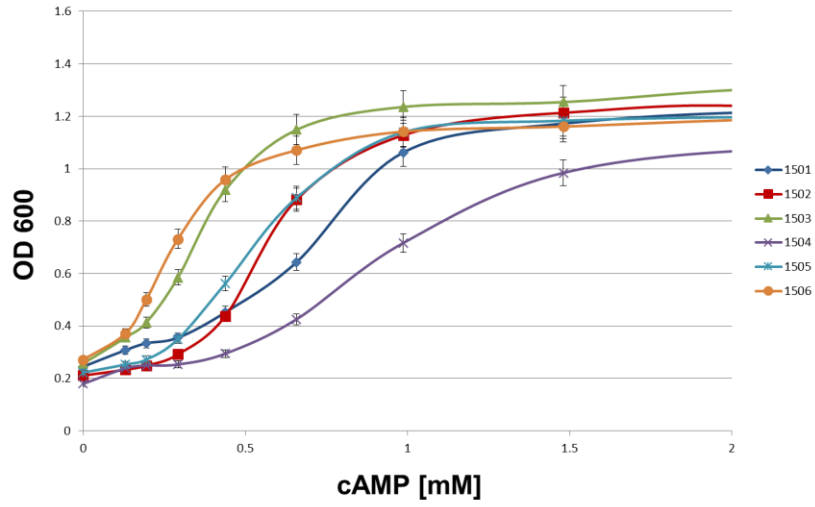
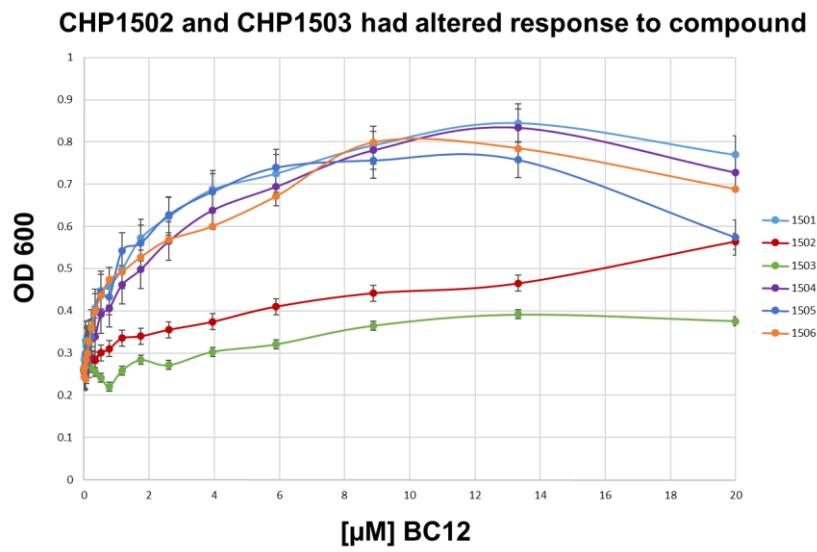


Figure A3. Growth response of candidate mutant PDE7B alleles to different compounds in 5FOA medium. PDE7B strains growth response in the presence of compounds: A) BC12, B) BC28, C) BC30 and D) BRL50481. Optical density of cultures of mutant PDE7B strains grown in 384 well microtiter wells. Values represent the average of $OD_{600} \pm$ standard error from two independent experiments. The values within each experiment represent an average of four replicate wells. Each experiment was incubated for a 48h growth at 30°C. Region of high sensitivity is highlighted by black rectangle and emphasized on top right (C).

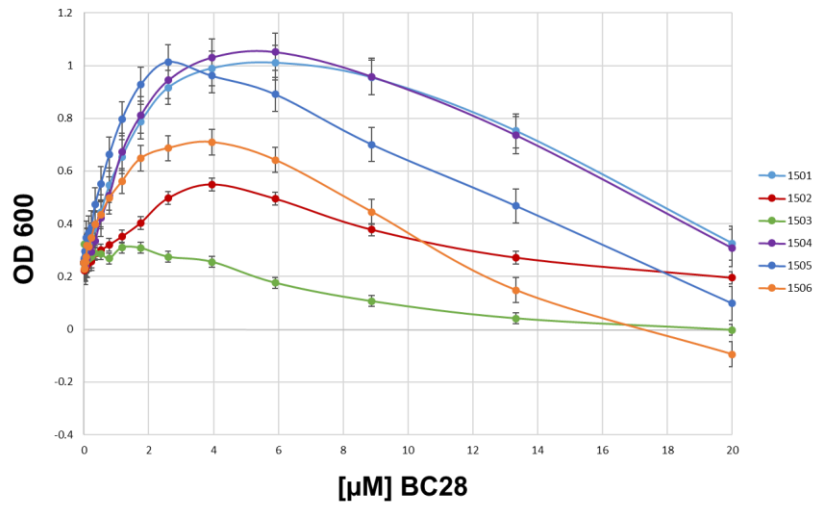
Figure A3 Growth response of candidate mutant PDE7B alleles to different compounds in 5FOA medium

A



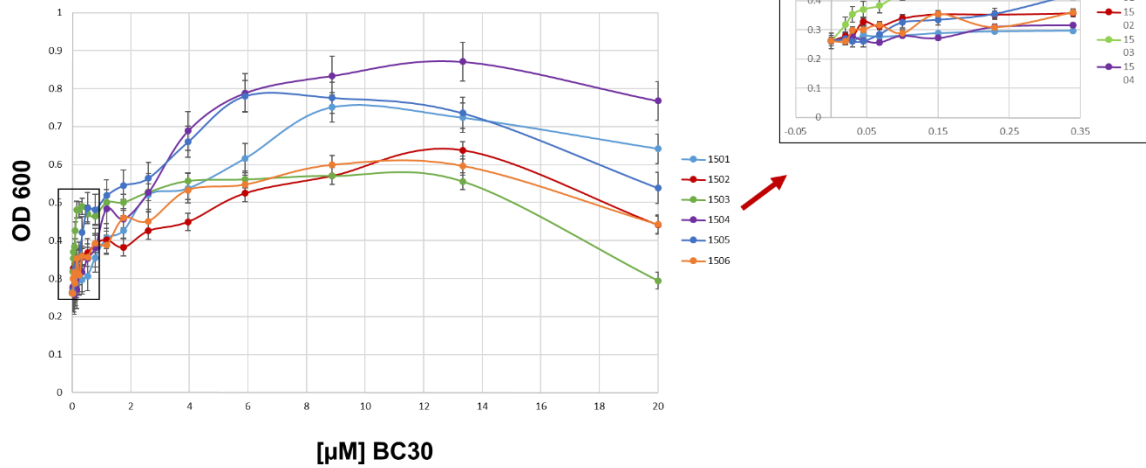
B

CHP1503 has no response to compound



C

CHP1503 is hypersensitive to compound



D

All PDE7B strains have similar response to compound

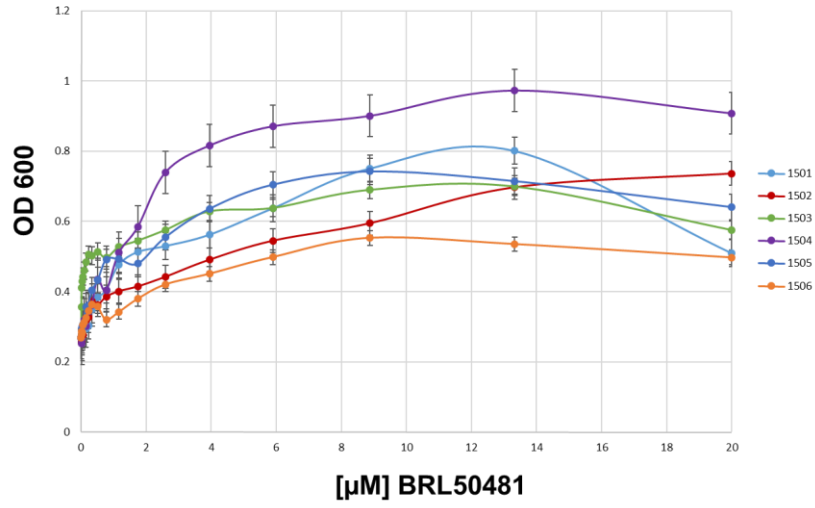
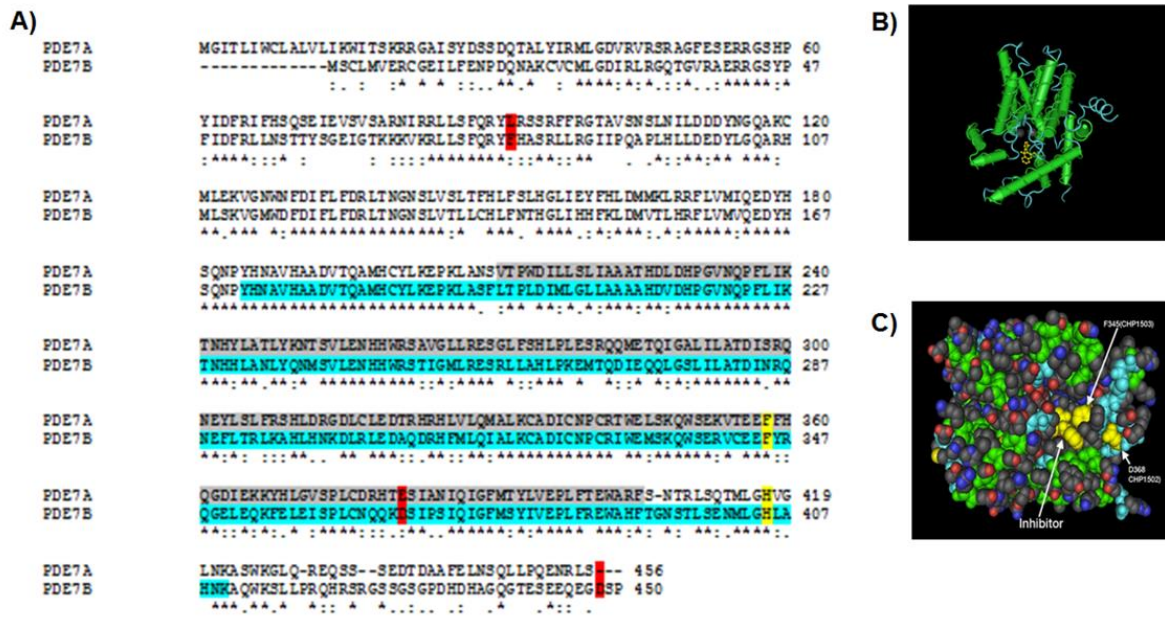


Figure A4. Sequence homology of PDE7A and PDE7B the catalytic domains. A) PDE7B catalytic domain is depicted in blue. PDE7A catalytic domain is depicted in grey. Location of plasmid D7 mutations (Strain CHP1503) are in yellow. Location of plasmid C7 mutations (Strain CHP1502) are in red. B) Co-crystal structure of PDE7A. C) Co-crystal structure of PDE7A depicting localization of the two residues of mutant PDE7B alleles (F345L in CHP1503; D368G in CHP1502).

Figure A4 Sequence homology of PDE7A and PDE7B the catalytic domains



CONCLUSIONS

Yeast genetics can be used to study mammalian genes. In this study, compound sensitivity, mating, growth phenotype and cell viability can be associated with PKA activity. In this study, I have successfully developed a genetics screens to study human PDEs analyzing the mating phenotype in the presence of PDE7B inhibitors. These mutants PDEs were isolated and further characterized. However, the initial phenotype was not confirmed suggesting the altered behavior was a result of a combination of mutations and not to a specific amino acid change. In future experiments, it will be important to optimize conditions that will generate mutants carrying point mutations for confirmation of the phenotype and, consequently, understanding the PDE and its specific inhibitors mechanism of interaction. In conclusion, we have successfully developed a genetic screen looking for altered mating phenotype. In the future, it will be interesting to develop other screens analyzing other phenotypes associated with PKA activity.

LITERATURE CITED

de Medeiros, AS, Magee, A., Nelson, K., et al (2013). Use of PKA-mediated phenotypes for genetic and small-molecule screens in *Schizosaccharomyces pombe*. *Biochem Soc Trans.*, **1**(6):1692-5.

Egel, R. (1989). In Nasim, A., Young, P., Johnson, B.F. (eds). *Molecular biology of Fission Yeast: Mating-type genes, meiosis, and sporulation*. San Diego: Academic Press, Inc., 31-35.

Hoffman, C. S., and Winston, F. (1990). Isolation and characterization of mutants constitutive for expression of the *fbp1* gene of *Schizosaccharomyces pombe*. *Genetics*, **124**:807–816.

Hoffman, C.S. and Winston, F. (1987). A ten-minute DNA preparation from yeast efficiently releases autonomous plasmids for transformation of *Escherichia coli*. *Gene*, **57**:267-272.

Mudge, D.K, Hoffman, C.A., Lubinski, T.J., Hoffman, C.S. (2012). Use of a *ura5⁺-lys7⁺* cassette to construct unmarked gene knock-ins in *Schizosaccharomyces pombe*. *Curr. Genet.*, **58**:59-64.

APPENDIX B

CHARACTERIZATION OF BC54 ANALOGS IN LIQUID AND SOLID MEDIA

INTRODUCTION

As described in Chapter 2, compound BC54 is a potent and selective inhibitor of PDE4 and PDE7 enzymes. Here, we examined a collection of compounds related to BC54 in an effort to identify important functional groups in the compound. This was done using two assays. In the first, compounds were assessed for their ability to inhibit growth on SC-ura medium of strains expressing either PDE4B or PDE7B (Ura⁺ growth due to *fbp1-ura4* expression is associated with low PKA activity). In the second assay, compounds were assessed for their ability to stimulate 5FOA^R growth due to activation of PKA to repress *fbp1-ura4* expression.

MATERIALS AND METHODS

B1. MATERIALS

B1.1 Growth media

Sensitivity to compound PDE inhibitors was determined in (5FOA) and SC-solid medium as described by Hoffman and Winston (1990).

B1.2 Yeast strains

The genotype of yeast strains, CHP1209 and CHP1268, used in this study are listed in Table 2.1 (section 2.1.2). These strains carried the the *fbp1-ura4⁺* construct, a translational fusions integrated

at the *fbp1*⁺ locus, as previously described by Hoffman and Winston (1990). Strains were grown at 30°C.

B2. Methods

B.2.1 Cell-based assay

5FOA assays were performed in the presence of BC54 and its analogs, as previously described (2.1.3.1).

B2.2 Growth in SC-ura

The SC-ura growth phenotype is associated with PKA activity, as previously mentioned (section 1.19) and depicted in Figure 6.

RESULTS

The activity of twelve BC54 analogs have been tested in solid media by growth in SC-ura medium and 5FOA assays. The results observed will be described in the sections below.

B1. Profiling the potency of BC54 analogs

The growth phenotype of yeast strains in SC-ura is associated with reduced PKA activity. Strains expressing either PDE4B (CHP1268) or PDE7B (CHP1209) in SC-Ura medium. Growth occurs in the presence of DMSO due to PDE activity. The PDE inhibition prevents growth by activating PKA in the presence of dual PDE7B/4B inhibitor, as depicted in the further left in Figure B1. Five out of twelve BC54 analogs (BC54-1/3/6/8/11) had moderate action against either PDE4B or PDE7B (Figure B1). The analogs BC54-1/-3/-8 seemed to inhibit more strongly strains expressing PDE4B plasmid (Figure B1, lower panel). While analogs BC54-6/-11 seemed to selectively inhibit strains expressing PDE7B plasmid (Figure B1, top panel). BC54 derivatives (BC54-4/5/7/9/10/12) had not

effect against either PDE4B or PDE7B (data not shown). The lack of activity of seven of the BC54 analogs may be due to a failure to be taken up by the cell.

B2. Profiling of BC54 analogs in cell-based assays with an effect

5FOA Growth assays with strains expressing either PDE7B or PDE4B in the presence of BC54 derivatives were performed. As already mentioned in previous sections, BC54 is a very potent inhibitor with dual specificity targeting PDE4 and PDE7 previously screened by our lab. In these assay, BC54 is the most potent inhibitor with dual specificity in both PDE7B and PDE4B strains (Figure B2a, b). While, BC54-6 and BC54-8 had a moderate inhibition against both strains in comparison to BC54 treatment, but more specifically against PDE7B (Figure B2a) and PDE4B (Figure B2b), respectively. BC54-1 had a weaker inhibition only against PDE4B (Figure B2b). The other BC54 derivatives (BC54-3 and BC54-11) initially screened in solid medium (Figure B1) did not inhibit in the secondary screen (Figure B2a, b), which it could suggest that the initial screen was a toxicity effect instead of inhibition.

B3. Analyzing the structure of BC54 analogs

The most potent derivatives, BC54-6 and BC54-8, don't have cyclohexyl side group attached to nitrogen in the pyrimidine ring (Figure B3, top panel). Instead of the cyclohexyl side group isobutyl group and BC54-6 has an isopropyl group near the pyrimidine ring. In addition, BC54-11 has a moderate effect, contains a methyl furan instead of the cyclohexyl present in BC54 (Figure B3, left lower panel). While BC54-1 and BC54-3 compounds differ structurally from BC54 for the absence of the acetylimino group (Figure B3, mid and lower panel). From these two, BC54-1 has a methyl carboxyl group and BC53-3 has the ethyl carboxyl groups that is present in BC54.

Seven compounds did not have any effect either in solid or liquid media (Figure B4). Compounds BC54-2 and -4 have the cyclohexyl group, but lack the acetylimino and ethyl carboxyl groups. The acetylimino group is also altered in compound BC54-7. Compounds BC54-5, -7 and -9 through -

12 (has a similar structure to BC54-11) lack the cyclohexyl group, which was substituted by other side groups.

CONCLUSIONS

Yeast genetics can be used to study mammalian genes. We have previously screened for mutant PDEs resistant to BC54. Screening for BC54 derivatives is a good way to understand BC54 structure and, consequently, potency. Based on our data, it seems that the cyclohexyl and acetylimino groups present in BC54 are important for its dual specificity targeting PDE4 and PDE7. In future experiments, it will be good test other BC54 analogs and perform *in vitro* assays to determine their IC₅₀ concentrations. In conclusion, chemical screens can help elucidate the mechanism of interaction of PDEs and their specific inhibitors.

Figure B1. Growth phenotype in SC-Ura medium. Strains expressing either PDE4B (lower panel) or PDE7B (top panel) treated with BC54 analogs. Plates were incubated for 3 days at 30°C.

Figure B1 Growth phenotype in SC-Ura medium

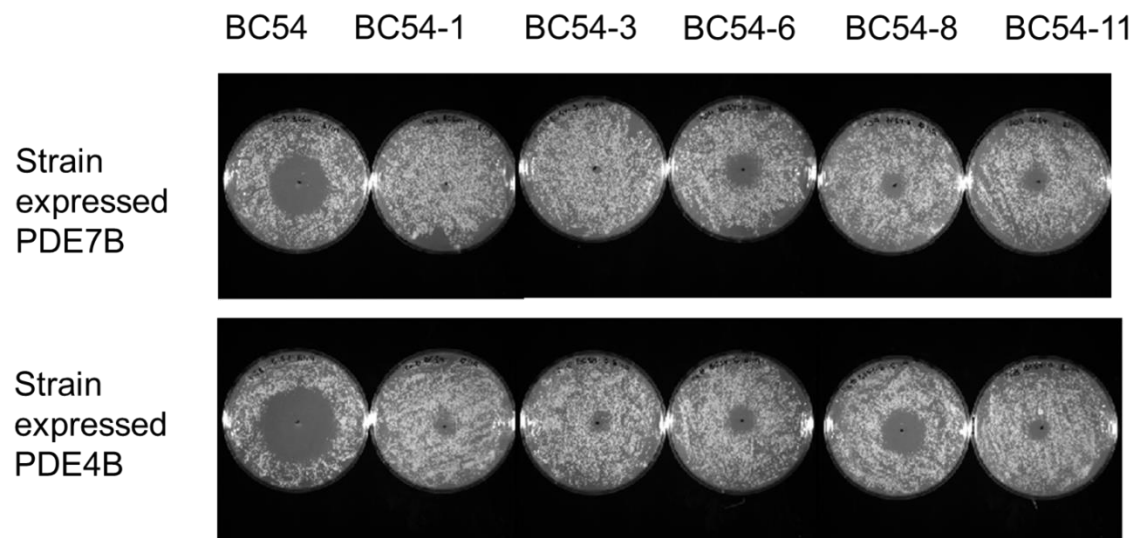
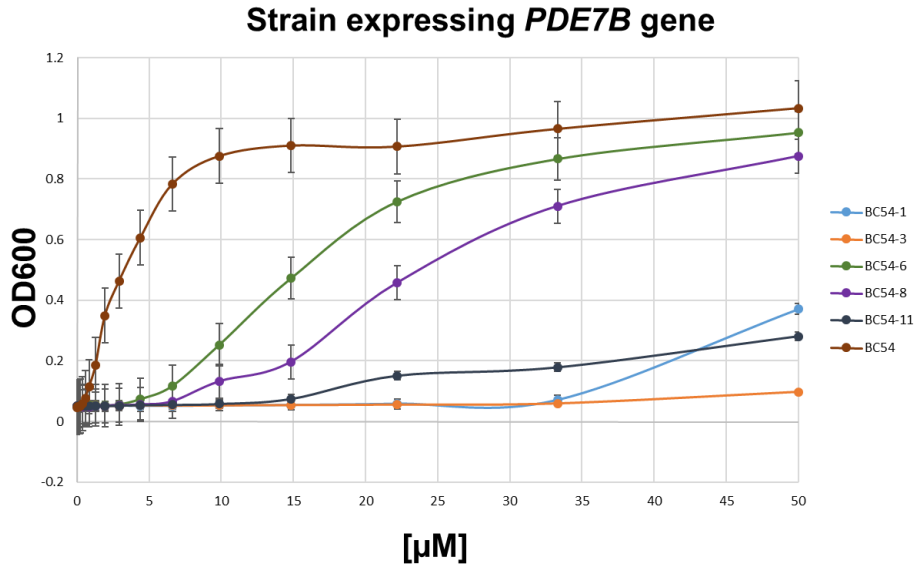


Figure B2. 5FOA Growth assays in the presence of BC54 derivatives. A) Strain expressing either PDE7B or B) Strain expressing PDE4B were treated with five BC54 analogs along with BC54. Values represent the average of $OD_{600} \pm$ standard error from three independent experiments. The values within each experiment represent an average of four replicate wells. Each experiment was incubated for a 48h growth at 30°C.

Figure B2 5FOA Growth assays in the presence of BC54 derivatives

A



B

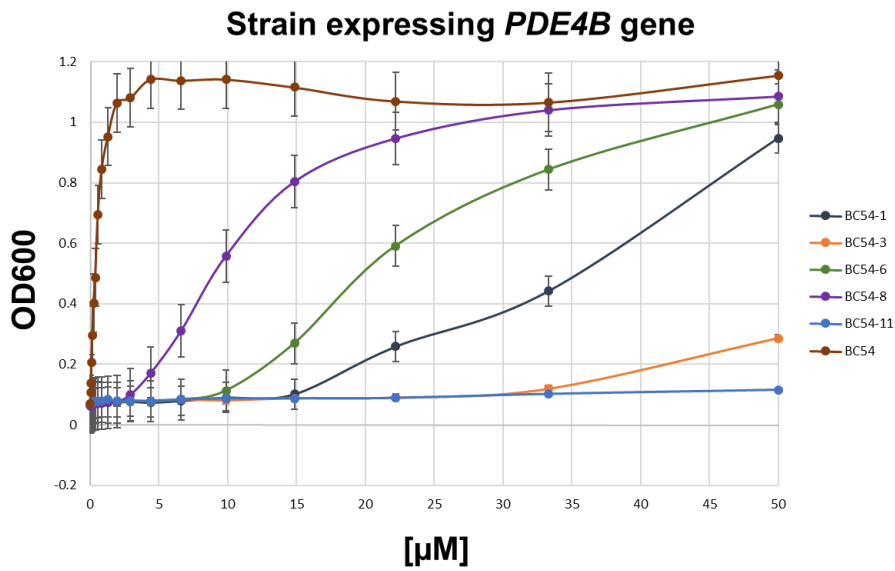


Figure B3. Chemical structure of BC54 analogs with an effect

From top left to right indicate the structures of the following: BC54, BC54-4 and BC54-8.

Structural differences are highlighted with red arrow. From bottom left to right indicate the structures of the following: BC54-11, BC54-1, BC54-3.

Figure B3 Chemical structure of BC54 analogs with an effect

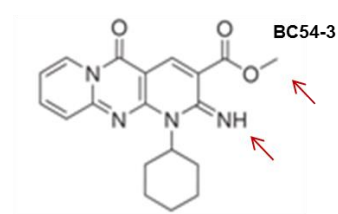
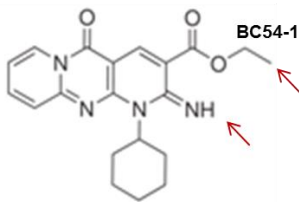
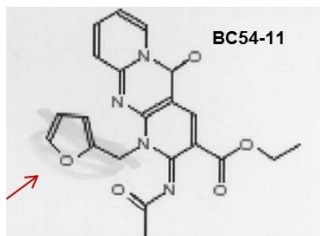
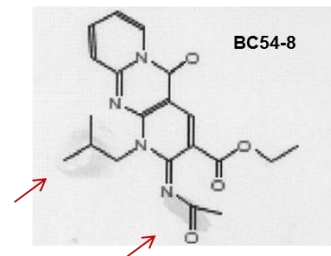
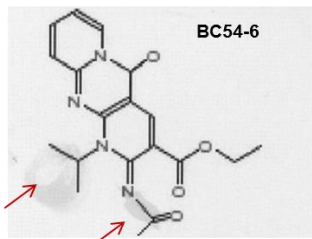
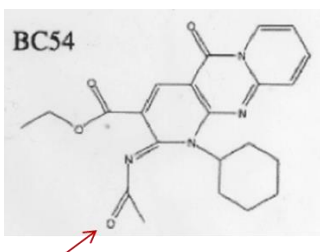
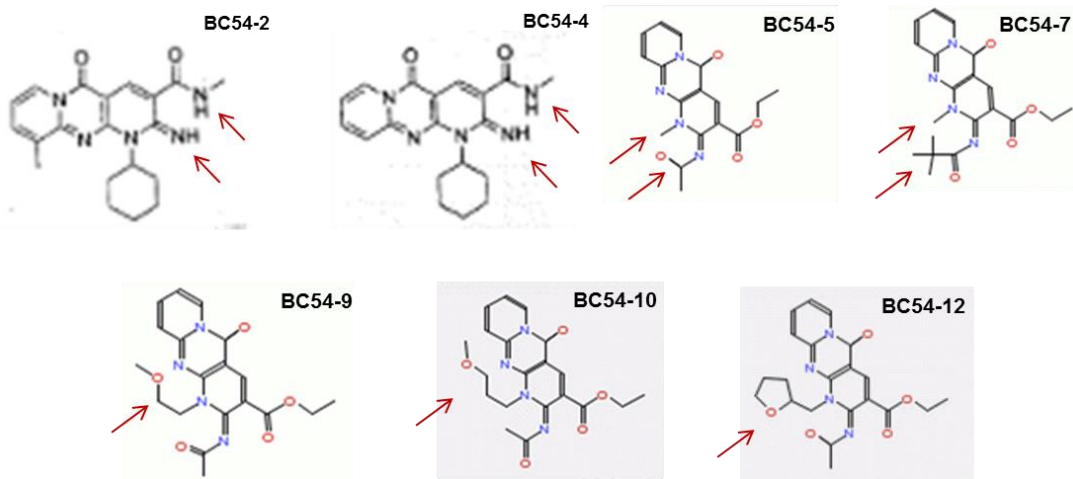


Figure B4. Chemical structure of BC54 analogs with no effect

From top left to right indicate the structures of the following: BC54, BC54-4 and BC54-8.

Structural differences are highlighted with red arrow. From bottom left to right indicate the structures of the following: BC54-11, BC54-1, BC54-3.

Figure B4 Chemical structure of BC54 analogs with no effect



LITERATURE CITED

Hoffman, C. S., and Winston, F. (1990). Isolation and characterization of mutants constitutive for expression of the *fbp1* gene of *Schizosaccharomyces pombe*. *Genetics*, 124:807–816.